TU Clausthal

Experimental Investigation of Sulfate-Modified Water and Polymer Flooding for Enhanced Oil Recovery

Doctoral Thesis
(Dissertation)

to be awarded the degree
Doctor of Engineering (Dr.-Ing)

submitted by
Muhammad Tahir

from Muzaffargarh, Pakistan

Approved by the Faculty of Energy and Economic Sciences
Clausthal University of Technology

Date of oral examination
June 30, 2020

Dean

Prof. Dr. rer. nat. habil. Bernd Lehmann

Chairperson of the Board of Examiners

Prof. Dr. rer. nat. habil. Bernd Lehmann

Supervising Tutor

Prof. Dr. mont. Leonhard Ganzer

Reviewer

Prof. Dr. habil. Philip Jaeger

Eidesstattliche Erklärungen

Hiermit erkläre ich an Eides Statt, dass ich die bei der Fakultät für Energie- und Wirtschaftswissenschaften der Technischen Universität Clausthal eingereichte Dissertation selbständig und ohne unerlaubte Hilfe angefertigt habe. Die benutzten Hilfsmittel sind vollständig angegeben.

Signature: _____

Date: _____

Abstract

Modified/smart water flooding is a low-cost enhanced oil recovery (EOR) technique that works through the manipulation of injected water chemistry to disturb the established ionic equilibrium in a reservoir system. Chemical manipulation is achieved by the addition/removal of active/non-active ions, respectively. Added active ions are known as potential determining ions (PDI) while removed non-active ions are known as non-potential determining ions (non-PDI). The focus of this study is to investigate the role of sulfate ions as PDI to select an optimum injection scheme and initiation time. This work investigates the combination of two EOR methods (also known as the hybrid method)—modified water flooding in the secondary mode and low-concentration polymer flooding in the tertiary mode—to enhance the capability of the flooding process. Modified water triggered fluid-fluid and rock-fluid interactions, and follow-up polymer flood improved the macroscopic sweep efficiency due to a favourable displacement mobility ratio. Hence, the hybrid EOR method is expected to be low-cost (as low polymer concentrations are required) and to provide the combined benefits of both EOR processes. This research work is focusing on experimental work. Evaluations were performed through comprehensive laboratory evaluations that included measurements of rheological behaviour, contact angle, interfacial tension, oil drop snap-off volume, and wettability alteration. Furthermore, the synergetic effects of modified water and polymer flooding were defined by flooding experiments using two types of micromodels with modified-wettability and complemented with core flooding in Bentheimer outcrops.

The objective of the study is to investigate whether the main recovery mechanism should be rock-fluid interaction, fluid-fluid interaction, or a combination of both as a potential lead. Synthetic seawater (SSW) was used as the benchmark. Brine optimization was performed by tuning the brine salinity and concentration of the sulfate, by either diluting the brine to achieve total dissolved solids of around 5g/L or maintaining the salinity of the SSW. Further, two types of formation brine (SSW, 2*SSW) were used to compare the impact and significance of the presence of divalent cations (the hardness contrast between the injection and formation brine). Subsequently, to investigate wettability alteration, Bentheimer core plugs and glass-silicon-glass micromodels were used as porous media for flooding experiments and to cross-validate the results. Three-week and six-week aging of core plugs were considered to establish the attachment of oil polar compounds resulting in mixed-wet and oil-wet core plugs. Similarly, oil-wet, complex/mix-wet, and water-wet micromodels were used for oil recovery comparison. Brine floods were performed as the secondary mode and polymer flooding as the tertiary mode to optimize the synergies and benefits of the hybrid EOR techniques. In addition, single-phase core-flooding experiments were performed to investigate the role of sulfates,

salinity, and hardness for the polymer viscoelastic properties.

Oil recovery from core plugs was mainly obtained by alteration of the local wettability to water-wet, which resulted from strong rock-fluid interaction as well as fluid-fluid interaction at the fluid interface. However, the recovery factor from the oil-wet/mixed-wet micromodel was achieved only through fluid-fluid interaction. The main reason for this is that the oil-wetting condition in the micromodel was achieved by the chemisorption of fluorinated silane at the matrix structure, which made it impossible for the modified water to promote a change of the micromodel's wettability to a water-wet state. Oil recovered from the two porous media approaches support the finding that wettability and fluid-fluid interactions result in more oil recovery when the injected brine is spiked with sulfate than SSW alone. Oil recovery comparison of oil-wet/mixed-wet with water-wet micromodels demonstrates that an initial oil-wetting condition is a basic requirement for the success of modified water flooding. Moreover, comparing data on the wettability alteration of core plugs and micromodels shows this recovery mechanism dominates over fluid-fluid interfacial interaction. Further, polymer flooding after modified water injection produced significantly higher recovery compared to the seawater base brine combined with polymer flooding. According to the single-phase polymer flooding data, the presence of sulfate increased polymer sensitivity to mechanical degradation. Further, polymer spiked with sulfate had higher pressure in two-phase polymer flooding due to the interfacial ionic layer developed between the pre-flushed brine and dead oil. Finally, a brief exercise evaluating the economic scenario of the project showed that sulfate-modified brine is a cost-effective process based on oil recovery.

Zusammenfassung

Wasserfluten gehört zu den Standardverfahren bei der Ölgewinnung. Hierbei wird produziertes Lagerstättenwasser genutzt, welches hohe Salzkonzentrationen besitzt. Der Einfluss der im Wasser gelösten Ionen auf den Verdrängungsprozess ist Gegenstand der aktuellen Forschung. Wasserfluten mit chemisch modifiziertem Wasser ist eine verhältnismäßig kosteneffektive EOR-Methode, bei der die chemische Zusammensetzung des injizierten Salzwassers verändert wird. Hierdurch wird das Gleichgewicht der Ionen im Reservoir verändert. Bei der chemischen Manipulation werden die Konzentrationen von aktiven und passiven Ionen verändert. Aktive Ionen werden als potentialbestimmende Ionen bezeichnet (PDI). Diese Arbeit untersucht den Einfluss von Sulfat-Ionen, um den optimalen Injektionszeitpunkt und ein passendes Injektionsschema zu ermitteln. Es wird eine Kombination aus zwei EOR-Methoden (Hybridmethode) genutzt. (1) Wasserfluten mit modifizierter Ionenkonzentration im sekundären Modus und (2) Polymerfluten mit geringer Konzentration im tertiären Modus. Das modifizierte Injektionswasser verändert die Wechselwirkungen zwischen den Fluiden sowie zwischen Fluid und Gestein. Anschließendes Polymerfluten optimiert die makroskopische Verdrängung von Öl durch eine stabilisierte Verdrängungsfront. Es wird erwartet, dass eine Hybridmethode kosteneffektiv ist (geringe Polymerkonzentration) und die mikroskopischen und makroskopischen Effekte beider Methoden kombiniert werden. Der Fokus dieser Forschungsarbeit liegt auf experimentellen Untersuchungen. Die Laboruntersuchungen beinhalten rheologische Messungen, Kontaktwinkel-Messungen, Grenzflächenspannung, dynamische Grenzflächenspannung sowie die Veränderung der Benetzbarkeit. Des Weiteren wurden Synergieeffekte zwischen modifiziertem Wasserfluten und Polymerfluten untersucht. Hierfür wurden Flutversuche in Mikromodellen mit zwei unterschiedlichen porösen Strukturen sowie unterschiedlicher Benetzbarkeit durchgeführt. Abschließend wurden Kernflutversuche in Bentheimer Sandstein durchgeführt.

Das Ziel dieser Untersuchung ist die Klärung, ob der Verdrängungsmechanismus auf Wechselwirkung zwischen den Fluiden, zwischen Fluid und Gestein oder auf einer Kombination basiert. Als Standard dienen Flutversuche mit synthetischem Meerwasser (SSW). Durch Veränderung der Salinität und durch Zugabe von Sulfat-Ionen wurde die Zusammensetzung der Salzlösung modifiziert. Zwei Salzlösungen mit unterschiedlicher Salinität wurden eingesetzt (SSW, 2*SSW), um den Einfluss divalenter Ionen auf den Gewinnungsprozess zu untersuchen (unterschiedliche Härte zwischen Injektionslösung und Reservoir-Lösung). Anschließend wurde die Benetzbarkeitsänderung untersucht. Hierfür wurden Flutversuche in Bentheimer Sandsteinkernen und Glass-Silizium-Glass Mikromodellen durchgeführt. Die Gesteinskerne wurden für drei bzw. sechs Wochen gealtert, um die Adsorption polarer Ölkomponenten auf der Gesteinsoberfläche sicherzu-

stellen. Die Gesteinskerne besaßen somit gemischte Benetzbarkeit bzw. waren ölbenetzend. Zum Vergleich wurden die Mikromodelle modifiziert, um ölbenetzende, gemischt benetzende und wasserbenetzende Oberflächen zu erhalten. Salzwasserfluten im sekundären- und Polymerfluten im tertiären Modus wurden durchgeführt. Zusätzlich wurden Einphasen-Versuche vorgenommen, um den Einfluss von Salinität, Härtegrad und Sulfat-Gehalt zu untersuchen.

Die zusätzliche Ölausbeute war Folge der Änderung der lokalen Benetzbarkeit von ölbenetzend hin zu wasserbenetzend. Dies war eine Folge starker Gestein-Fluid Wechselwirkungen, sowie Fluid-Fluid Wechselwirkungen. Im Mikromodell war die Ölgewinnung jedoch eine Folge von Fluid-Fluid Wechselwirkungen. Dieser Unterschied rührt aus der Tatsache, dass die ölbenetzende Eigenschaft des Mikromodells durch Chemisorption flourinierter Silane erzeugt wurde und somit keine Änderung der Benetzbarkeit während des Experiments möglich war. Die Ergebnisse unterstützen die Annahme, dass die Injektion einer mit Sulfaten versetzter Salzlösung zu einer Änderung der Benetzbarkeit sowie Fluid-Fluid Wechselwirkungen führt. Als Folge wird eine zusätzliche Ölgewinnung beobachtet. Ölbenetzende Eigenschaften des porösen Mediums sind hierfür eine grundlegende Voraussetzung. Der Vergleich von Gesteinskernen und Mikromodellen macht deutlich, dass die Änderung der Benetzbarkeit der dominierende Mechanismus ist. Des Weiteren führte das Polymerfluten im Anschluss an das Wasserfluten mit Sulfat dotierter Salzlösung zu einer deutlich höheren Ausbeute im Vergleich zum Benchmark. Einphasenversuche zeigten, dass die Präsenz von Sulfat-Ionen mechanische Degradation des Polymers verstärkt. Des Weiteren führte der Einsatz von Sulfat-Ionen zu einem erhöhten Differenzialdruck beim anschließenden Polymerfluten. Diese Beobachtung wird auf Ionen-Wechselwirkungen an der Grenzfläche zwischen der Salzlösung und dem Öl zurückgeführt. Abschließend zeigte eine vereinfachte ökonomische Bewertung, dass Wasserfluten eine kosteneffektive EOR Methode ist.

Acknowledgment

I would like to express sincere gratitude to my advisor **Prof. Dr. Leonhard Ganzer** for the continuous support of Ph.D. study and related research, for his supervision, motivation, and immense knowledge. His guidance helped me in all the time of research and writing of this thesis. In addition, I would like to thank **Prof. Dr. Philip Jaeger** on the acceptance to be part of committee and to review thesis. Besides, I would like to thank **Dr.-Ing. Rafael E. Hincapie R.** for his continuous support, technical assistance and valuable time to complete this big challenge.

Very special gratitude to family and friends, especially my **wife** and **parents**, for their moral and emotional support in my life in every good and bad time. I thank my fellow colleagues **Calvin Gaol** and **Dr.-Ing. Hendrik Foedisch** for their valuable suggestion and technical discussions to complete this task. Special thanks to **Gion-Joèl Strobel** and **Stefanie Saefken** for the continuous support of the experimental setup. I would also like to thank **Bettina Jenei** for her support to assist in practical sessions as well as creative ideas for the colleagues' get-together. With a special mention to **Nils Langanke** for technical, socio-political and cultural discussions we had, as well for the nickname of *Helmut*. Also thanks to **Dr.-Ing. Birger Hagmenn**, **Ms. Jessica Lüer**, **Ke Li** and **Maximilian Wirth** for all the nice time we had while working at ITE.

Last but not least, I would like to thank **Higher Education Commission (HEC) of Pakistan** for the financial support to complete my studies under the funding program of "Faculty Development of MSc leading to Ph.D. for Universities of Engineering, Science and Technology (UESTP) – Germany."

Contents

List of Figures

List of Tables

Abbreviations

2*SSW	Double salt concentration of synthetic seawater
A	Polymer solution viscosity of effluent from flowlines
API	American petroleum institute
B	Polymer solution viscosity before injection
bbl	Barrels
BG	Brine group
BR	Bump rate
CF	Core flood
CG	Core group
DR	Degradation rate
DSSW	Ten timed diluted synthetic seawater
DSSW+2SO_4^{-2}	Ten times diluted synthetic seawater with double amount of sulfate
DW	Deionized water
Elong.	Elongational
EOR	Enhanced oil recovery
e-VROC	Extensional viscometer rheometer on a chip
FP	Flopaam 6035 S
GB	Bramberge reservoir formation brine
GBP	Great Britain pound
HF	Hengfloc 63026
HPAM	Partially hydrolyzed polyacrylamide
IFT	Interfacial tension
JD	Jordanian dirham
MM	Micromodel
M_R	Mobility ratio
N1	Normal stress difference
N_2	Nitrogen gas
OOIP	Original oil in place
PDI	Potential determining ions
PF	Polymer flood
ppm	Parts per million
PV	Pore volume
PVI	Pore volume injected
RF	Recovery factor
ROS	Remaining oil saturation
RT	Relaxation time
SAOS	Small amplitude oscillatory shear
Sec.	Secondary
SSW	Synthetic seawater
SSW+2SO_4^{-2}	Synthetic seawater with double amount of sulfate
SSW+4SO_4^{-2}	Synthetic seawater with four times amount of sulfate
SSW-Na	Synthetic seawater without sodium chloride
STOIIP	Stock tank oil initial in place
Tert.	Tertiary

Symbols

L	Length, L
D	Diameter, L
ΔP	Pressure drop, [M.L^{-1}.T^{-2}]
V	Interstitial velocity, [M.T^{-1}]
Soi	Initial oil saturation , dimensionless
Swc	Initial water saturation, dimensionless
Φ	Porosity, dimensionless
k	Permeability, [L^2]
η	Shear viscosity, [M.L^{-1}.T^{-1}]
μ	Viscosity, [M.L^{-1}.T^{-1}]
k_{ro}	Relative permeabilty of oil, dimensionless
k_{ra}	Relative permeabilty of polymer, dimensionless
G'	Elastic modulus, [M.L^{-1}.T^{-2}]
G"	Viscous modulus, [M.L^{-1}.T^{-2}]
γ	Shear rate, [T^{-1}]

Chapter 1

Introduction

To meet the increasing demand for hydrocarbon energy, it is essential either to discover new fields or to apply new/existing technologies that enhance the recovery of oil in existing reservoirs. Typically, oil recovery from reservoirs is classified into three stages, namely primary, secondary, and tertiary recovery. Primary recovery includes oil production using the reservoir's natural energy. Secondary recovery normally occurs after primary recovery and provides assisted energy for further oil production. This recovery stage involves maintaining the pressure of the reservoir either by water flooding or gas injection. After both conventional recovery stages (i.e., primary and secondary recovery), a significant amount of oil is left in reservoirs. A good portion of the unflushed oil can be produced during the tertiary recovery stage, known as enhanced oil recovery (EOR) [12]. This stage deals with the injection of components or fluids not present in the reservoir (e.g., chemicals, gases, or heat energy).

EOR is often divided into four main classes: thermal recovery, miscible gas injection, chemical flooding (e.g., polymer flooding), and other methods [13] [14] [15]. The latter class includes non-mature EOR techniques and mostly comprises EOR processes under research and development, such as the injection of foam, microbial techniques, and mechanized/modified/smart water [15]. Common practices suggest that detailed screening criteria based on rock-fluid properties are utilized to select the most suitable EOR technique for the target reservoir [16] [13] [14] [15]. Further, financial constraints and economic analysis also play a vital role in the selection of a specific EOR technology.

1.1 From Water Flooding to Modified/Smart Water Injection

Water flooding is a widely accepted technique that has been used in oil reservoirs for decades to maintain reservoir pressure and hence improve oil recovery. Conventional water flooding uses either the produced formation brine or available water resources (i.e., back-produced water or seawater) for injection. However, for a long time, little attention has been paid to injected water chemistry and its compatibility with the rock-oil-brine system. To date, various recovery mechanisms have been proposed based on the chemical composition of injected water and its impact on rock-fluid interaction. One such mechanism, proposed by the British Petroleum (BP) company, is low-salinity water flooding (LoSal) [17]. Martin [18] made the first attempt to study the LoSal process (subsequently referred to as modified water injection) and concluded that the injection of water with a composition close to freshwater could improve oil displacement due to the presence of clay in the rock matrix. Gradually, many core flooding experiments and pilot tests validated his claims and thus confirmed the impact of chemically adjusted water flooding in sandstone reservoirs [19] [20] [21] [22]. In the 1990s, significant advancements were made in research on the possible effects of low salinity [23] [21] [24], and many recovery mechanisms involving modified water injection were proposed. Most mechanisms appoint a key role to change the reservoir rock wettability from oil-wet or mixed-wet to water-wet [25].

Modified water injection disturbs the established rock-oil-brine ionic equilibrium due to the role of active ions (also known as potential determining ions, PDI) and helps produce more oil. Morrow et al. [26] first proposed the concept of modified/smart water flooding, which led to further investigations of the impact of injected water composition on oil recovery. In a simple sense, modified water flooding involves either the addition of active ions/salts or the removal of inactive ions/salts from the injection brine. This addition or removal of specific salts changes not only the salinity but also the hardness of the brine. Among these active divalent ions, sulfate (SO_4^{-2}) is the most effective ion in both sandstone and carbonate reservoirs for the design of modified water [27]. The oil recovery mechanism from SO_4^{-2} is controlled by the ionic interactions taking place in the reservoir. Clay and quartz present in the rock matrix are negatively charged surfaces, and the negative polar compounds of the oil are attached to the rock surface with the divalent ions serving as a bridge (Ca^{+2} and Mg^{+2} present in formation brine), as shown in Figure 1.1(A) [28]. The positive polar compounds of the oil are attached to the negatively charged rock surfaces, and the created chemical bonds result in the oil-wetting condition of the sandstone reservoir. The negative polar compounds of the

oil are replaced by SO_4^{-2} through Ca^{+2}, Mg^{+2}, causing bridging of the rock surface and subsequently altering wettability towards a water-wet state [28], as illustrated in Figure 1.1(B). However, the wettability alteration process is catalysed if low-salinity modified water flooding is performed. Low salinity further dilutes the divalent cations in the formation brine, hence weakening the strength of the bonds.

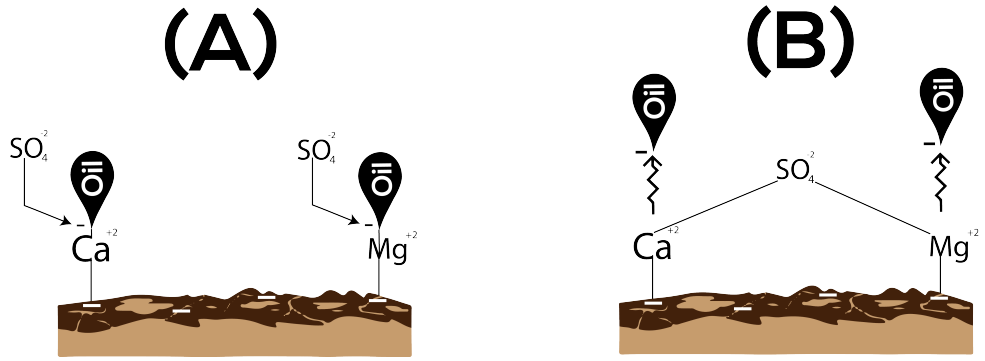

Figure 1.1: *Wettability alteration mechanism of SO_4^{-2} in sandstone. (A) refers to oil-wet; (B) refers to water-wet condition of reservoir*

Fluid-fluid interaction between oil and brine at the interface is another recovery mechanism responsible for additional oil recovery during modified/smart water flooding [29] [1] [30]. This interaction is developed at the oil-brine interface and results from the ionic activity between modified brine and oil polar compounds (asphaltenes and naphthenic acids) [31] [28] [32] [33]. However, this layer is sensitive to the salinity of injected brine. Mahzari and Sohrabi [34], Morin et al. [35], and Sohrabi et al. [36] demonstrated that low-salinity flooding produces a more stable and elastic surface at the oil-brine interface. For instance, Morin et al. [35] found that this stable layer is resistant to rupture and assists the continuous oil-phase transportation in porous media, hence contributing to higher oil recovery.

1.2 Polymer Flooding

Polymer flooding is a well-established tertiary recovery mechanism and mature EOR process. As water flooding has been adopted in most mature fields, adding polymers to the injected water costs less than other chemical EOR methods, which require, for instance, the use of surfactants. Polymer flooding has been the most widely used chemical EOR process since the 1960s [37]. As the mode of action, polymer increases viscosity in the injected aqueous phase, generating higher ultimate recovery due to improved mobility control and sweep efficiency [38]. Increasing the viscosity of the injected aqueous phase produces a favourable mobility ratio, M_R;

$$M_R = \frac{(\frac{k_{ra}}{\mu_a})}{(\frac{k_{ro}}{\mu_o})} \tag{1.1}$$

Subscript "a"= aqueous phase (polymer)

Subscript "o"= oil phase

where the numerator represents the displacing fluid (polymer) and the denominator refers to the displaced phase (oil). Polymer flooding improves the volumetric sweep efficiency due to a favourable mobility ratio, leading to late breakthrough and eliminating fingering effects.

1.2.1 Polymer Rheology

The rheological behaviour of polymer is a key factor not only for the design of the EOR technique but also for its economics and performance. Polymer injection is often designed based on a target viscosity (e.g., oil viscosity at reservoir conditions), and surface rheology is an excellent tool to predict and support this process. Polymer solutions are non-Newtonian, meaning the viscosity of polymer solutions is shear-rate dependent. A polymer solution can exhibit two types of viscosity—shear-thinning and shear-thickening viscosity. Shear thinning is observed with a decrease in shear viscosity with an increase in the shear rate, while shear thickening is observed with a proportional increase in shear viscosity with an increase in the shear rate. Two types of polymers, namely biopolymers and copolymers of acrylamide, are used in the petroleum industry. Biopolymers exhibit only shear-thinning response due to a rod-like molecular structure; however, hydrolysed polyacrylamide can exhibit both responses depending on the molecular weight and salinity of the brine. Note that the shear-thickening response it is commonly associated with viscoelasticity, which describes fluids (e.g., polymer diluted solutions) that exhibit elastic and viscous properties simultaneously [39] [5]. Polymers with high molecular weight used for EOR have been reported to have good viscoelastic response, with debatable acceptance [40] [5] [41] [11] [39].

Rheological measurements performed in the laboratory (using a rheometer) can predict the shear-thinning response of polymer solutions. However, these measurements cannot completely describe the shear-thickening response. One of the main reasons for this is a lack of representation of the pore structure, mainly the change in flow geometries causing interstitial velocity, which causes shear-thickening behaviour. The converging-diverging geometry of porous media produces the contraction and extension

of the polymer molecular structure and results in the shear-thickening response. Several authors have reported different ways to define and predict the shear-thickening behaviour of polymer used for EOR using either small amplitude oscillatory shear (SAOS), first normal stress difference (N_1), in-situ rheology, or elongational/extensional viscosity [5] [42] [40] [43] [44] [45] [46].

Elongational or extensional viscosity is often associated with shear-thickening behaviour during flow through porous media, hence helping with the further understanding of the flow dynamics of polymer solutions through porous media. These measurements include single-phase polymer flooding through core plugs/sand-packs, extensional measurements (e.g. eVROC®), and filament stretching devices [47].

1.2.2 Pilot Projects of Polymer Flooding

Polymer flooding has been performed in many pilot projects as a response to the poor sweep efficiency of water flooding. The application of polymer flooding is expected to result in additional oil recovery due to the higher aqueous viscosity of polymer. However, formation brine salinity is a major challenge for application of the process at a field scale. The higher salinity of formation brine significantly decreases polymer's in-situ viscosity and hence presents economic challenges for such projects [48] [49] [50]. These economic constraints motivate companies to perform low-salinity pre-flush to optimize the process. Water pre-flush is commonly used to decrease the salinity of the formation brine, which is expected to improve polymer flooding performance [51] [52] [53].

- A pilot study performed in Marmul Field (Oman) and reported by Koning et al. [54] describes polymer flooding with low salinity as a pre- and post-flush. The salinity of the formation brine was reported as 3 g/L, and low-salinity pre-flush/post-flush with 0.6 g/L NaCl brine was injected. A combination of polymer injection with pre- and post-flush resulted in 59% of stock tank oil initially in place (STOIIP).
- Wang et al. [55] presented pilot test data of the well-known polymer flooding (PO as pilot one and PT as pilot two) application in Daqing Field (China). The formation brine salinity was 7 g/L, and a pre-flush of low-salinity brine of 0.8–1.3 g/L was performed before polymer flooding (1000-ppm concentration of polymer). Interestingly, the produced water salinity was reported in concentrations of 2 g/L to 4 g/L. The combined oil recovery from pre-flush and polymer flooding increased by 14% (pilot one) and 11.6% (pilot two) compared to water flooding.
- Al-Qattan et al. [53] presented a single-well chemical tracer test (SWCT) per-

formed in one Wara producer of the Greater Burgan Field (Kuwait). The reported connate water salinity was 160 g/L TDS. Low-salinity brine (diluted SWCT chemicals) flooding was performed as SWCT Test #2. and low-salinity polymer injection was performed as SWCT Test #3. The associated reduction of residual oil saturation (S_{or}) was 7% from low-salinity pre-flush and low-salinity polymer flooding.

- Polymer flooding in the Adorf Field (Germany) was applied after a low-salinity pre-flush [54] with formation brine with an initial salinity of 250 g/L. In this case, polymer flooding did not contribute to the expected additional oil recovery. The main reason for the poor performance was a reaction between the injected low-salinity brine and the rock minerals. This reaction significantly increased the brine hardness, hence limiting the viscosity control and performance of the polymer flooding.

Observations from pilot projects support the hypothesis that pre-flush results in a reduction of formation brine salinity and additional oil recovery that is produced mainly through the viscosity-driven mechanism of polymer flooding. However, little attention has been paid to the pore-scale mechanism triggered by low-salinity pre-flush. Subsequent studies found that not only low salinity but also the chemical composition of injection water could lead to increased oil recovery.

Based on the latest research, it is uncertain whether it was only the polymer flooding process that contributed to the additional oil recovery in the pilot tests. It is assumed that a significant amount of oil was also recovered due to the wettability alteration actuated through the low-salinity brine flooding performed as a pre-flush. This assumption summarises the concept of combining two EOR recovery processes, also known as hybrid EOR, to contribute to significant additional oil recovery.

1.3 Combined EOR Mechanisms

The combined EOR mechanism can be defined as the combination of multiple EOR processes, also known as the hybrid EOR method. Different methods have been combined in the search for cost-effective EOR processes that could bring additional benefits to applications with possible capital and operating expenditures optimization.

Combined processes are expected to displace oil more efficiently compared to the application of a single technique due to multiple recovery mechanisms. For example, combining polymer flooding with other EOR techniques (e.g., alkali, surfactant or low salinity) has demonstrated positive effects on oil recovery [56] [7] [57] [58] [59]. The per-

formance of polymer flooding mainly depends on the ionic composition of reservoir brine [14] [47] [39]. The higher the ionic composition of the formation water, the more drastic the decrease in polymer viscosity, with this also negatively affecting its viscoelasticity [14] [5] [39] [41] [11]. As previously discussed, in practice, a reservoir is pre-flushed with low-salinity water to reduce the salinity of the reservoir brine and produce additional oil. Accordingly, polymer flooding after the low-salinity flooding is expected to lead to the recovery of even more oil. Diluted brine injection combined with polymer flood has been shown to increase recovery in sandstone core plugs [7] [59] [60]. However, the availability of low-salinity brine resources limits the application of this combined process. Further treatment of produced brine or seawater to prepare the low-salinity water requires initial investment and operational costs [61] [62]. These economical restrictions further motivate injecting modified water as a pre-flush for polymer projects. Modified water is accomplished by adding cheap and active salts/ions in the produced brine and seawater.

Similar to low-salinity brine, the combined recovery mechanism of modified/mechanized water in combination with polymer flooding is expected to produce higher oil recovery. Modified water alters the reservoir wettability (rock-fluid interaction) from an oil-wet to water-wet condition and detaches the oil polar compounds (asphaltenes and naphthenic acids). Modified water is also expected to produce fluid-fluid interaction between the detached oil and brine in parallel with wettability alteration to a water-wet state. Follow-up polymer flooding after modified water is expected to lead to the recovery of additional oil because of the improved mobility ratio [63] [58]. Thus, the combined process of both EOR techniques is expected to produce significant additional oil compared to only one EOR process. Moreover, the combined injection of modified water with polymer flooding has been commercially proposed as an economical EOR process. Modified brine is prepared by mixing low-cost and easily available salts/active ions in produced brine or seawater. Moreover, low-concentration polymer is prepared and injected after modified brine for mobility control. The low-concentration polymer solution directly reduces the cost of the polymer required.

In summary, modified brine can be prepared at low cost and can initiate rock-fluid (wettability alteration) and fluid-fluid interaction inside a reservoir to detach and produce oil polar compounds. Follow-up, low-concentration (low-cost) polymer will produce additional oil due to favourable mobility control and good viscoelastic properties.

1.4 Motivation

This work investigates the combination of two EOR methods (modified brine injection and polymer flooding), known as the hybrid EOR method, to enhance the capability of the flooding process. Particular attention is given to the presence of sulfate in the injection brine as a key parameter for comparison and optimization.

This work focuses on describing the flow behaviour of oil recovery from the injection of sulfate-modified/low-salinity water in combination with polymer. It provides a detailed microscopic visualization and macroscopic observations of the displacement taking place during modified water flooding at a pore-scale level while evaluating the effect of wettability on oil recovery. A comprehensive workflow for the evaluation is proposed that includes fluid-fluid and rock-fluid interactions. On one hand, polymer flooding is expected to improve the macroscopic sweep efficiency due to a favourable displacement mobility ratio. On the other hand, modified water will affect the microscopic sweep efficiency by triggering fluid-fluid and rock-fluid interactions. Hence, the hybrid process is expected to provide the combined benefits of both EOR methods.

Modified water injection as a pre-flush is expected to change the reservoir wettability from oil-wet to water-wet and change the fluid distribution in the reservoir. Detached oil droplets are expected to move from small pores to large or medium pores. Polymer flooding after modified brine is expected to produce the redistributed oil phase easily due to improved sweep efficiency. Low-concentrations polymer solutions will be required for combination with a pre-flush of modified water, which will decrease the cost of EOR projects.

1.5 Scope of the Study

The main objective of the study is to investigate the synergies and benefits of modified water injection combined with polymer flooding. The role of sulfate to disturb the established ionic equilibrium in the reservoir (rock-oil-brine) is investigated with various injection brine recipes. Follow-up low-concentration/viscosity polymer flooding in the tertiary mode is investigated to propose a cost-effective hybrid EOR process. An experimental investigation is performed to study the possible rock-fluid and fluid-fluid interactions of the modified water and the viscoelastic response of diluted polymer solutions. Further, this study provides clear insights on the dominant recovery mechanism of the rock-fluid and fluid-fluid interactions directing different porous media (i.e., Bentheimer core plugs and glass-silicon-glass micromodels). Further, the impact of sulfate,

brine salinity, and hardness are investigated on polymer viscoelastic properties by performing single-phase core flooding. The scope of this study is summarised in the following objectives:

- Assess the modified water design, focusing on the injection of brines with low salt compounds ($\leqslant 5g/L$).
- Investigate the modified water design based on the presence of sulfate using synthetic seawater composition ($\approx$ 42 g/L).
- Evaluate and define the synergies and benefits of the hybrid EOR process, which comprises modified water injection combined with polymer flooding.
- Appraise the visualization of the displacements taking place in micromodels during various brine flooding while evaluating the effect of wettability on oil recovery.
- Evaluate, compare, and investigate modified water flooding using experimental data, including fluid-fluid and rock-fluid interactions, to understand the dominant recovery mechanism.
- Determine the impact of sulfate and evaluate the influence of semi-harsh conditions (i.e., salinity, hardness, and temperature) on polymer viscoelastic properties during polymer flooding.
- Perform basic economic analysis of the preparation of modified water and low-salinity brine for the project.

1.6 Outline of the Thesis

This work is presented in ten (10) chapters. The first two chapters are an introduction and literature review, and the final chapter is the conclusion. The other chapters describe the scope of the study (objectives) and provide an outline to answer open questions. Figure 1.2 summarises the outline of the thesis. Note that a majority of the data presented in the chapters have been published either in conference or journal pre-review papers.

The objectives of the study are addressed and presented in the following chapters.

Chapter 2: State of the Art and Literature Review

This chapter briefly introduces the evolution of the water flooding process and the development of modified/smart water technology. It also summarises the proposed recovery mechanisms of low-salinity and modified water flooding, as well as the role of

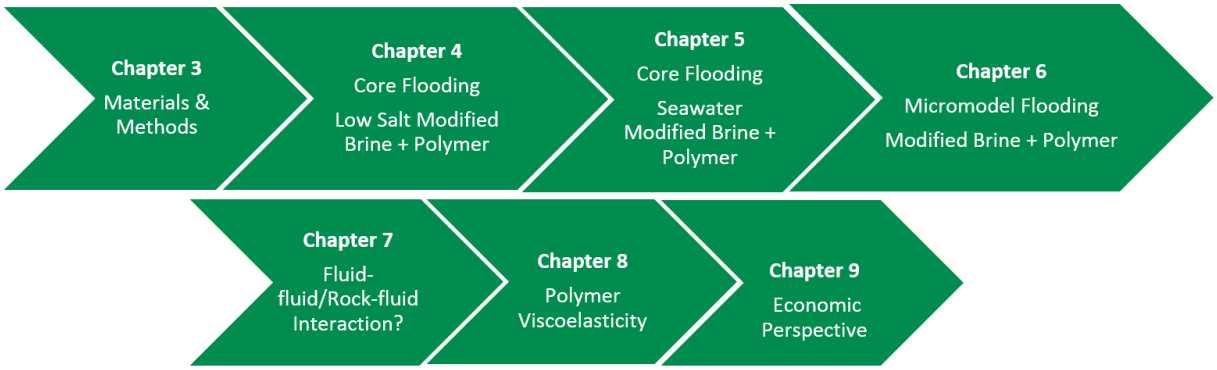

Figure 1.2: *Overview of Thesis Outline*

active ions in designing the injection water recipe. Moreover, it summarises the hybrid/-combined EOR investigation performed to provide an understanding of the importance of multiple combined EOR processes.

Chapter 3: Materials, Methods, and Experimental Setup

This chapter presents the chemicals used to prepare different brine recipes, the dead oil samples, and porous media utilized for flooding experiments. Further, it briefly describes the experimental setup as well as the steps adopted to perform the experimental investigation.

Chapter 4: Modified Low-salinity Flooding Combined with Polymer Flooding

This chapter compares oil recovery factors and pressure data for low-salinity brine flooding, low-salt sulfate-modified water injection, and polymer flooding in the secondary stage into oil-wet Bentheimer core plugs. Moreover, a comparison is drawn for the application of low-salinity and modified water flooding between secondary- and tertiary-mode flooding scenarios to select the optimum injection scheme.

Chapter 5: Modified Seawater Flooding Combined with Polymer Flooding

This chapter investigates the approach of utilizing synthetic seawater to design modified water from oil-wet Bentheimer core plugs. It describes the impact of injection brine composition on fluid-fluid interaction, focusing on the oil drop snap-off volume and static interfacial tension. The chapter also describes the wettability alteration achieved by the aging process of Bentheimer core plugs.

Chapter 6: Sulfate-modified Sea Water Flooding in Micromodels

This chapter presents a visual analysis of images obtained during brine floods to validate the oil recovery results obtained from core plugs investigated in Chapters 4 and 5. Two types of micromodel chips and three types of wettability are investigated to

understand the recovery mechanism based on fluid-fluid and rock-fluid interactions.

Chapter 7: Comparative Investigation of Modified Water Injection

This chapter provides a comparative analysis of the results obtained in Chapters 4 through 6. This comparison helps to conclude that the primary recovery mechanism of low-salt and modified water injection is either wettability alteration or fluid-fluid interaction. Further, this chapter describes the limitations of micromodels compared to core floods, focusing on rock-fluid interaction.

Chapter 8: Polymer Viscoelastic Properties

Chapter 8 investigates polymer viscoelastic properties using single-phase polymer flooding in Bentheimer core plugs. Investigation parameters are salinity, hardness, and temperature as well as the presence of sulfate in the mixing brine of polymer solutions.

Chapter 9: Economic Perspective Analysis

This chapter provides a fundamental economic analysis and compares the different brine recipes, focusing on capital investment and operational costs required versus the recovery factor obtained.

Chapter 10: Conclusions

This chapter summarises the present study and the key findings of the considered work.

Chapter 2

State of the Art and Literature Review

This chapter describes the evolution of the water flooding technique from its beginning to the present use of modified water flooding. Further, it discusses the role of active ions and the previously proposed concept of potential determining ions (PDI) and non-potential determining ions (non-PDI) to assess its possible contribution to additional oil recovery. Subsequently, the chapter addresses the main recovery mechanisms of modified water and polymer flooding to clarify the pore-scale mechanisms of the hybrid EOR process. Moreover, it concisely presents the hybrid EOR process that combines modified injection with polymer flooding based on previous investigations.

2.1 Salinity Aspects during the Water Flooding Process

Water-quality control is an important aspect of process applications, mainly from the operational point of view [64]. Quality control leads to better results when the water flooding process is applied for the purpose of enhanced oil recovery. Martin [18] first observed an increase in oil recovery using low-salinity water in sandstone reservoirs. Subsequent studies found that not only low-salinity water flooding but also chemically modified/smart water flooding can lead to increased oil recovery. Some researchers have used the terms low salinity and smart water synonymously [65].

Low salinity involves the dilution of injected water (i.e., seawater/produced brine) with fresh water to reduce the total dissolved solids (TDS) [66] [67]. This reduces the

ionic strength of the injected water but the hardness may remain the same. On the other hand, smart/modified water involves manipulating the ionic strength (hardness) of the injected water [68]. This manipulation is aimed at disturbing the established rock-oil-brine ionic equilibrium, which could result in optimum oil recovery by improving the microscopic displacement efficiency. Hence, the hardness of injected water is also manipulated by the ionic concentration.

In a simple sense, modified water flooding involves either the addition of active ions/salts or the removal of inactive ions/salts from the injection brine. This addition or removal of specific salts changes not only the salinity but also the hardness of the brine [69]. Morrow et al. [26] first proposed the concept of smart water, which led to later investigation of the impact of injected water composition on oil recovery [17] [70] [71] [72] [24] [73] [22] [27]. Chemically modified water flooding has been studied as an enhanced oil recovery technique through sandstone core plugs and field tests [74] [75] [19] [1] [68] [76]. Modified water flooding has received significant attention as an EOR technique due to its low cost and environmental friendliness compared to other EOR methods. Modified water is created through the manipulation of injected brine chemistry [74] [77] [75] [78]. This manipulation includes the removal of specific inactive ions/salts as well as the addition of some active ions/salts. The modification of injected brine's salinity and hardness establishes rock-fluid and fluid-fluid interactions in the reservoir and initiates the various recovery mechanisms responsible for higher oil production.

2.1.1 Recovery Mechanisms of Low Salt and Modified/Smart Water

Smart water flooding and low-salinity flooding have common recovery mechanisms, namely wettability alteration [79] [80] [81] [82], multicomponent ion change (MIE) [19], clay swelling [79] [19] [80] [82], change in pH value [75] and fluid-fluid interaction at the oil-brine interface [31] [83] [84]. However, this research mainly focuses on the investigation of wettability alteration and the interfacial mechanism at the fluid interface. Both mechanisms are based on the ionic activity among the injection brine, formation brine, oil polar compounds, and rock matrix. The expectation is that modified water injection disturbs the established rock-oil-brine ionic equilibrium due to the role of active ions (potential determining ions, PDI), helping to produce more oil.

Wettability Alteration

Wettability alteration of the reservoir from an oil-wet to water-wet state is a well-established recovery mechanism of low-salinity/modified water flooding, as many studies have reported [79] [80] [81] [82]. The injection of modified water disturbs the established rock-oil-brine ionic equilibrium, which, in turn, releases the oil polar compounds attached to the rock surface. The detachment of oil compounds causes wettability alteration from oil-wet to water-wet. According to information reported in the literature [28] [69] [67], the basic requirements for the successful application of either process, low-salinity or smart water flooding, are similar. The following are requirements for wettability alteration of rock formations from an oil-wet to water-wet state to be the primary oil recovery mechanism:

- Reservoir rock should be oil-wet/intermediate-wet [22] [67] [25]

  In an oil-wet/intermediate-wet state, oil polar compounds are attached to the rock surface through ionic interactions. Low-salinity/modified water flooding targets these polar compounds, detaching them from the rock surface, as shown in Figure 1.1, and hence producing additional oil recovery through wettability alteration from oil-wet/intermediate-wet to water-wet.

- Existence of polar compounds in the oil [31] [83] [84]

  Polar compounds are mainly composed of asphaltene and naphthenic acids (NAs) and act as surface active compounds. These two surface active compounds are known not only to stabilize water-in-crude oil emulsions but also to constitute the interfacial film at the fluid-fluid interface. Asphaltene is insoluble in low molecular weight alkanes (n-heptane or n-pentane) but soluble in aromatics (toluene). The interfacial viscoelastic layer at the brine-oil interface is produced due to the slow and irreversible adsorption process of asphaltene at the fluid interface [85] [86] [87]. Acevedo et al. [88] described the positive effects of asphaltene to develop the oil-brine interface's rheological properties. Another fraction of crude oil is NAs which are composed of cycloaliphatic carboxylic acids (R-COOH) [84] [89]. These NAs are hydrophilic compounds and are accumulated at the oil-brine interface. Further, NAs can also dissociate in the aqueous phase and reach cations present in the brine to form naphthenic salts. These salts can accumulate at the oil-brine interface. However, the role of NAs remains uncertain because some studies claim that NAs improve oil-brine interface elasticity [84], while others claim they soften the interfacial film [90].

- High content of divalent cations in the formation brine [17] [91]

Divalent cations provide the bridging connection between oil polar compounds and rock surfaces. Mainly, Ca^{+2}, Mg^{+2} play a significant role to create a bond, as shown in Figure 1.1.

In addition, contrary to previously reported cases, recent research has proposed that the presence of clay is not important for wettability alteration from an oil-wet to water-wet condition [29].

Oil-Brine Interfacial Interactions

Some authors have proposed the role of fluid-fluid interfacial interactions as a recovery mechanism other than wettability alteration [29] [1] [30]. They claim that wettability alteration cannot be the only factor in low-salinity/smart water flooding contributing to high oil recovery [29] [1] [30]. Therefore, another parameter that plays an important role in modified water flooding is the interfacial interaction between the brine and oil phases (fluid-fluid interaction).

These properties are static interfacial tension as well as dynamic interfacial rheology caused by ionic interfacial interactions at the fluid interface [92] [31]. Additionally, in recent years, a great deal of research has investigated the role of interfacial rheology (dynamic interface response) in the brine-oil system, as presented in Figure 2.1 [1] and in Figure 2.2 [2].

Figure 2.1 reports the impact of sulfates on brine-oil interfacial elastic moduli, viscous moduli, and viscoelasticity. Figure 2.1 summarises that three times and five times higher (spiked) sulfate (3S and 5S) in seawater results in the highest response of viscoelasticity and viscous and elastic moduli. Similarly, Figure 2.2 shows the impact of sulfates on elastic moduli. Figure 2.2 shows that Na_2SO_4 results in the highest elastic moduli over time (hours) at the oil-brine interface compared to $NaCl$ and $CaCl_2$.

From the results in Figure 2.1 and Figure 2.2, it can be concluded that the spiked amount of sulfate improves the oil-brine interfacial interaction. Mohamed and Alvarado [1] reported that 3S and 5S brine produced optimum interfacial viscoelasticity. Improved dynamic stability forms a mechanically stable interfacial surface at the brine-oil interface and prevents snap-off oil droplets. Further, detached oil compounds develop liquid-liquid interaction with modified water to develop a stable layer at the interface [68] [93]. Some researchers believe the formed fluid interface (oil-brine) is the main recovery mechanism other than wettability alteration [29] [30] [33].

In light of these findings, ionic manipulation plays a key role in developing inter-

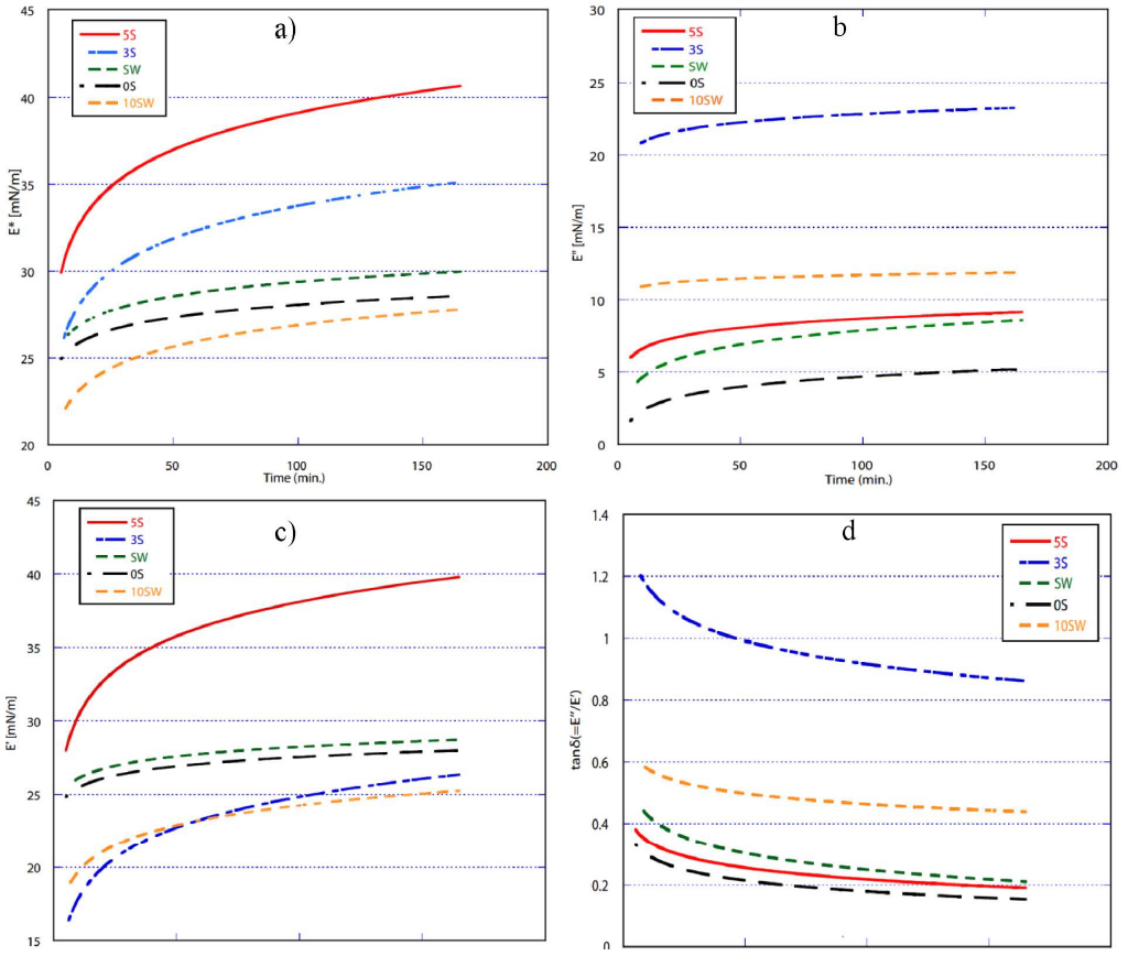

Figure 2.1: *Interfacial a) viscoelasticity b) viscous and c) elastic moduli; d) tanδ (=E"/E') for crude oil and five brines with different concentrations of sulfate ions in seawater. Adapted with permission from [1]. Order License ID:101369-1*

facial interaction between brine and oil (fluid-fluid interaction). Studies show that the interfacial film forms when the NAs and asphaltene present in crude oil and divalent ions in the aqueous phase accumulate at the interface [32] [33]. However, this layer is sensitive to brine salinity and forms a more stable layer under low-salt brines. According to Mohamed et al. [1], sulfates improve interfacial rheology between the two phases, resulting in higher oil recovery. In other words, from a fluid-fluid interaction point of view, sulfates could improve the stable interface resulting in oil-phase snap-off suppression and increase the oil drop size [3] [1] [93]. The fluid-fluid interaction is developed at the interface between the oil polar compounds and ions present in the brine forming a layer. The layer assists in transporting the continuous oil phase and resists the oil snap-off, hence producing more oil [35].

While the above-described studies of both recovery mechanisms—wettability alteration and fluid interfacial interactions—provide valuable information, the role of the main recovery mechanism of these two remains uncertain and needs to be investigated.

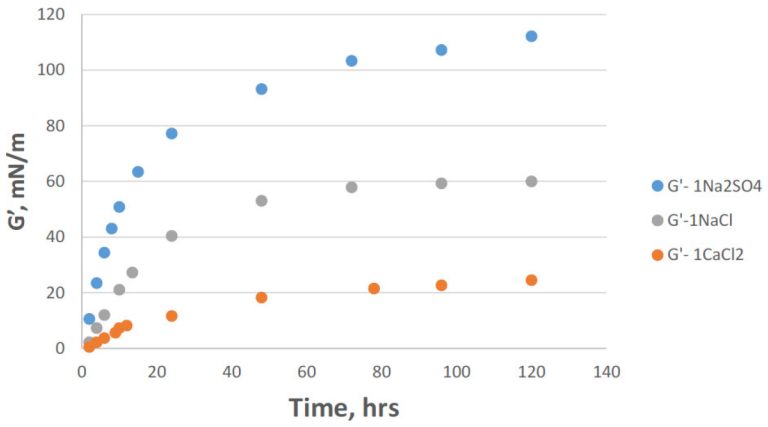

Figure 2.2: *Elastic modulus for crude oil and different brines with the same ionic strength. Adapted with permission from [2]. Order License ID:101369-2*

2.1.2 Sulfate as the Effective Potential Determining Ions (PDI)

Multivalent ions play a significant role in designing effective modified water. Therefore, most laboratory studies have investigated the impact of spiked SO_4^{-2}, Ca^{+2}, Mg^{+2}, BO_3^{-3} and PO_4^{-3} on oil recovery [94] [69] [93] [27]. These ions are called potential determining ions (PDI) [22]. Due to their high ionic charge, these ions disturb the established ROB ionic balance and cause the release of polar oil compounds. In other words, PDI catalyses the fluid-fluid and rock-fluid interaction process inside the reservoir. One important aspect is that among these PDIs, sulfate SO_4^{-2} has proven to be the most effective for application in sandstone and carbonate reservoir rock [1] [27] [22].

Mohamed and Alvarado [1] investigated sulfate as a key parameter to design a smart water recipe for Berea sandstone core plugs, as shown in Figure 2.3. In Figure 2.3, x-axis represents the composition of injected brines. The first brine, 0S, represents seawater without sulfates, and the second brine, SW, is the base reference seawater. The third and fourth brines, 3S and 5S, represent three times and five times increased sulfate (spiked amount) in seawater. The last brine, 10SW, depicts ten times diluted seawater. The last three brines produced the highest oil recovery; however, 3S and 5S brine showed promising results for oil-brine interfacial viscoelasticity, according to the authors. Therefore, the amount of sulfate to be added in the modified water is a critical factor in the effective flooding process.

The wettability alteration process in sandstone reservoirs (clay and quartz) by a spiked (increased) amount SO_4^{-2} is summarized in Figure 1.1. A spiked (increased) amount of SO_4^{-2} in injected brine disturbs the ionic equilibrium of the system, resulting in the replacement of negative oil polar compounds with SO_4^{-2} through Ca^{+2} and Mg^{+2} bridging the rock surface. Thus, oil polar compounds are released, and SO_4^{-2} is attached

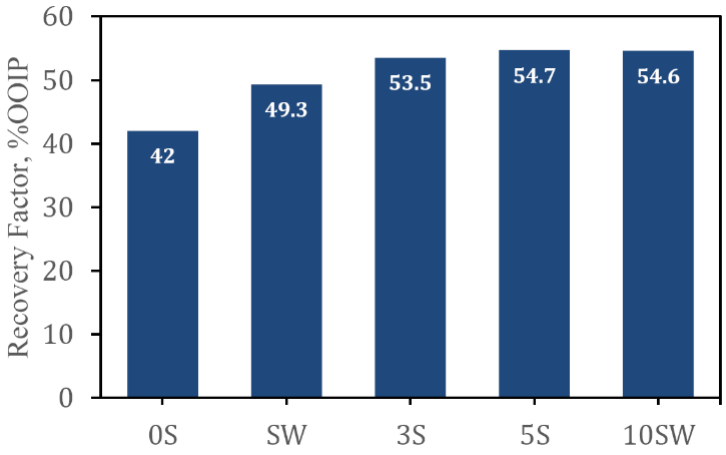

Figure 2.3: *Oil recovery factor as a function of the amount of sulfates in injection brines. Adapted with permission from [1]. Order License ID:101369-1*

to the rock surface through ionic bridging, resulting in a water-wet rock surface.

Nevertheless, a higher concentration of sulfate can be problematic when there are significant amounts (supersaturation) of divalent cations (Ba^{+2}, Sr^{+2} and Ca^{+2}) in the formation water. Due to supersaturation and chemical reactions, precipitation of $CaSO_4$, $BaSO_4$ and $SrSO_4$ can occur. If the reservoir temperature is high enough, then this scaling issue can be even worse compared with lower temperatures, as high temperature enhances the precipitation process [95] [96]. This process, in turn, will cause major injectivity issues due to the generated formation damage and pore plugging around the wellbore [97] [98] [99]. Precipitation and pore-plugging problems challenge the efficiency of sulfate-modified water injection and can make any project uneconomical. Recently, Ghosh et al. [98] studied the prediction of precipitation formation using a simulation technique and presented scale control methods.

Similarly, monovalent ions have no significant impact on additional oil recovery and are defined as non-PDI (Na^{+1} and Cl^{-1} and K^{+1}). Thus, monovalent ions should be either removed or diluted to design the modified water. To enhance the wettability alteration of rock formations from oil-wet to water-wet, some researchers have proposed decreasing the Na^{+1} concentration in the injected water to design optimum modified water for the target reservoir system [3]. Figure 2.4 and Figure 2.5 show the impact of decreasing the amount of non-PDI (Na^{+1}) and increasing the amount of PDI sulfates (SO_4^{-2}) in injection brines [3]. The results shown in Figure 2.4 and Figure 2.5 indicate that increasing the amount of SO_4^{-2} and decreasing the amount Na^{+1} produces higher cumulative oil recovery. However, pore volumes injected to achieve oil recovery from core plugs are less realistic compared to field-scale applications. Therefore, oil recovery obtained below 5PV injected is relevant, focusing on the field-scale application.

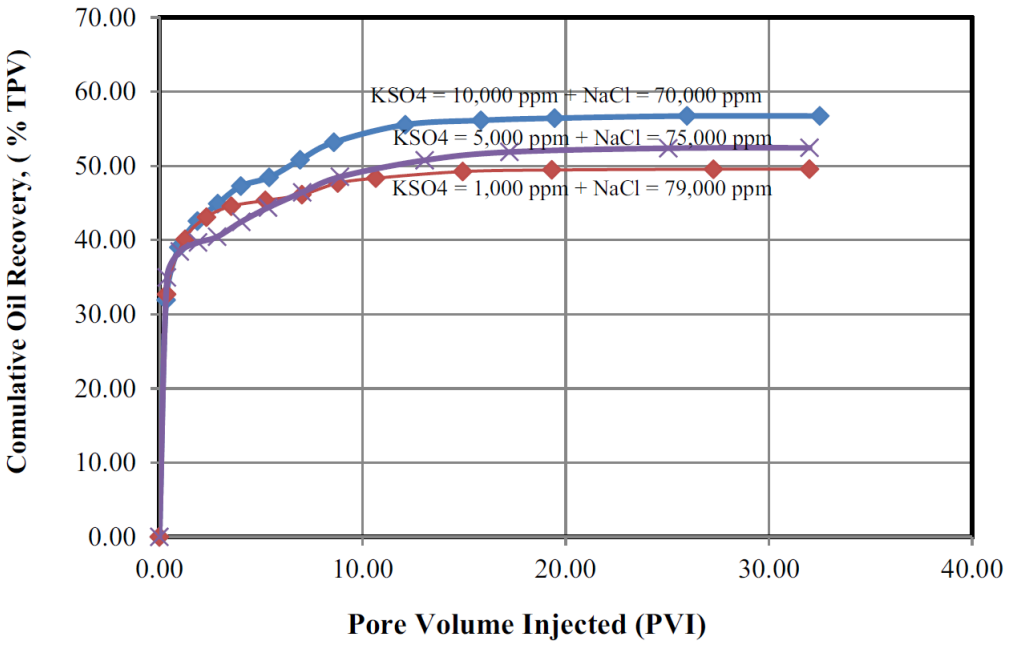

Figure 2.4: *Oil recovery factor as a function of the amount of Potassium Sulfates in injection brines [3]. Permission under Creative Commons Attribution-NonCommercial-No Derivatives License*

Turning to recent research on designing smart/modified water, mostly spontaneous imbibition experiments and fluid interfacial measurements have been performed to investigate the impact of sulfates [94] [28] [98] [1] [3] [100] [31]. A selected number of published experiments have been performed using core flooding and sand-pack [29] [78] [100] [74] [75] [101]. Some authors have proposed wettability alteration as the main recovery mechanism while others have proposed fluid-fluid interaction at the interface. The presented research is clear evidence an investigation be made to assess whether the dominating recovery mechanism of spiked SO_4^{-2} is wettability alteration or fluid interfacial interactions.

2.2 Recovery Mechanisms of Polymer Flooding

A significant amount of remaining oil saturation is left in the reservoir due to the poor sweep efficiency of brine flooding [102] [103] [14]. Hence, polymer flooding is performed to recover the unswept and distributed oil saturation remaining. The literature [104] [5] has reported many recovery mechanisms of polymer flooding, for instance, viscous fingering reduction [105], relative permeability reduction [58], pull-out in dead-end pores [106], stripping from oil-wet surfaces [107], enhanced flow between heterogeneous layers [14] [58], shear thickening [5], and elastic turbulence [108]. However, all of the mentioned recovery mechanisms are associated with polymer's improved mobility ratio and

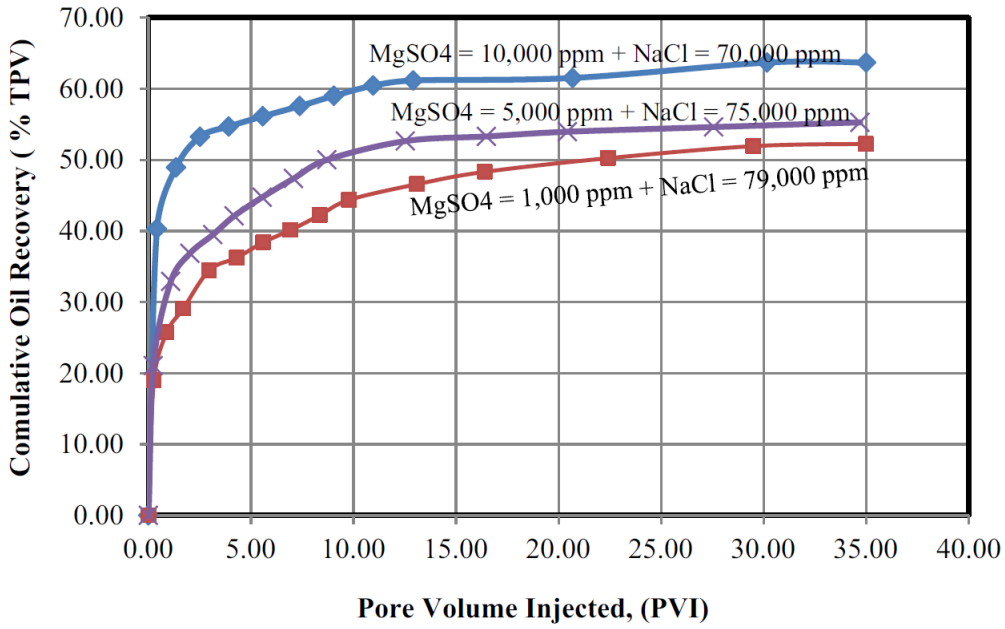

Figure 2.5: *Oil recovery factor as a function of the amount of Magnesium Sulfates in injection brines [3]. Permission under Creative Commons Attribution-NonCommercial-No Derivatives License*

its viscoelastic properties.

2.2.1 Mobility Control

Polymer increases aqueous phase viscosity and hence improves the sweep efficiency of the reservoir [109] [52]. The main recovery mechanism of polymer flooding is improved mobility control, as defined in Equation 1.1, in the porous media to produce a uniform displacement front and hence improve oil bank recovery. However, mobility control of the polymer solution is challenged by the salinity of formation brine. This limitation is encountered in multiple approaches, as outlined in the following:

- Polymer solutions are prepared in high concentrations to overcome the effects of formation brine salinity. There is a decrease in polymer in-situ viscosity, but high concentrations of polymer solutions can sweep the reservoir to contribute to additional oil recovery. On a commercial scale, high-concentration polymer flooding was performed in the Daqing Field and produced 20% original oil in place (OOIP) [110]. Field tests concluded that high-concentration polymer injection is safe and commercially economical.
- A couple of pilot tests and many laboratory experiments have concluded that low-salinity pre-flush can be performed to decrease the salinity and hardness of

formation brine [111] [51] [55]. Polymer flood after the pre-flush is expected to have suitable in-situ polymer viscosity, hence contributing to higher oil recovery.

- Recently, the concept of the hybrid EOR method using combined low-salinity water flooding with polymer flooding has also shown promising results for oil recovery [7] [53]. Low salinity also decreases the salinity of formation brine in a similar manner as pre-flush and polymer flooding afterward retains good mobility control.
- Mixing polymer solutions in low-salinity water is also an effective approach to handling harsh conditions for reservoir brine [112] [113] [60]. This method produces high-viscosity polymer solutions utilizing the lower concentrations of the polymer product.

The presented information is good evidence of the dependence of polymer mobility control on formation brine and will thus be advantageous for investigating the role of modified water injection as pre-flush for polymer flooding.

2.2.2 Polymer Viscoelasticity

Hydrolysed polyacrylamides (HPAMs) are the most widely used polymers in the oil industry due to their low cost and commercial availability [114]. Some HPAM polymers with high molecular weight have viscoelastic properties, behaving like a solid or liquid depending on interstitial flow conditions. Due to viscoelasticity and their non-Newtonian nature, HPAMs may depict shear-thinning behaviour at low shear rates and shear thickening behaviour at medium-high shear rates [4] [5]. Shear-thinning behaviour is defined as a decrease in shear viscosity as the shear rate increases, while shear-thickening behaviour is an increase in shear viscosity as the shear rate increases, as depicted in Figure 2.6 and Figure 2.7.

Shear-thickening behaviour also depends on the relaxation time of polymer when it flows through converging-diverging geometry (elongational viscosity) [5]. Various authors have asserted that HPAMs increase displacement efficiency due to their elastic properties [103] [115] [116]. Thus, recovery efficiency, which is a product of displacement efficiency (E_D) and volumetric sweep efficiency (E_V), is increased by viscoelastic HPAM polymer flooding.

$$E = E_D * E_V \tag{2.1}$$

Viscoelasticity of HPAMs used for EOR is restricted by various factors, such as:

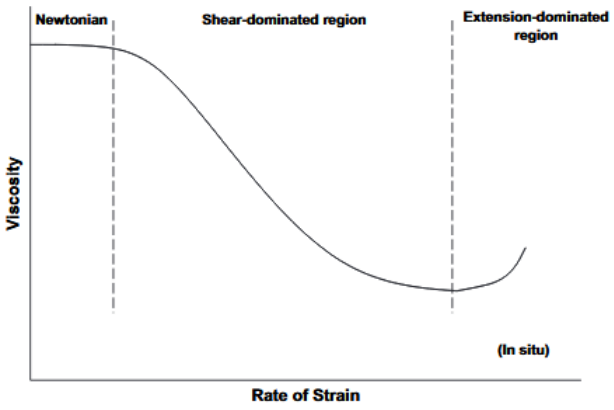

Figure 2.6: *Viscoelastic flow with shear-thinning region and shear-thickening region. Adapted with permission from [4]. License Nr.:4750180422492*

- Degradations caused by mechanical shear and chemical reactions [117] [118] [119]

  Mechanical shear is caused during polymer solution preparation through mixing devices, injection pumps, flow lines, and valves from storage tanks to injection wells. Chemical degradation is caused by a chemical reaction. For example, the polymer may be sensitive to oxygen and thus oxygen scavengers are added to the solution.

- Reservoir temperature [120] [47] [121]

  Polymer solutions are sensitive to temperature. High temperature causes breakdown of the molecular backbone chain structure, which, in turn, decreases polymer viscoelasticity.

- Hardness of the water (brine) in the reservoir [122] [47]

  Hardness is the amount of cations in the brine. A high amount of cations will result in low polymer viscosity. Polymer's ball-like molecular structure is composed of negative charges, and the repulsive forces of negative charges result in a larger ball-like molecular structure. High concentrations of cations react with the negative charge of polymer, hence decreasing the ball-like molecular size. A reduction in molecular size results in the loss of polymer viscosity and hence also reduces viscoelasticity.

These conditions place a strain on project economics as they negatively affect polymer performance [123] [124]. Surprisingly, however, until recently, a majority of the research has neglected the impact of sulfates/modified brine as pre-flush on polymer viscoelastic properties.

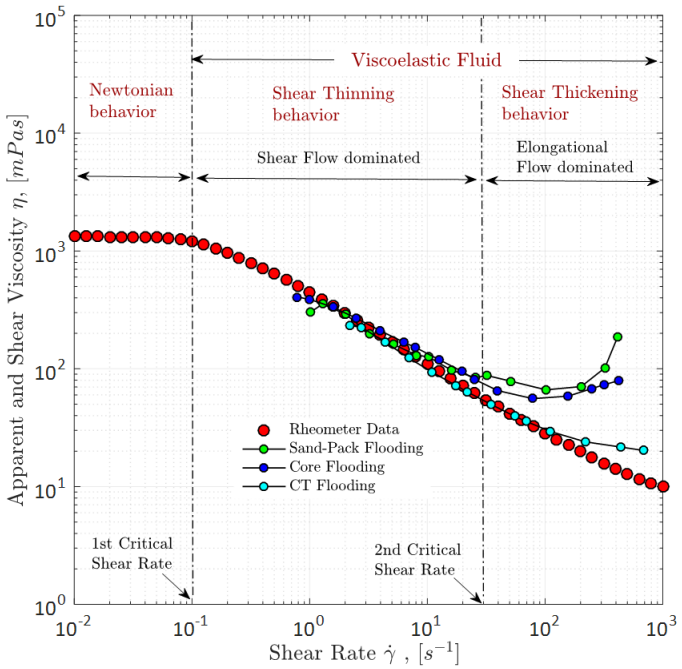

Figure 2.7: *Graphic illustration of viscoelastic flow behaviour [5] [6]*

2.3 Combined EOR Processes

Modified water with an increased amount of sulfates, combined with other EOR methods, is expected to produce additional oil recovery due to multiple recovery mechanisms. Similarly, the combination of polymer flooding with other EOR techniques has demonstrated positive effects on oil recovery [56] [7] [57] [58] [59]. Figure 2.8 presents the impact of the hybrid/combined EOR process of low salt combined with polymer flooding on the reduction of remaining oil saturation [7]. Figure 2.8 depicts low-salinity flooding in the secondary stage and low-concentration polymer (300 ppm) flooding in the tertiary mode. A significant amount of oil is produced through the hybrid EOR method.

A potential benefit of the hybrid EOR method is the role of multiple recovery mechanisms in enhancing the capability of the flooding process. Further, this technology can be used for a proposed commercially economical EOR method. During the combined EOR flooding process, low-viscosity/concentration polymers are injected after the modified water [7] [93]. However, recovery factors obtained are promising compared with high-concentration polymer flooding alone. Moreover, small concentrations of polymer in the hybrid method also reduce the potential environmental risks.

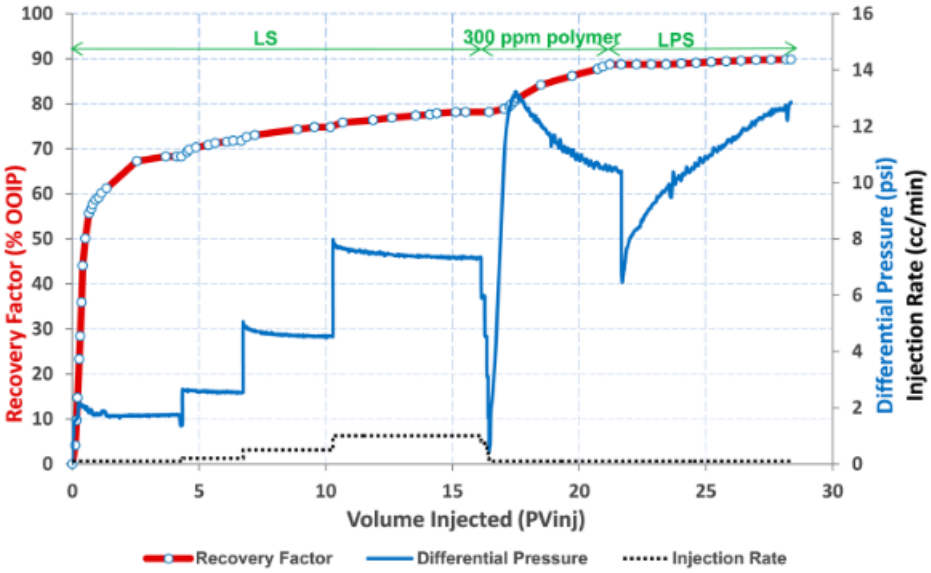

Figure 2.8: *Oil recovery factor, pressure profile, and injection rate as functions of injected volume during hybrid lowsalt and lowsalinity-polymer injection for intermediate-wet core. Adapted with permission from [7]. Copyright (2020) American Chemical Society*

Chapter 3

Materials, Methods, and Experimental Setup

This chapter describes the chemical composition of brines utilized for the flooding experiments conducted to design optimized sulfate-modified water for sandstone reservoirs. Moreover, it presents two types of porous media used with petrophysical rock characteristics. Further, it explains in detail approaches used to investigate rock-fluid interaction (contact angle) and fluid-fluid interaction (static interfacial intention and oil drop snap-off volume). The chapter also documents the experimental set-up adopted to perform the flooding experiments, as well as the preliminary procedural steps. Concise details of the methodologies used for the preparation of polymer diluted solutions with the required viscosity are also a vital part of this chapter.

3.1 Fluids

3.1.1 Brines

Different salt components are mixed with deionized water to prepare brines. Four groups of brines (BG1, BG2, BG3, and BG4) were prepared for this study. The brines were filtered through a 0.2-μm millipore filter by applying 2.0 bar of N_2 pressure to avoid any undissolved components.

Table 3.1: *Chemical composition of brines (formation, injection, and polymer preparation brines)*

Chemical Formula	Units	Total Dissolved Solids (g/L)											
		BG1		**BG2 ($\leq$ 5g/L): Chapter 4, 6 and 7**		**BG3 ($\approx$ SSW g/L): Chapter 5, 6 and 7**				**BG4 : Chapter 8**			
		Formation Brines		**Injection Brines**						**Single-phase Polymer Flood**			
		Brine 1	**Brine 2**	**Brine 1**	**Brine 2**	**Brine 3**	**Brine 4**	**Brine 5**	**Brine 6**	**Brine 7**	**Brine 8**	**Brine 9**	**Brine 10**
	g/L	SSW	2*SSW	SSW	DSSW	DSSW + $2SO_4^{-2}$	SSW + $2SO_4^{-2}$	SSW + $4SO_4^{-2}$	SSW - Na	SSW2	GB	SSW	SSW + $4SO_4^{-2}$
$NaCl$		23.97	47.94	23.97	2.397	2.39	23.97	23.97	0	27.4	34.3	23.97	23.97
KCl		0.8	1.6	0.8	0.08	0.08	0.8	0.8	0.8	0.77	0.29	0.8	0.8
$CaCl_2.2H_2O$		1.11	2.21	1.11	0.111	0.11	1.11	1.11	1.11	1.5	13.7	1.11	1.11
$MgCl_2.6H_2O$		11.04	22.08	11.04	1.104	1.1	11.04	11.04	11.04	10.8	10.9	11.04	11.04
$SrCl_2.6H_2O$		0.03	0.05	0.02	0.003	0.003	0.03	0.02	0.02	0	0	0.03	0.02
Na_2SO_4		3.93	7.86	3.93	0.393	0.78	7.86	15.73	3.93	0	0	3.93	15.73
$NaHCO_3$		0.27	0.55	0.27	0.027	0.02	0.27	0.27	0.27	0	0	0.27	0.27
TDS		41.15	82.31	41.15	4.12	4.5	45.09	52.95	17.18	40.47	59.19	41.15	52.95
Hardness		0.13	0.13	0.13	0.13	0.11	0.11	0.09	0.48	0.13	0.27	0.13	0.09
Density (g/cm^3) @22°C		1.03	1.04	1.03	0.98	0.99	1.02	1.04	1.02	1.03	1.05	1.03	1.04
η (mPa.s) @45°C		0.63	0.7	0.63	0.67	0.67	0.68	0.68	0.65	0.63	0.69	0.63	0.68

The first group (BG1) was used to evaluate the effects of hardness and the amount of divalent cations present in the formation brine. In other words, this group provided a comparison based on the formation brine composition to design effective sulfate-modified water for the target reservoir. $2{*}SSW$ represents the doubled amount of salts of synthetic seawater used to prepare the brine. The second group of brines (BG2) was prepared to design a low salinity sulfate-modified water based on sulfates. The brine composition was optimized using synthetic seawater (SSW) as a base brine. Brine optimization was achieved by diluting (in freshwater) the SSW-brine (DSSW) and SSW with the doubled sulfate amount to a tenth of its initial concentration (DSSW + $2SO_4^{-2}$). The objective was to keep the total dissolved solids $\approx 5g/L$ to investigate the impact of low-salt brine and low-salt sulfate-modified water injection. The third group of brines (BG3) was designed to optimize the modified water recipe with total dissolved solids of $\approx 42g/L$ (equal to seawater). SSW was used as the base brine and, therefore, was a benchmark. Brine optimization was performed by the addition of sulfates or removal of sodium ions. Table 3.1 describes in detail the brines used. $SSW + 2SO_4^{-2}$ represents the base brine (SSW) with a doubled amount of sulfates while $SSW + 4SO_4^{-2}$ indicates a quadrupled amount of sulfates. While $SSW{-}Na$ represents the complete removal of sodium ions from SSW. The last brine group, BG4, was used to investigate the brine hardness, salinity, and impact of sulfates on polymer viscoelasticity. Brine hardness is calculated using the proportion of divalent ions in each brine. The parameter R^{+1}(hardness) is defined according to Equation (3.1) by weight, as explained by Tabary [125] and Tay [126]. Table 3.2 presents an example of hardness calculation for SSW.

$$R^{+1} = \frac{\sum(Divalent_{Cations})}{\sum(Total_{Cations})} \tag{3.1}$$

Table 3.2: *Hardness calculation of synthetic seawater (SSW)*

Composition	**g/L**	**Cation At. Mass**	**Tot. At. Mass**	**Molar Mass**	**Tot. At. Mass/Molar Mass**
		Dalton	Dalton	g/mol	mol.Dalton/g
$NaCl$	23.97	22.98	550.93	58.44	9.43
KCl	0.80	39.00	31.24	74.55	0.42
$CaCl_2.2H_2O$	1.11	40.00	44.31	147.01	0.30
$MgCl_2.6H_2O$	11.04	24.00	264.99	203.30	1.30
$SrCl_2.6H_2O$	0.03	83.91	2.25	158.53	0.01
Na_2SO_4	3.93	45.96	180.77	142.04	1.27
$NaHCO_3$	0.28	22.98	6.33	84.00	0.08
TDS	41.16			Dival. Cations	1.62
			Total cations		12.74
			R^{+1} (Dival. Cations/Total cations)		0.13

3.1.2 Polymer Solutions

A synthetic viscoelastic polymer with high molecular weight (i.e., Flopaam 6035 S) was used to prepare the diluted solutions for two-phase flooding experiments, as mentioned in Table 3.3. Further, a Hengfloc 63026 polymer was used to prepare a diluted solution with a 3000-ppm concentration to investigate the polymer viscoelastic properties. Diluted solutions were prepared using the approach adopted by Hincapie [5]. Polymer had a viscosity ratio (oil to polymer) of one or two to investigate the flooding scenarios. Moreover, different polymer concentrations were prepared in various brines with corresponding polymer viscosity as presented in Table 3.3. Further, Table 3.3 provides the temperatures at which viscosity was measured as well as a list of porous media used for the flooding experiments. Diluted solutions were filtered using a 5.0-μm membrane filter to avoid any undissolved fish eyes. Only high-concentration polymers were used for the single-phase viscoelastic investigation because low polymer concentrations cannot predict the viscoelastic response of solutions using linear viscoelastic measurements (those observed in small-amplitude oscillatory SAOS measurements).

Table 3.3: *Steady shear viscosity of polymer solutions and dead oil at a shear rate of $10s^{-1}$ at specific temperatures and adopted flooding medium*

Nr.	HPAM Conc.	Brine Group	Chapter	Brine For Polymer	*Polymer Viscosity*	*Oil Viscosity*	Temperature	Flooding Medium	Porous Media
	PPM	***From Table 3.1***			***mPas***	***mPas***	***^oC***		
1	300	BG2	4 & 7	Brine 2, Brine 3	≈4 (Half to oil)	8	45	Core	Two phase
2	750	BG2, BG3	5 & 7	Brine 1, Brine 4/5	≈4 (Half to oil)	8	45	Core	
3	1000	BG2, BG3	6 & 7	Brine 1, Brine 4	≈ 10 (Half to oil)	22	22	Micromodel	
4	1500	BG2, BG3		Brine 1, Brine 4	≈ 24 (Equal to oil)	22	22	Micromodel	
5	2000	BG4	8	Brine 9, Brine 10	Viscoelastic study		45	Core	Single phase
6	3000	BG4		Brine 7, Brine 8	Viscoelastic study		45	Core	

3.1.3 Dead Oil

Centrifuged and degassed dead oil was used for all experiments. Oil was filtered through a 5.0 µm millipore filter to avoid solid particles and thick residue. Table 3.4 presents the main crude oil properties measured at 22°C.

Table 3.4: *Oil properties at room temperature*

Oil Properties at 22°C	
Density (g/cm3)	0.879
API	29.42
η **(mPa.S)**	23

3.2 Porous Media

Two types of porous media, core plugs and micromodels, were used for the flooding experiments to investigate fluid-fluid and rock-fluid interactions.

3.2.1 Core Plugs

Bentheimer core plug samples were used in this study. Plugs were trimmed with an average length and diameter of 60mm and 30mm, respectively, as shown in Figure 3.1, and stored in the oven at 50°C for at least three days. Porosity was measured using a Micromeritics1340 pycnometer and permeability was measured using a gas permeameter (Syroperm). Brine was injected at five injection rates (0.5. 1.0, 2.0. 5.0, and 2.0 ml/min) to measure the brine permeability. Table 3.5 shows the routine core analysis (RCA) parameters. Three groups of core plugs were used in this study. The first group (CG1) was selected to design low-salt sulfate-modified water (BG2 in Table 3.1) in combination with polymer flooding. Similarly, the second group of cores (CG2) was selected to investigate the impact of brine composition for slightly higher salinity, as with BG3 in Table 3.1, in combination with polymer flooding. On the other hand, the third group (CG3) was used for single-phase polymer flooding experiments to investigate the polymer viscoelastic properties (polymer solutions prepared in BG4). Moreover, Figure 3.2 presents the porosity-permeability plot of the Bentheimer core plugs mentioned in Table 3.5. This plot describes the range of the high porosity-permeability values for the used plugs.

The experimental set-up used for core flooding, including a detailed description of the design and components, was explained in Foedisch et al. [127] and can be seen in

Table 3.5: *Bentheimer core plug characteristics with formation brines as initial water saturation*

Groups	Core	L	D	ϕ	k_g^*	k_b^{**}	Swc	Soi	Formation Brine
		mm	mm	%	mD	mD	%	%	
CG1(Ch. 4, 7)	Bent 5.1	60.10	29.55	23.33	2510	1684	18.15	81.85	SSW
	Bent 5.2	59.95	29.55	23.69	2714	1964	24.60	75.40	
	Bent 5.3	60.10	29.50	23.54	2835	1976	24.60	75.40	
	Bent 5.4	60.00	29.55	24.10	2848	1608	20.60	79.40	
	Bent 5.5	60.05	29.55	24.10	3029	2114	20.70	79.30	
CG2(Ch. 5, 7)	T1	59.99	29.52	27.18	3272	2148	20.61	79.39	SSW
	T2	60.11	29.36	26.53	3231	2067	15.66	84.34	
	T3	60.40	29.08	26.22	3775	2051	21.39	78.61	2*SSW
	T4	60.08	29.34	26.20	3464	2113	20.52	79.48	
	T5	60.37	29.31	28.56	3434	1946	20.97	79.03	
	T6	60.22	29.30	26.41	3438	1944	17.80	82.20	
	T7	60.09	29.44	26.76	3244	1952	17.89	82.11	SSW
	T8	59.93	29.33	26.06	3112	1970	18.67	81.33	
	T10	59.87	29.33	26.43	3370	2108	26.36	73.64	
CG3(Ch. 8)	C3	60.47	29.51	24.6	2988	1292	Single-phase Polymer Flood		
	C5	59.89	29.29	24.68	3046	1541			
	C6	60.07	29.31	25.06	3226	986			
	C8	59.97	29.35	24.71	2980	1548			
	C11	59.84	29.56	23.83	2666	1052			

k_g^*= Permeability measured with gas
k_b^{**}= Permeability measured with brine

Figure 3.1: *Bentheimer core plugs used for core flooding experiments*

Figure 3.3. Oil saturation of core plug groups CG1 and CG2 was performed using a porous plate with a maximum injection pressure of 8.0 bar. Core plugs of CG1 were aged for three weeks, and core plugs of CG2 were aged for six weeks at 50°C before each flooding experiment to alter their wettability (rock-fluid interaction), and core flooding experiments were performed at 45°C. The wettability alteration of Berea and Bentheimer sandstone core plugs through a two- or three-week aging process has established by many researchers [101] [29] [1] [102].

Different scenarios were adopted for the core flooding evaluations, namely formation brines, in the secondary and tertiary modes (see Table 3.6, and Table 3.7). The chosen injection rate was also defined to mimic the injection velocity of 1-2 ft/day. Moreover, bump rate injection was performed to eliminate capillary end effects before tertiary mode injection. Chapters 4 and 5 present the results of core flooding experiments for oil recovery.

Table 3.6: *Adopted workflow for the low-salt/low-salt and sulfate-modified water core flooding experiments*

Chapter 4 & 7 Flooding Plan					
Formation Brine	**Core**	**Secondary**	**Bump Rate**	**Tertiary**	**Post-Tertiary**
SSW	Bent 5.1	Polymer-DSSW	-	DSSW	
	Bent 5.2	DSSW	Bump Rate	Polymer-DSSW	
	Bent 5.3	DSSW+2SO_4^{-2}	Bump Rate	Polymer-DSSW+2SO_4^{-2}	
	Bent 5.4	SSW	Bump Rate	DSSW	Polymer-DSSW
	Bent 5.5	SSW	Bump Rate	DSSW+2SO_4^{-2}	Polymer-DSSW+2SO_4^{-2}
Q(ml/min)		0.1	0.33	0.15	0.15

The methodology for the single-phase core flood experiments consisted of polymer

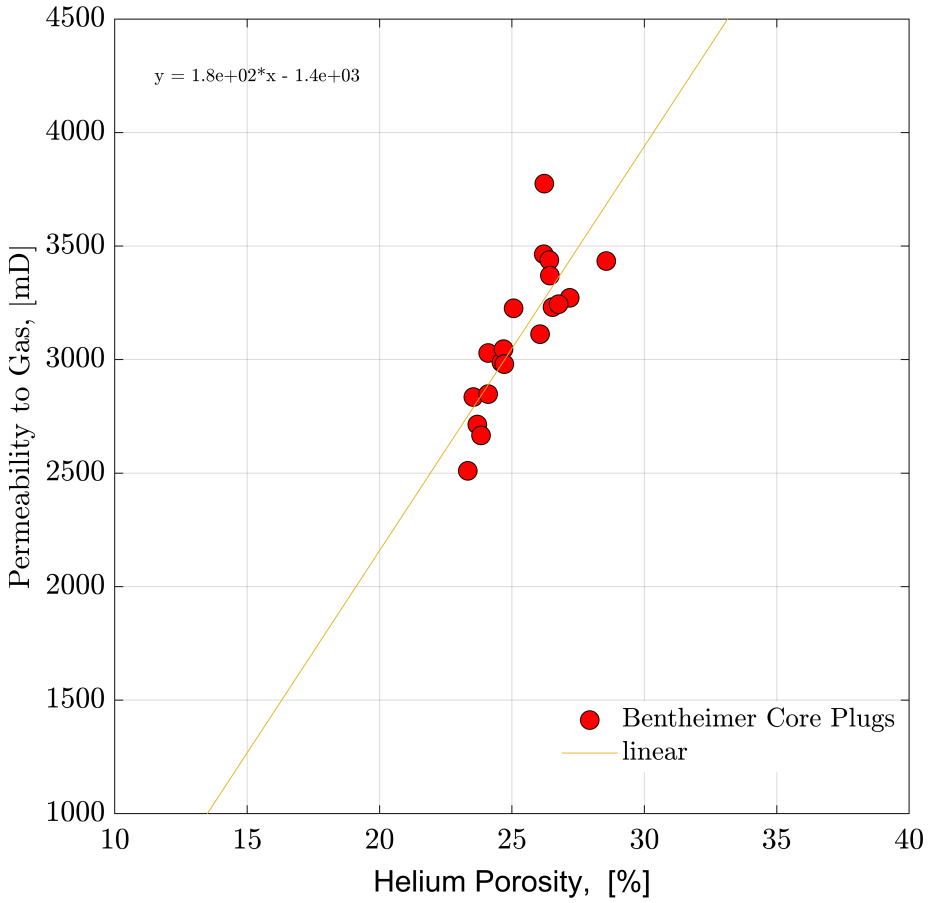

Figure 3.2: *Porosity-permeability plot of analogue core plugs*

flooding through the core plugs at relevant temperatures (22°C and 55°C) with a wide range of injection rates (37 μL/min to 29mL/min). Chapter 8 presents the results of single-phase polymer flooding through core plugs.

Contact Angle Measurements

Measurements were performed at room temperature (i.e., 22°C) using the SSW brine. The core plug face was polished to achieve maximum smoothness and hence saturation with SSW. The core plug was placed with the smooth surface inside brine, and an oil drop was introduced from the bottom with a syringe system developed in house. The oil drop came in contact with the plug surface, and contact angle measurements were performed over time. Furthermore, the core plug was saturated with dead oil to achieve connate water saturation, and plug aging was performed at 50°C in an oven for six weeks. The aged core plug was immersed in SSW using the same procedure described earlier, to measure the contact angle between the oil-drop and rock-surface, as shown in Figure 3.4. The core plugs were initially assumed as water-wet, and the aged plug was expected

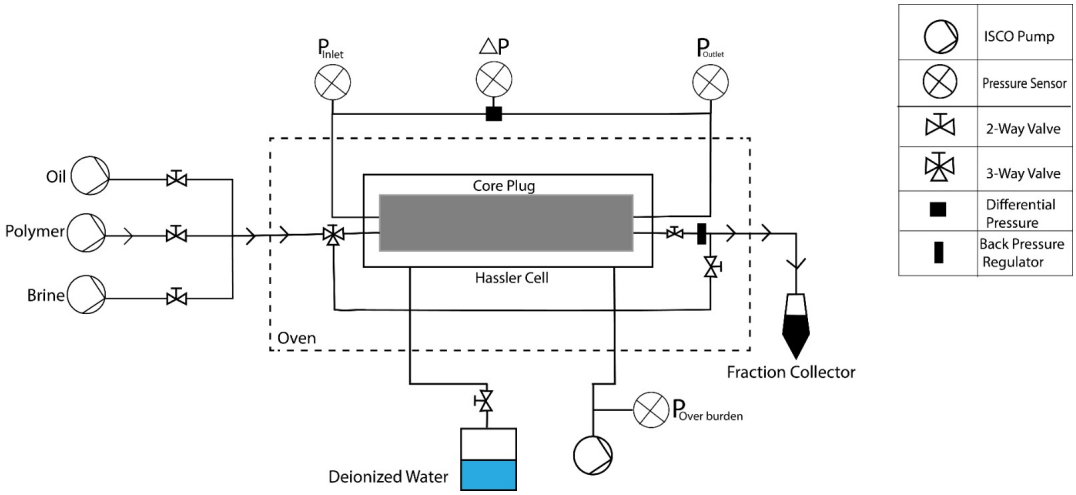

Figure 3.3: *Sketch of core flood experimental setup*

Table 3.7: *Adopted workflow for the seawater-based modified water core flooding experiments*

Chapter 5 & 7 Flooding Plan					
Formation Brine	**Core**	**Secondary**	**Bump Rate**	**Tertiary**	
2*SSW	T6	SSW	Bump Rate	Polymer prepared in SSW	
	T4	SSW+$2SO_4^{-2}$	Bump Rate	Polymer prepared in SSW +$2SO_4^{-2}$	
	T5	SSW+$4SO_4^{-2}$	Bump Rate	Polymer prepared in SSW +$4SO_4^{-2}$	
	T3	SSW-NaCl	Bump Rate	Polymer prepared in SSW +2SO4-2	
SSW	T2	SSW	Bump Rate	Polymer prepared in SSW	
	T7	SSW+$2SO_4^{-2}$	Bump Rate	Polymer prepared in SSW+$2SO_4^{-2}$	
	T8	SSW+$4SO_4^{-2}$	Bump Rate	Polymer prepared in SSW+$4SO_4^{-2}$	
	T1	SSW-NaCl	Bump Rate	Polymer prepared in SSW+$2SO_4^{-2}$	
SSW	T10	SSW	Bump Rate	SSW +$2SO_4^{-2}$	Polymer prepared in SSW
Q(ml/min)		0.15	0.33	0.15	0.15

to become oil-wet due to the aging process, or mix-wet in the other case. Note that some additional measurements were performed using the pendant drop method (OCA 15 from Data Physics OCA-Serie with some modifications) for cross-validation purposes, as shown in Figure 3.5. Modification of the pendant drop method included the oil-drop production procedure using the technique described earlier in this section. Image processing for contact angle measurements was performed using the OCA 15 device from DataPhysics. Contact angle measurements were performed for the core plugs aged for six weeks. Chapter 5 presents the results.

Figure 3.4: *Contact angle measurement between aged core plug and oil-drop in-house device*

Figure 3.5: *Contact angle measurement by the pendant drop method [OCA 15 from Data-Physics OCA-Serie [8]]*

3.2.2 Microfluidics

Two glass-silicon-glass (GSG) micromodels based on pore structures were used for this study as porous media for the flooding experiments shown in Figure 3.6. The first micromodel is an artificial structure micromodel or homogeneous micromodel, due to its random distribution of circular grains. Such micromodels have been previously used for several EOR investigations [9] [128] [10]. The second micromodel is also known as a real structure micromodel or heterogeneous micromodel. Its structure is based on a μ CT image of a Bentheimer core plug. The real structure model has three permeability zones, two lower permeability zones on the sides and a high permeability zone in the middle. Both micromodel types have been previously used for microbial flooding experiments by

Gaol et al. [9]. Figure 3.6 shows pore structure images and dimensional measurements of both models, and Table 3.8 provides porosity and permeability values.

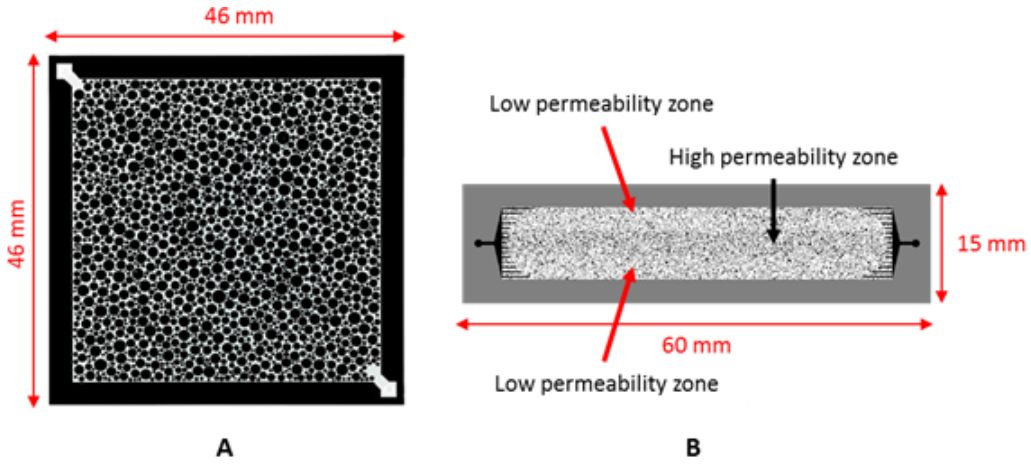

Figure 3.6: *Micromodels used in this study. A) artificial-structure micromodel and B) real-structure micromodel [9]*

Table 3.8: *Rock characteristics of the micromodels used*

	Parameter	Glass-silicon-glass (GSG) Micromodel	
		Artificial	**Real**
Chapters 6 & 7	**Porosity (%)**	27.6	19.2
	Brine Permeability (mD)	13000	1237
	Min. Pore diameter (μm)	8	12.21
	Max. Pore diameter (μm)	2610	112.52
	Avg. Pore diameter (μm)	178.2	31.5

Wettability Evaluation of the Micromodels

The micromodels were chemically modified to generate three types of wettability based on the presented structures, namely water-wet, oil-wet, and complex-wet/mixed-wet, as shown in Table 3.9. The complex/mixed wettability type addresses the local variation of wettability areas, which occurs when some parts/zones are oil-wet while others are water-wet. The wettability alteration was achieved by chemisorption of fluorinated silane that was applied on the micromodels' inner glass and silicon surfaces. Silicon and glass were initially water-wet with a contact angle (water) below 20°. After treatment, this angle was increased to 112°. The oil contact angle of the modified surface was significantly lower at 77°. The mixed-wet micromodel was obtained by fragmentary acid-induced abrasion of the coating. The wettability alteration process was confirmed through a visual inspection of the concave/convex interface of the fluids and is shown in Figure 7.5.

Table 3.9: *Description of micromodels according to the wettability approach*

Chapters 6 & 7	Parameter	Glass-silicon-glass (GSG) Micromodel	
		Artificial	**Real**
	Water-wet	Yes	Yes
	Oil-wet	Yes	No
	Complex/Mix-wet	Yes	No
	Injection Rate (μl/min)	0.3	0.1
	Bump rate (μl/min)	1.5	0.5

Microfluidics Setup and Flooding Sequence

For flooding experiments, the InspIOR microfluidics-flooding rig from HOT Microfluidics was used. This is a compact experimental set-up that includes injection pumps, a micromodel holder, a DSLR camera for imaging, pressure sensors (connected to the inlet and outlet of the micromodel holder), and fluid and waste reservoirs. An upgraded version of the experimental set-up and components, as described by Schumi et al. [10] and shown in Figure 3.7, was used for the flooding experiments. The flooding process was performed at an injection flux of 1.0 ft/day, with corresponding injection rates included in Table 3.9. Bump rate injection was performed at a higher flux rate of 5.0 ft/day. Flooding experiments were performed at room temperature (i.e., 22°C) and a system pressure of 1.0 bar (gas) with the following steps:

- Micromodel is installed into the holder and water injection is performed to remove air bubbles and pursued until the differential pressure stabilizes.
- Brine flooding is performed to measure the permeability of the model.
- Oil saturation is established through continuous and increasing oil injection rates until no further water can be produced.
- Two hours stabilization interval is provided to establish a possible ionic reaction in the model.
- Brine flooding is performed to observe the oil recovery and the pressure data.
- During the flooding process, images are gathered/captured at different time intervals and recovery analysis is performed through an imaging processing tool developed in MATLAB.

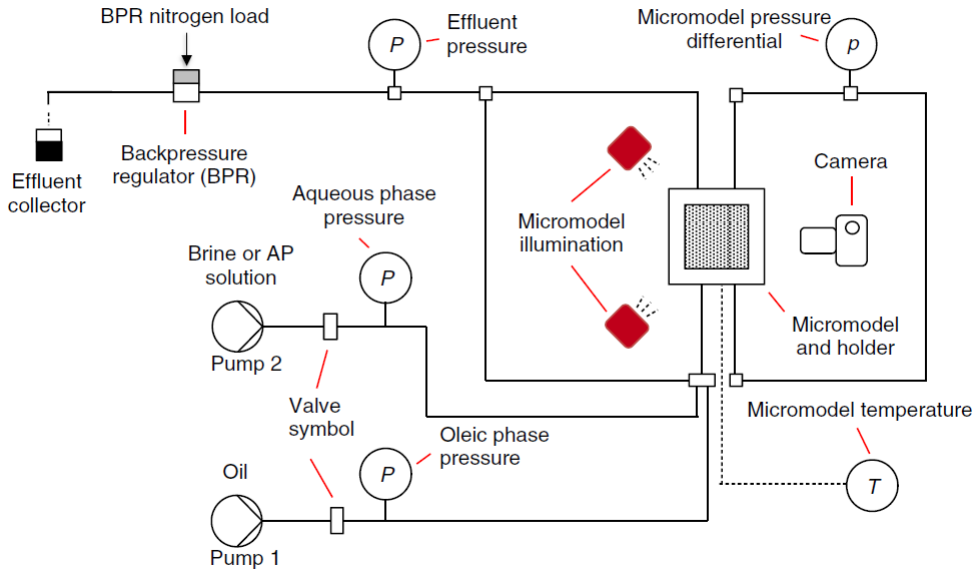

Figure 3.7: *Sketch of microfluidics experimental setup [10]. Order License ID:1017373*

3.3 Fluids Investigation

3.3.1 IFT Measurements (Fluid-fluid Interaction)

Oil-brine IFT measurements are performed to investigate the impact of brine chemistry (monovalent and divalent ions) at the oil-brine interface. The measurements are performed using the Du Noüy ring method (Prozessor- Tensiometer KRUESS GmbH K12), as shown in Figure 3.8, at room temperature of 22°C. The input parameters of the device are oil and brine densities and the steps for the evaluation can be described as:

- A metallic ring is placed on a fire for a few seconds to burn any organic compound if present.
- The sample holder is filled with the brine sample, and a measurement ring is inserted in the brine.
- Device calibration is performed.
- The oil phase is filled at the top of the brine phase to the marked level.
- Measurement is performed by selecting the ring movement from bottom to top (brine to oil phase).
- Towards the end of the measurement, IFT at the oil-brine interface is measured through the force experienced by a sensor attached to the metallic ring.
- IFT measurements are performed between the dead oil and the five brines (BG2 and BG3) presented in Table 3.1.

Chapter 5 and Chapter 7 briefly discuss the results obtained.

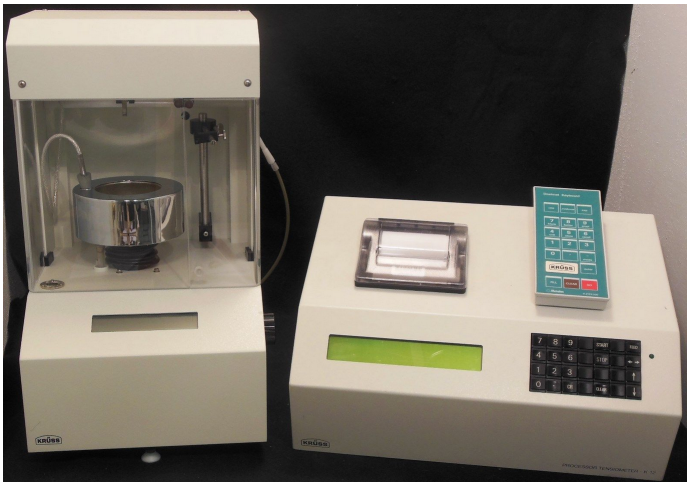

Figure 3.8: *IFT measurement device: Prozessor- Tensiometer KRUESS GmbH K12*

3.3.2 Oil Drop Snap-off Volume Measurements (Fluid-fluid Interaction)

Oil-brine interfacial interactions were investigated through the analysis of oil-drop volume at the snap-off point. This approach does not provide direct measurements of interfacial viscoelasticity (G' and G"). Rather, indirect measurement of oil-drop size at the snap-off point correlates with the interfacial interactions. An oil drop of 2.5 μL volume was produced through a syringe in the specific brine phase. A settlement time of 10 minutes was established for ionic equilibrium between both fluids. During this time, ionic interaction between oil polar compounds and brine divalent/monovalent ions was expected to happen at the interface. After 10 minutes, 2.5 μL of oil was further injected to increase the oil drop size. After a further 10 minutes of ionic interaction, the time between both phases was established. Subsequently, 2.5 μL of oil was injected to increase the oil-drop volume further. This process continued until oil-drop snap-off happened from the needle. Figure Figure 3.9 summarizes the measurement process.

Oil drop experiences two opposite forces before snap-off happens. One force is buoyancy, which is an upward force due to oil density. The second force is interfacial interaction, which is a downwards force that establishes the oil-drop attachment to the needle and controls the oil-drop snap-off. Oil-drop size continues to increase in the case that the downward force at the interface is higher than the upward force. After a specific increase in drop size, buoyancy dominates the interfacial elastic force and oil-drop detachment from the needle happens.

This investigation helped to study the formation of the interfacial elastic layer at the

fluid interface due to ionic reactions. The strong interfacial elastic layer is expected to produce a more significant oil-drop volume before the snap-off point. Morin et al. [35], and Mohamed and Alvarado [1] demonstrated that elastic interfacial film is found to be more stable and resistant to snap-off. This will assist with stable and continuous oil flow during flooding while limiting oil trapping in porous media and is hence correlated with the higher oil recovery during core flooding experiments. Chapter 5 and Chapter 7 present these measurements.

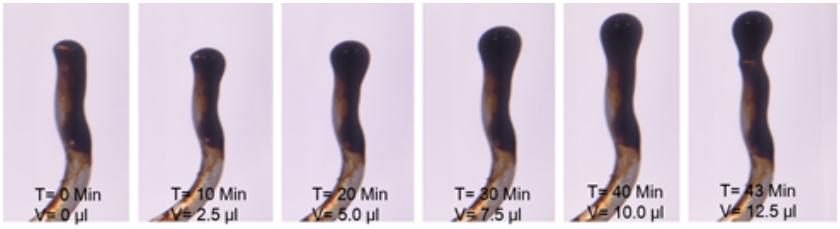

Figure 3.9: *Indirect measurement of ionic oil-brine interfacial interaction through the oil-drop snap-off point*

3.3.3 e-VROC Extensional Viscometer

The e-VROC (extensional viscometer-rheometer on a chip) is a device capable of measuring elongational viscosity. It measures extensional viscosity by monitoring the fluid flow through a microfluidic hyperbolic shape of converging-diverging geometry within a cell. The pressure response before and after the converging-diverging geometry is measured via micro-electrical-mechanical systems (MEMS) pressure sensors, which help interpret viscosity changes across the geometry. Figure 3.10 provides a schematic of this converging-diverging geometry. This device is used to investigate the elongational response of diluted polymer solutions. Further detail on the working principle and associated physics can be found in Hincapie [5].

This device is used to investigate the non-Newtonian behaviour of fluids. A small amount of polymer diluted solutions is injected through a converging-diverging geometry, as shown in Figure 3.10. The converging point at the contraction zone resembles the pore throat and the diverging point resembles the pore space. Polymer molecules' structure is elongated while flowing through the contraction zone and hence they are expected to demonstrate viscoelastic response. The viscoelastic response of solutions is expressed in terms of extensional/elongational viscosity. Chapter 4 and Chapter 8 present the results obtained from this device.

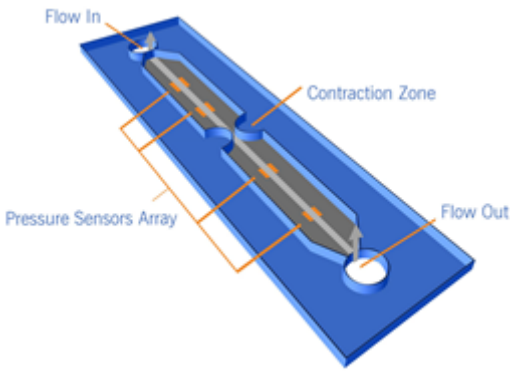

Figure 3.10: *Hyperbolic converging-diverging geometry used to measure elongational viscosity [11]*

3.3.4 Polymer Degradation Analysis

This study investigates polymer viscosity reduction due to mechanical degradation that occurs during the pipe flow, based on the principles explained by Severs [129]. Degradation is studied by measuring polymer viscosity (rheology) before and after injection into the pipeline (collected fluids). As reported, the polymer solution experiences the shear rate exerted by the pipeline and while flowing through valves and connections. The degradation rate (DR) of solutions is defined using Equation 3.2. The degradation rate is defined as the viscosity loss in the designed polymer solution, focusing on a viscosity ratio of two or one between the oil and polymer solutions. Chapter 4 and Chapter 5 present the results of polymer degradation.

$$Degradation Rate(DR) = \frac{(\eta_o - \eta_e)}{\eta_o} * 100 \tag{3.2}$$

where, η_o= viscosity of the original solution, and η_e= viscosity of the degraded solution.

Chapter 4

Modified Low-salinity Flooding Combined with Polymer Flooding

Oil recovery using modified/smart water technology can be maximized by optimizing the composition of the injected water. Brine optimization is also believed to improve polymer flooding performance. This chapter assesses and defines the potential impact of combining low-salt modified water with polymer flooding, based on the presence of sulfate in the injection water. The impact of sulfates (sodium sulfates) on polymer viscoelasticity and its performance in porous media are studied based on oil recovery and pressure response. Brine composition is optimized using SSW as the base brine. As the chapter title indicates, the objective is to design low-salinity sulfate-modified water with TDS of around 5g/L (BG2 from Table 3.1). Diluted polymer solutions are prepared in Brine 2 and Brine 3 from BG2, as indicated in Table 3.1. Further, this study investigates the role of the spiked amount of sulfates in low-salt injection brine. The focus is on performing fluid optimization following core flooding experiments. Secondary, tertiary, and post-tertiary (quaternary) mode experiments are performed to evaluate the feasibility of applying both processes (modified water and polymer flooding). Further, low-salt brine flooding and low-salt sulfate-modified water injection are compared based on recovery performance. The workflow is summarised in the flow chart presented in Figure 4.1. This work was published under the title "Influence of Sulfate Ions on the Combined Application of Modified Water and Polymer Flooding—Rheology and Oil Recovery" in Energies 2020 (ISSN 1996-1073), 13(9), 2356; https://doi.org/10.3390/en13092356

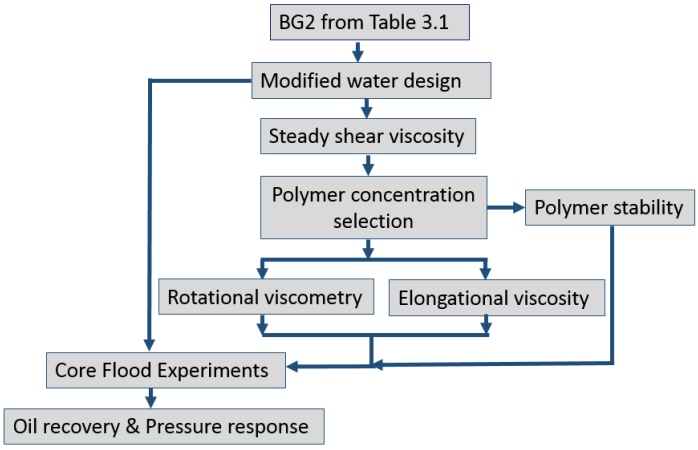

Figure 4.1: *Adopted work flow for combined low-salinity injection and polymer flooding*

4.1 Overall Methodology and Approach

To evaluate the influence of sodium sulfate on 1) polymer viscoelasticity, under the assumption that the phenomenon exists, and 2) oil recovery and pressure response due to the injection of optimized brine in porous media, the following steps or methodology were adopted to gather the data and draw conclusions:

- ***Brine preparation and optimization***: Three brines were prepared, including sulfate concentration changes and varying TDS and hardness, presented as BG2 in Table 3.1.
- ***Polymer preparation and comprehensive rheological characterisation***: Polymer solutions were prepared, mainly with a viscosity ratio of 2 between oil and polymer, shown as Nr. 1 in Table 3.3. Subsequently, solutions were characterised in a detailed manner using steady shear viscosity, elongational viscosity measurements, first normal stress differences (N_1) and oscillatory shear (the latter two were attempted).
- ***Mechanical degradation of polymer solutions***: This step defines any possible degradation prior to the core face and enables better conclusions to be drawn regarding polymer performance using Equation 3.2.
- ***Two-phase core flooding experiments***: Core plugs were saturated to initial water saturation using the porous plate method, presented as CG1 in Table 3.5, before each experiment took place. Subsequently, different chemical slugs were injected following the flooding sequence mentioned in Table 3.6 to observe pressure response and determine oil recovery.

4.2 Fluids Optimization

4.2.1 Steady Shear Rheology (Shear Viscosity)

Figure 4.2 shows the measured viscosity for the utilized oil sample (mentioned in Chapter 3 and Table 3.4) at a temperature range of 22°C to 55°C. As expected, oil shear viscosity decreased proportionally with temperature increase, which is indicative of Newtonian behaviour. Note that this evaluation helps to define polymer concentrations with respect to oil viscosity. Core flooding experiments were performed at 45°C with an oil viscosity of 8.0 mPa.s at a $10s^{-1}$ shear rate.

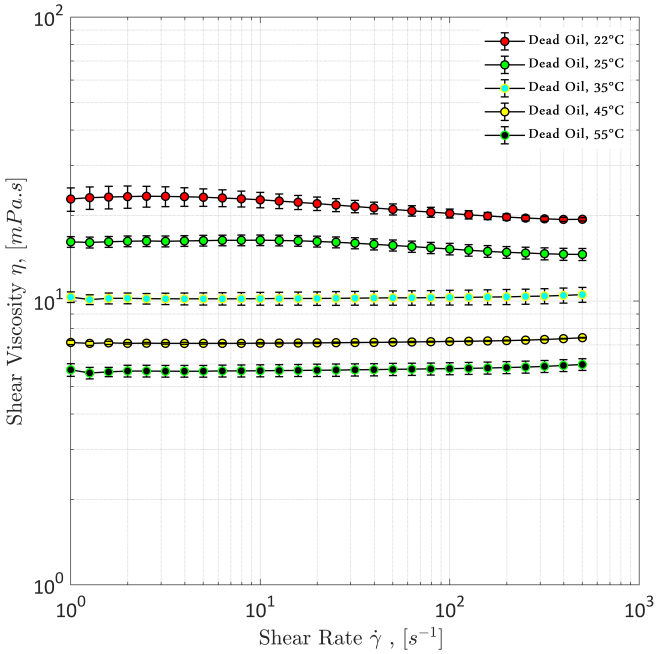

Figure 4.2: *Steady shear viscosity of the dead oil sample at a temperature range of 22°C to 55°C. Error was observed in the range of 3%*

Figure 4.3 shows the shear viscosity of the polymer solutions. The objective is to select the polymer concentration exhibiting half of the oil viscosity; thus, the results of Figure 4.3 indicate a concentration of 300 ppm (≈3.7 mPas). Moreover, for the polymer concentration of 300 ppm, there is a slightly higher viscosity for the diluted solutions containing a doubled amount of sulfates (DSSW+2SO_4^{-2}) compared to the typically diluted brine (3.67cp and 3.45 cp). In other words, the increase in polymer solution viscosity was due to experimentation involving the increase of sulfates. The main factor is a decrease in brine hardness with an increase in sodium sulfates (per Equation (3.1)). Therefore, the hardness of the brine has a stronger impact compares to salinity (TDS). It can also be observed that solutions with 200-ppm polymer concentration have higher measurement errors. This error is assumed to be due to the low polymer concentration, which leads

to less stable solutions. Thus, stability in viscosity measurements is established with an increase in concentration, as can be seen in Figure 4.3, resulting in reduced measurement error. The time to measure steady shear viscosity measurement time for 200 ppm was longer compared to higher polymer concentrations due to stability issues.

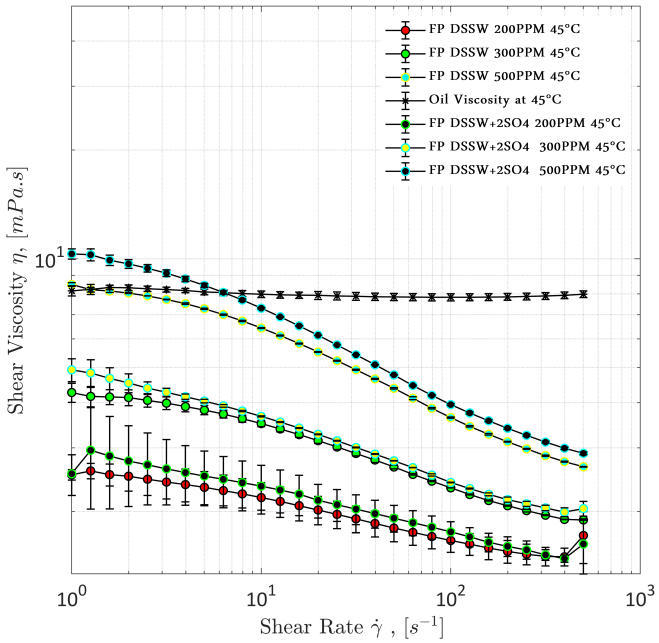

Figure 4.3: *Steady shear viscosity of polymer solutions at 45°C. Polymer solutions are prepared in Brine 2 and Brine 3 of the BG2 group in Table 3.1 (concentrations of 200 ppm, 300 ppm, and 500 ppm)*

4.2.2 Oscillatory Measurement and First Normal Stress Differences

Polymer viscoelastic behaviour is evaluated using SAOS response and first normal stress differences measurements. Oscillatory measurements are performed to define the viscous and elastic properties of the polymer solutions. The characterisation focuses on the elastic modulus (G') and viscous modulus (G"), measured against the angular frequency. A viscoelastic material has both liquid-like (viscous) and solid-like (elastic) properties depending upon the deformational stress and relaxation time (time required for the material to relax). If the stress is applied for a shorter time than the relaxation time of a material, then it regains its original molecular structure and exhibits solid-like behaviour. However, if the applied stress interval exceeds the relaxation time of a specific material, permanent deformation is caused in the molecular structure and the material liquid-like behaviour. Relaxation time is measured as the inverse of angular frequency (rad/sec) at the crossover point of both moduli (viscous and elastic G'=G"). Materials with a higher

relaxation time have strong viscoelastic properties. However, with no or less relaxation time, they have mainly viscous properties.

Similarly, normal stress differences (N_1) caused by force normal to shear flow also represent the elastic behaviour of the polymer solutions. N_1 effects are measured due to tension in the flow streamlines. N_1 is a quantitative measurement to evaluate non-linear viscoelastic response by monitoring the normal forces on a rotational rheometer. Mathematically, N_1 is defined as $N_1 = \sigma_{xx}$ - σ_{yy} where σ_{xx} is the stress induced in the direction of applied stresses, and σ_{yy} is the normal stress in the force direction.

Based on observations in the literature [116] [106] [107], it can be concluded that high-molecular-weight hydrolysed polyacrylamides have good viscoelastic properties and can contribute to additional oil recovery. Therefore, it is essential to characterise polymer viscoelastic properties before performing polymer flooding to understand the flow dynamics in porous media.

Repeated measurements were performed to gather information on viscosity response, with little success. In the first step, angular frequency measurements of G', G" for both polymer solutions (300 ppm) were performed at 45°C, but no crossover point was observed. Subsequently, the same measurements were performed at room temperature (i.e., 22°C), as presented in Figure 4.4. Once again, no crossover angular frequency (relaxation time) was observed for solutions diluted in synthetic seawater (DSSW). However, DSSW+$2SO_4^{-2}$ solution with a doubled amount of sulfates had a crossover point and very low relaxation time $\approx$ 0.1s. It can be argued that this crossover point is in the margin of error of the device or the torque limit, but it can be seen in Figure 4.4 that both solutions have almost the same values for G" while DSSW+$2SO_4^{-2}$ had slightly higher values for G' compare to the DSSW solution, as shown in Figure 4.4. Furthermore, the first normal stress differences measurement was performed to confirm the linear viscoelastic response of the solutions. However, no N_1 response could be measured for either solution (DSSW and DSSW+$2SO_4^{-2}$) at room temperature of 22°C and at 45°C. This investigation led to a further investigation of the polymer solution's elongational measurements. Viscoelastic response of solutions is prominent while flowing through pores and pore throats. Oscillatory measurements provide linear viscoelastic response but fail to predict the behaviour of solutions through converging-diverging geometry.

4.2.3 Elongational Measurements

Figure 4.5 shows the apparent elongational measurements at 45°C for polymer solutions prepared in DSSW and DSSW+$2SO_4^{-2}$. The objective is to analyse the impact of sulfates

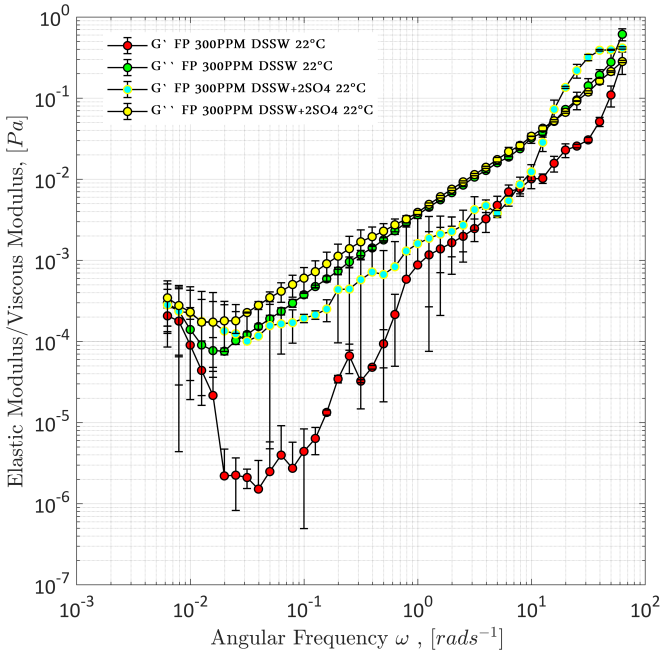

Figure 4.4: *Oscillatory measurements of G', G" as a function of angular frequency for Flopaam 6035 S at 22°C*

on polymer elongational properties. From Figure 4.5, two important features can be seen between low and high apparent extensional rates:

- The measurement errors, as described with error bars: At lower apparent extensional rates, both solutions exhibited a wider range of measurement errors compared to higher apparent extensional rates. One reason for the errors could be that the elongational measurement is not unique, and there is no device that can reproduce the same behaviour of fluids. Moreover, at lower extensional rates, the sensitivity of measurement is higher compared to higher rates. The error bar indicates that the polymer prepared in DSSW+$2SO_4^{-2}$ is more sensitive than the polymer solution in DSSW (wider range of error bar).
- The measurement response: Nearly the same elongational viscosity was observed for both solutions, considering the range of error bars between apparent extensional rates of 10-100s^{-1}. At high extensional rates, the DSSW solution (without sulfates) had slightly higher elasticity compared to DSSW+$2SO_4^{-2}$, but both exhibited a decline in elastic response between apparent extensional rates of 100-1000s^{-1}. For flow through porous media, the extensional rate for the low to medium range is more important compared to the high rates in Figure 4.5. Furthermore, the elongational response of a fluid can be different while flowing through porous media (core plug). Whereas flow through porous media fluid experiences series of converging-diverging geometries, for this measurement, only one hyperbolic shape

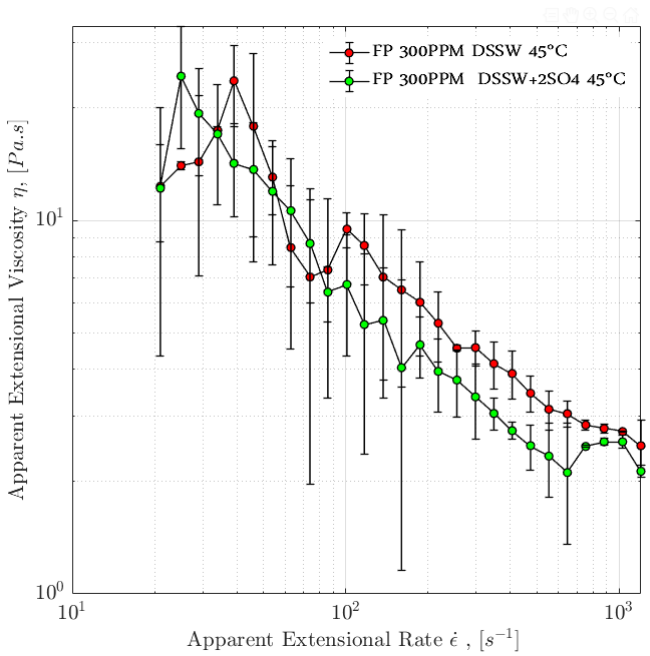

Figure 4.5: *Apparent extensional viscosity as a function of apparent extensional rate for polymer solutions of Flopaam 6035 S at 45°C*

converging-diverging geometry was used. Elongational response of fluid became stronger with multiple contraction and elongation of polymer molecules.

Summarising the results of oscillatory and elongation measurements, it can be concluded that both polymer solutions depicted almost the same viscoelastic response at field-scale low extensional rates and angular frequencies. The main factor is the low polymer concentration for these solutions. A clear difference can be justified by increasing the polymer concentration/viscosity. Viscoelastic response of both solutions can be further compared based on the pressure response during polymer flood in core plugs. Polymer solution with higher viscoelasticity exhibited higher pressure drop in the core plug at the same injection rate.

4.3 Core Flood Experiments

4.3.1 Core Flooding Sequence

Core plugs of group CG1 from Table 3.5 were used for the flooding experiments. Core flooding sequences with different scenarios and injection rates are summarised in Table 3.6. Core flooding started with secondary-mode flooding to mimic the primary mode of oil production through the natural energy of the reservoir. After the secondary mode,

the second phase of fluid flooding was performed as the tertiary mode. The post-tertiary stage represents the third phase of fluid injection after the tertiary mode.

Fluid viscosities (oil and polymer solutions) for core flooding experiments at 45°C are shown as Nr. 1 in Table 3.3 and are briefly explained in Section 4.2.1 on steady shear rheology. Oil viscosity was 8 mPa.s and the viscosity of polymer solutions was half that of the oil (viscosity 4 mPa.s). Lower-viscosity polymer solutions were selected to represent the low polymer concentration required and hence the cheaper EOR hybrid technique.

4.3.2 Oil Recovery and Pressure Observations

Table 4.1 summarises the recovered oil based on the core flood sequences adopted for this study. Secondary-mode and tertiary-mode flooding were performed for all core flooding, adopting the flood sequence in Table 3.6. Post-tertiary-mode flooding was performed in only two core plugs (Bent 5.4 and Bent 5.5). Polymer flooding was used for the post-tertiary-mode for mobility control after brine flooding in both experiments. The objective was to observe any extra oil recovery due to the viscosity difference between tertiary-mode and post-tertiary (quaternary) mode flooding. For the first core flood experiment, Bent5.1, Figure 4.6 describes the recovery profile and pressure differential across the core as the function of injected pore volumes. The oil recovery factor at the end of the secondary-mode polymer flooding was 41.85%. An increase in pressure response for polymer flooding can be seen in Figure 4.6. However, diluted SSW in tertiary mode injection did not change the recovery factor although 58.15% of oil (remaining oil saturation) was present in the core. This shows that the diluted SSW flood followed the same flow path, which was already adopted by polymer because of the viscosity difference. As polymer viscosity is half of the oil viscosity, diluted SSW could displace only pre-flushed polymer because of its lower viscosity compared to oil. Diluted SSW flood had no interaction with oil in the core to contribute to extra oil recovery and did not mobilize trapped and unflushed oil droplets. Nevertheless, the pressure profile in Figure 4.6 indicates slightly higher pressure for diluted SSW compared to the pressure profile of SSW before polymer flooding (Figure 4.7). The reason for this is the presence of a polymer solution in porous media for Bent 5.1.

In experiment-2 using the core plug Bent 5.2, the same fluids of experiment-1 were injected but in reverse order. As discussed in Chapter 3, bump rate injection for subsequent experiments was performed after secondary-mode brine flooding to eliminate the capillary end effects, if present. Oil recovery from bump rates is not reflected in the results. Figure 4.7 shows the results of the recovery profile and pressure response for this

Table 4.1: *Summary and comparison of core flood recoveries and flooding processes. Polymer concentration and fluid viscosities from Nr. 1 in Table 3.3*

Nr.	Flooding	Name	ϕ (%)	PV	k, brine (md)	*k, gas*	Soi	Swc	Add. RF	Total RF (OIIP)
	Secondary Mode 45°C									
1	Polymer-DSSW	Bent 5.1	23.33	9.61	1684	2510	81.85	18.15	-	40.85
2	DSSWF	Bent 5.2	23.69	9.74	1964	2714	75.4	24.6	-	36.9
3	SWF	Bent 5.3	23.54	9.67	1976	2835	75.4	24.6	-	37.87
4	SSW	Bent 5.4	24.1	9.91	1608	2848	79.4	20.6	-	32.22
5	SSW	Bent 5.5	24.1	9.92	2114	3029	79.3	20.7	-	35.27
	Tertiary Mode 45°C									
1	DSSWF	Bent 5.1	23.33	9.61	1684	2510	81.85	18.15	0	40.85
2	Polymer-DSSW	Bent 5.2	23.69	9.74	1964	2714	75.4	24.6	6.9	43.8
3	Polymer-SW	Bent 5.3	23.54	9.67	1976	2835	75.4	24.6	9.6	47.47
4	DSSWF	Bent 5.4	24.1	9.91	1608	2848	79.4	20.6	2.5	34.72
5	SWF	Bent 5.5	24.1	9.92	2114	3029	79.3	20.7	5	40.27
	Post-tertiary (Quaternary) Mode 45°C									
4	Polymer-DSSW	Bent 5.4	24.1	9.91	1608	2848	79.4	20.6	6.3	41.02
5	Polymer-SW	Bent 5.5	24.1	9.92	2114	3029	79.3	20.7	6.4	46.67

core (Bent 5.2). The recovery factor from diluted SSW as the secondary mode reaches to around 36.9% OOIP. A significant amount of oil (6.9% OOIP) was produced from the tertiary-mode 300-ppm polymer-DSSW flood. Pressure build-up for polymer flooding can be clearly seen in Figure 4.7. Comparing the pressure profiles of Bent 5.1 and Bent 5.2 core plugs, 0.05-bar higher pressure for polymer flooding was observed for the Bent 5.2 plug. Additional oil recovery from polymer-DSSW could be due to this higher pressure response. This pressure response also indicates that prior low-salt flooding helps alter the wettability of the rock and causes the release of oil compounds.

Follow-up tertiary-mode polymer flood experienced resistance in the flow because of the detached and trapped oil in this phase. Moreover, the polymer had slightly higher pressure compare to the polymer flood in Bent 5.1. Hence, polymer flood produces detached and trapped oil droplets because of improved sweep efficiency (additional recovery of 6.9% OOIP). For further comparison, Experiment 3 in Bent 5.3 was performed using modified water with doubled sulfates. The injection scheme is similar to that outlined in the previous section (Bent 5.2), but modified water with doubled sulfates is injected instead of the diluted SSW. The results show 1% higher oil recovery of about 37.87% OOIP in secondary-mode sulfate-modified water flooding compared to secondary-mode DSSW flooding in Bent 5.2. The incremental oil recovery from 300-ppm polymer-DSSW+$2SO_4^{-2}$ flooding in the tertiary mode was 9.6% OOIP. The final oil re-

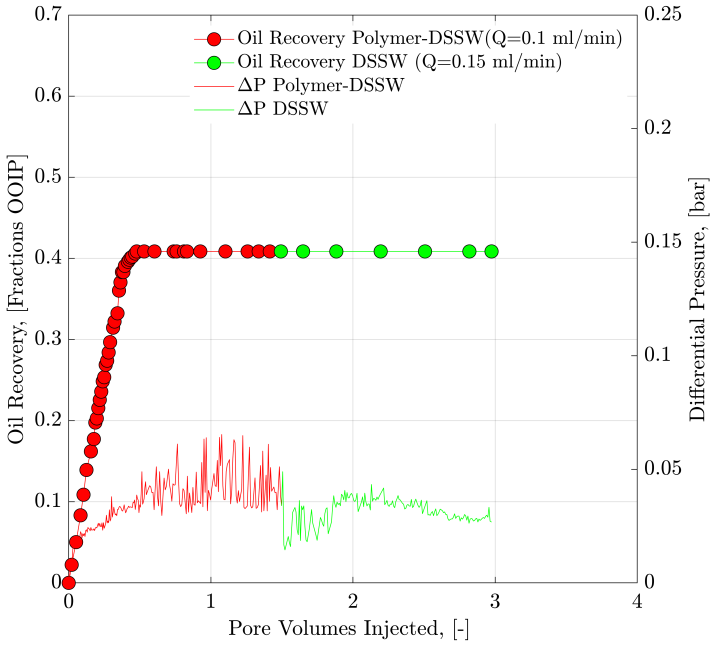

Figure 4.6: *Oil recovery and pressure drop versus pore volume (PV) injected for Bent5.1 core plug. Red represents the experimental data for secondary-mode injection of polymer-DSSW, and green represents the tertiary injection mode of DSSW*

covery reached 47.47% OOIP (Figure 4.8), leaving remaining oil saturation of 52.53% OOIP compared to the remaining oil saturation in the Bent 5.2 core, which was 56.20% OOIP. One reason for this high recovery is the pressure response, shown in 4.7 and Figure 4.8. The pressure drop along the Bent 5.3 core was double for Polymer-DSSW+$2SO_4^{-2}$ compared to polymer-DSSWF (at PV=2.5). Therefore, the increased oil recovery can mainly be attributed to improved viscoelastic properties of polymer-DSSW+$2SO_4^{-2}$ in porous media owing to sulfates. Fluid optimization in the previous section was not significantly different for the viscoelastic properties of both polymers. This behaviour further clarifies that linear viscoelastic (oscillatory and e-VROC) measurements cannot wholly predict the fluid response in porous media. As previously discussed, viscoelastic properties are controlled through the converging-diverging geometry of the flow path in porous media. Single-phase core flooding/sand packs/micromodel flooding can predict the viscoelastic response in porous media. The second reason for higher recovery could be the multi-EOR process in the secondary and tertiary modes, as explained by prior research [60] [59] [60]. The sulfate-modified low-salt water flood may have disturbed the ionic equilibrium in the oil-rock-brine system in the reservoir, which resulted in detaching the long-chain carboxylic acids (oil) adsorbed during the aging process (wettability alteration). Follow-up polymer-DSSW+$2SO_4^{-2}$ produced this oil due to improved mobility and viscoelastic forces. Polymer-DSSW+$2SO_4^{-2}$ produced 2.7% extra oil compared to the polymer-DSSW due to stronger viscoelastic response in porous media, which resulted

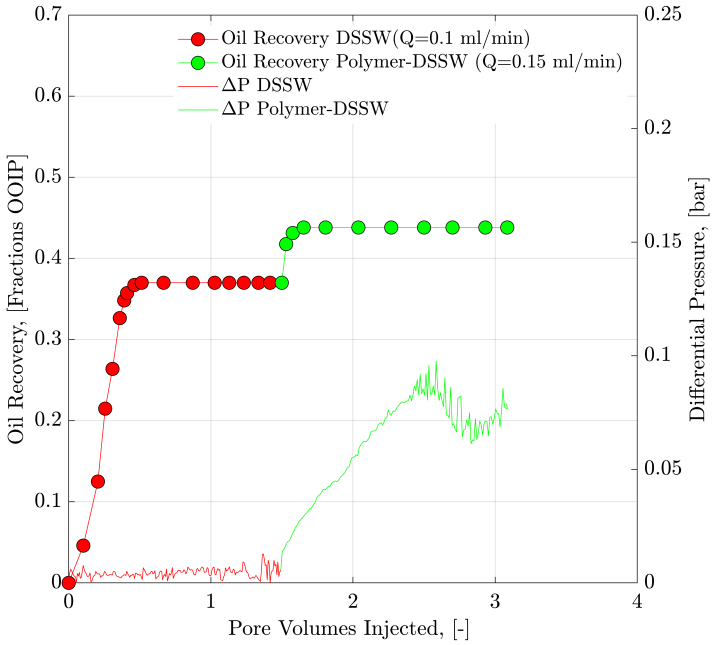

Figure 4.7: *Oil recovery and pressure drop versus PV injected for the Bent 5.2 core plug. Red represents the experimental data for secondary-mode injection of DSSW while green represents the tertiary-mode injection of polymer-DSSW*

in higher injection pressure at the same injection rate.

For further investigation, core flooding was performed using SSW as the secondary mode in the Bent 5.4 and Bent 5.5 core plugs, as shown in Figure 4.9 and Figure 4.10. Both core plugs produced lower recovery (29.68% and 33.50% OOIP) compared to DSSW flooding, DSSW+2SO_4^{-2} water flooding, and polymer flooding in the secondary mode, mentioned in previous sections. Although SSW has slightly higher viscosity than DSSW and DSSW+2SO_4^{-2} water as a result of higher TDS, extra recovery in Bent 5.2 and Bent 5.3 was due to the low-salt effect and modified water (proposed wettability alteration process). Both brines (DSSW, DSSW+2SO_4^{-2}) alter the wettability to be more water-wet compared to SSW and contribute to higher recovery. Furthermore, DSSW as the tertiary mode results in only 2.5% extra oil recovery, as described in Figure 4.9. Nevertheless, DSSW+2SO_4^{-2} tertiary-mode flooding in Bent 5.5 produced 5.0% extra oil recovery, which is double that compared to DSSW flooding in Bent 5.4. This 2.5% recovery difference further proves that wettability alteration through DSSW+2SO_4^{-2} is stronger than DSSW. We can also see from the secondary recovery of both brines in Bent 5.2 and Bent 5.3 plugs, DSSW+2SO_4^{-2} produced 1% higher recovery than DSSW. The last four core flooding experiments indicate that sulfate-modified low salinity water worked better than DSSW in altering the wettability. Interestingly, polymer flooding in the post-tertiary mode produced almost the same oil recovery in both core plugs (6.30% of OOIP). However, overall, the difference in recovery for both plugs increased to 3% OOIP

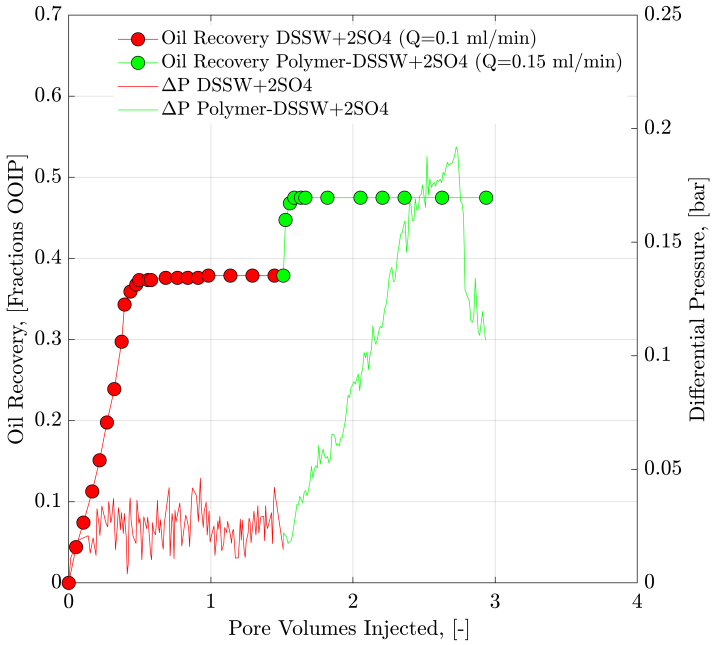

Figure 4.8: *Oil recovery and pressure drop versus PV injected for the Bent 5.3 core plug. Red represents the experimental data for secondary-mode injection of sulfate-modified low-salt water flooding while green represents the tertiary injection mode of polymer-DSSW+2SO_4^{-2}*

after polymer flooding due to multi-EOR processes. Lastly, comparing the recovery from five core floods in Table 4.1, it can be concluded that the multi-EOR application of DSSW+2SO_4^{-2} flooding in secondary and polymer-DSSW+2SO_4^{-2} in the tertiary mode performed efficiently, resulting in the highest recovery versus the lowest pore volume injected.

4.4 Polymer Stability Analysis

Figure 4.11 shows the DR of polymer solutions while flowing through flow lines before entering the core plugs. The DR was calculated using Equation 3.2. 300- ppm polymer-DSSW+2SO_4^{-2} was found to have a higher DR compared to 300-ppm polymer-DSSW at low to intermediate shear rates (same as an e-VROC response). The higher DR of 300-ppm Polymer-DSSW+2SO_4^{-2} was due to the increased amount of monovalent sodium cations present in the brine. Pipe flow supports the ionic interaction of sodium cations with anionic ions of polymer, which resulted in the increased DR. However, polymer-DSSW+2SO_4^{-2} has shown higher viscosity for fresh solutions but a significant decrease in polymer-DSSW+2SO_4^{-2} viscosity owing to mechanical degradation. This behaviour can be clearly seen in Figure 4.11. An increase in sulfates can enhance the polymer viscoelastic properties in porous media, but it can significantly develop polymer

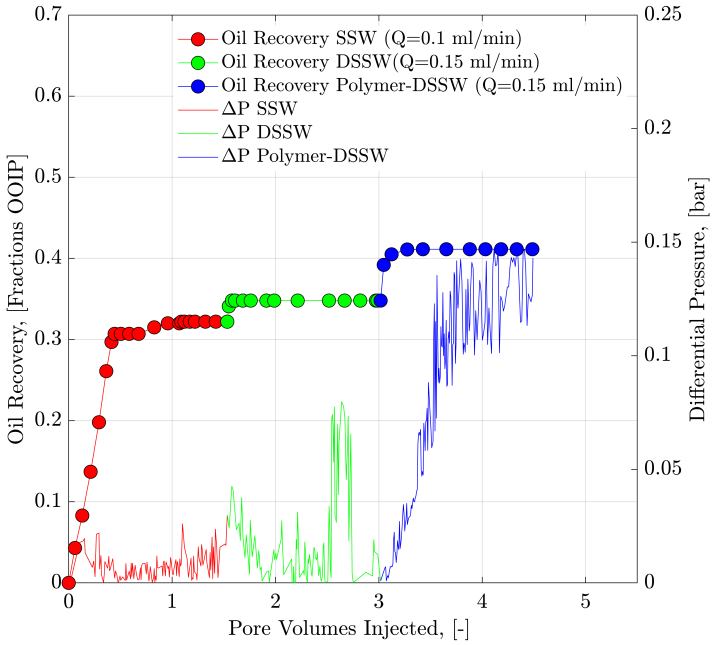

Figure 4.9: *Oil recovery and pressure drop versus PV injected for the Bent 5.4 core plug. Red represents the experimental data for secondary-mode injection of SSW, green represents the tertiary injection mode of DSSW, and blue represents the post-tertiary injection mode of polymer-DSSW*

sensitivity to mechanical degradation.

4.5 Results and Remarks

Based on the obtained data and observations of the experimental conditions presented here, the proposed sulfate-modified water process produced important results that indicate its potential influence on wettability alteration. Moreover, the work presented here provides a detailed workflow to evaluate the combined application of modified water and polymer flooding. Researchers assessing similar processes can implement this workflow.

The evaluation of polymer performance provides important findings; in particular, polymer solutions prepared in the presence of sulfate in the brine had higher viscosity compared to other brines with the same TDS (g/L). According to the rheological evaluation, linear viscoelastic measurements cannot clearly differentiate the viscoelastic response between the polymer solutions due to the lower concentrations implemented in this work. Nevertheless, the increase in sulfate led to an enhancement of the polymer viscoelastic properties determined through the increase in injection pressure observed from the core flooding experiments. The evaluation also shows that increasing the amount of sulfate made the solution more sensitive to mechanical degradation when flowing through

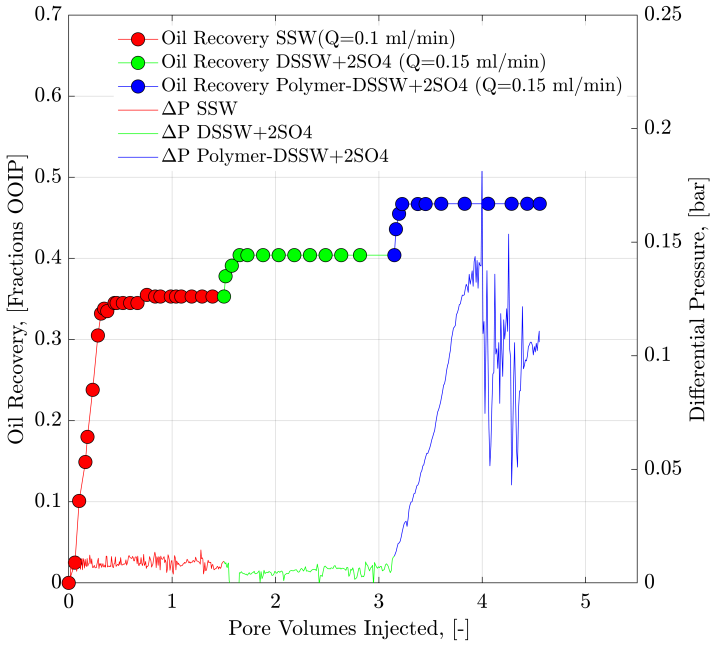

Figure 4.10: *Oil recovery and pressure drop versus PV injected for the Bent 5.5 core plug. Red represents the experimental data for secondary-mode injection of SSW, green represents the tertiary-mode injection of DSSW+2SO_4^{-2}, and blue represents the post-tertiary injection mode of polymer-DSSW+2SO_4^{-2}*

pipes and valves. Current industry applications seek to use low shear valves to minimize this impact.

For the two-phase flooding, core floods showed that low-salt or sulfate-modified water flooding should be performed before polymer flooding to achieve higher oil recovery. Otherwise, brine flooding after polymer flooding will follow the same path of pre-injected polymer without having contact with oil. Furthermore, DSSW+2SO_4^{-2} water flooding and DSSW injection produced almost the same recovery in the secondary mode. However, in the tertiary mode, polymer injection after DSSW+2SO_4^{-2} water flooding produced 4% more oil compared to polymer flooding after DSSW. It is assumed that this additional oil is due to the higher pressure/viscoelastic response for polymer-DSSW+2SO_4^{-2}. Finally, recovery experiments showed DSSW+2SO_4^{-2} and DSSW contributed to extra recovery compared to SSW in the secondary mode due to wettability alteration; however, the overall combination of DSSW+2SO_4^{-2} and polymer resulted in the higher recovery. The findings obtained by the two-phase flooding experiments support that both brines (DSSW+2SO_4^{-2} and DSSW) induce wettability alteration of the rock, pointing out that the wettability change for the case of sulfate-modified water strongly follows the presence of 2SO_4^{-2} as a catalyst for the alteration to take place.

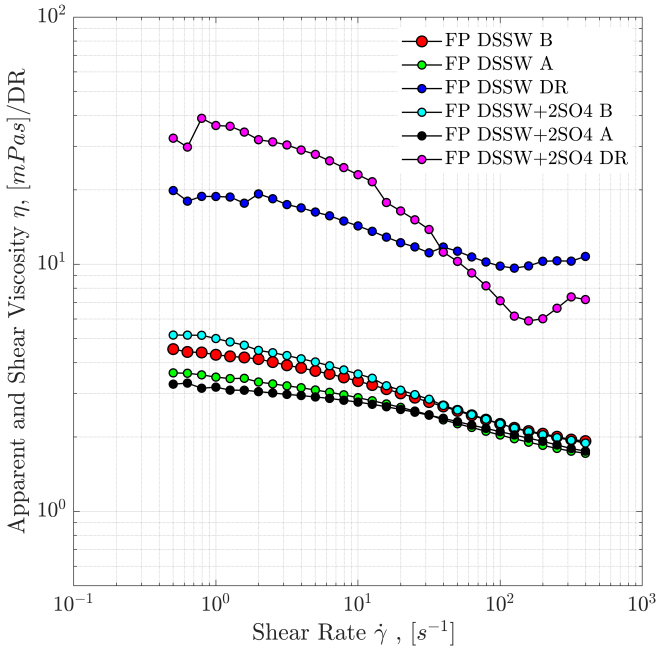

Figure 4.11: *Viscosity loss and mechanical degradation of polymer solutions through stainless steel pipe before entering the core plug. B represents the fresh solution while A represents the degraded solution through stainless steel pipe connections*

Chapter 5

Modified Sea Water Combined with Polymer Flooding

This chapter assesses the design of sulfate-modified water to analyse its impact on the reduction of remaining oil saturation and hence improved oil recovery. Moreover, it evaluates and defines the synergies/benefits between high-salt modified water and polymer flooding. SSW is used as the base brine, and optimization is performed by adding/removing specific chemical components of the SSW. Secondary- and tertiary-mode experiments were performed to evaluate the feasibility of applying modified water injection and its synergies with polymer flooding. Modified water with spiked sulfate changed the interfacial tension and developed interfacial interactions, compared with SSW. Hence, modified water injection contributed to extra oil recovery, resulting in the reduction of the remaining oil saturation. Furthermore, the higher concentration of the divalent cations in formation brine and complete removal of Na^{+1} in the injected brine, as well as the combination of modified water and polymer flooding, resulted in a significant decrease in the remaining oil saturation. The adopted workflow for this hybrid EOR study is summarised in Figure 5.1. The findings of this chapter were organized for journal publication with title of "Unlocking the Effects of Fluid Optimization on Remaining Oil Saturation for the Combined Sulfate-Modified Water and Polymer Flooding" in Energies 2020 (ISSN 1996-1073), 13(12), 3049; https://doi.org/10.3390/en13123049.

5.1 General Methodology and Approach

The chapter investigates the ability of combined EOR techniques (modified brine injection and polymer flooding), known as the hybrid method, to enhance the capability

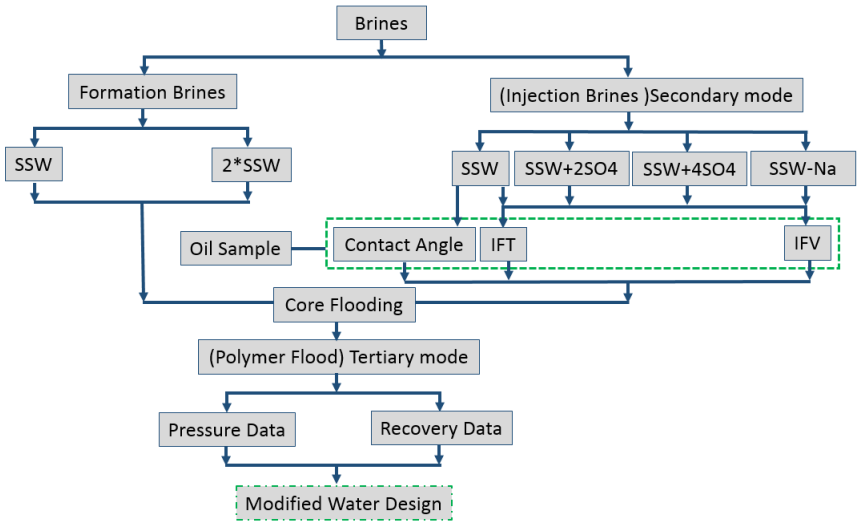

Figure 5.1: *Adopted workflow for SSW-based hybrid EOR process combined with polymer flooding*

of the flooding process. The objectives of this chapter are achieved using the following methodology to gather data and evaluate the results:

- ***Optimization of Formation and Injection Brines***: Two types of formation brine (BG1 in Table 3.1) and four types of injection brine (SSW as the base case and BG3 in Table 3.1) were generated. The primary approach was to prepare brines, focusing on the role of increasing the sulfate and varying the TDS of the SSW to correlate with the impact of salinity on oil recovery.
- ***Polymer Diluted Solutions at Target Concentration***: Low-concentration (750 ppm) polymer solutions were prepared to achieve a viscosity ratio of 2 between the oil and polymer, shown as Nr. 2 in Table 3.3. Polymer solutions were prepared to investigate the synergies and benefits of the combined EOR processes.
- ***Evaluation of Fluid-fluid Interactions***: Interfacial tension and oil-drop snap-off volume measurements were performed to investigate the ionic interaction between oil polar compounds and active ions in brine (Sections 3.3.1 and 3.3.2 from Chapter 3). The results of fluid-fluid interactions were incorporated to determine the possible impact on oil recovery.
- ***Contact Angle Measurements***: Contact angle measurements were performed to confirm the wettability alteration of Bentheimer core plugs from a water-wet to oil-wet condition (Section 3.2.1 from Chapter 3). Two approaches were adopted to cross-validate the results.
- ***Mechanical degradation of polymer solutions***: This step allowed helped to understand and define any possible degradation prior to the core face using

Equation 3.2 and to draw better conclusions on polymer performance.

- ***Two-phase Core Flooding Experiments***: Different brines were flooded through oil-wet core plugs, (CG2 in Table 3.5) as the secondary mode, followed by tertiary-mode polymer flooding. The purpose was to investigate the synergies of the promising hybrid EOR process. The experiments followed the flooding sequence explained in Table 3.7 to observe pressure response and to define oil recovery.

5.2 Fluid Optimization

5.2.1 Wettability Alteration

Contact angle measurements of aged Bentheimer core plugs confirmed the attachment of the polar oil compounds to the rock surface and wettability alteration from water-wet (Figure 5.4) to an oil-wet (Figure 5.5). The water wetness of the Bentheimer core plug, saturated with SSW, was determined as the oil drop did not result in any change in the contact angle over time (see Figure 5.2 and Figure 5.4). For the oil-saturated and aged core, a change in the contact angle was observed over time, confirming a possible wettability alteration due to the attachment of polar compounds with the rock surface over the aging period (Figure 5.3 and Figure 5.5). Per assumptions, Bentheimer has a negligible amount of clay (less than 1%), so quartz causes this wettability modification. The result is supported by Al-Saedi et al. [29], who reported that quartz behaves similarly to clays. According to Skauge et al. [102], the aging of Bentheimer cores at 50°C for three weeks would induce the attachment of oil polar compounds to the rock surface.

Figure 5.2: *Contact angle between SSW saturated core plug and oil drop at 0 minutes (left side) and after 60 minutes (right side)*

Additional observations were made using the pendant drop method to validate the contact angle measurements. This approach was used to measure the contact angle between the saturated core plugs (seawater and dead oil) and oil drop, as shown in Figure 5.4 and Figure 5.5, respectively. A similar trend was observed, as core plugs saturated with brine showed a water-wet condition while oil-saturated, aged core plugs were altered to an oil-wet condition.

Contact angle results obtained from both approaches, in-house measurements and

pendant drop method measurements, are in line. The brine-saturated core plug indicated water wettability of the core plug. However, the six-week aging process of the oil-saturated core plug resulted in wettability alteration from a water-wet to oil-wet condition. This wettability alteration to an oil-wet state was caused by the oil polar compounds' attachment to the rock surface through the bridging reaction of divalent cations present in the formation brine, as shown in Figure 1.1A.

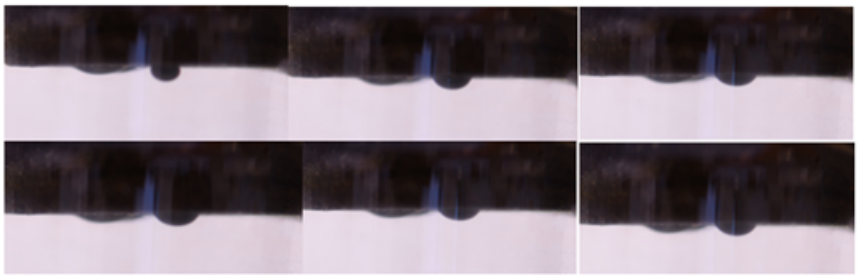

Figure 5.3: *Contact angle between oil-saturated, six-week aged core plug and oil drop at 0 minutes (top left) and after 60 minutes (bottom right)*

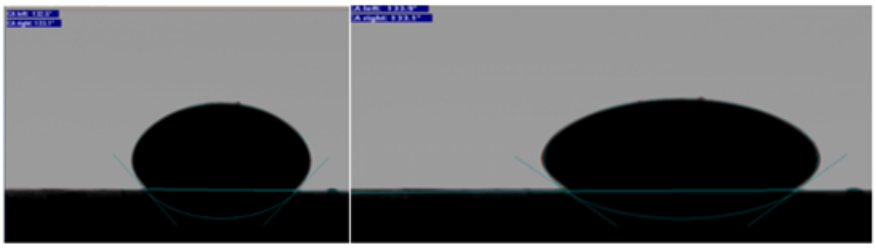

Figure 5.4: *Pendant drop method contact-angle measurement between brine-saturated core plug and oil drop at 0 minutes (left) and after 60 minutes (right)*

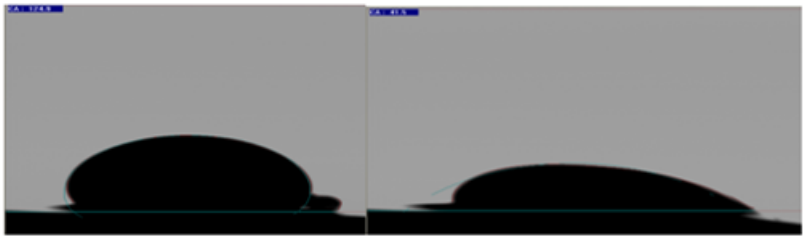

Figure 5.5: *Pendant drop method contact-angle measurement between oil-saturated, six-week aged core plug and oil drop at 0 minutes (left) and after 60 minutes (right)*

5.2.2 Impact of Sulfates on IFT

Table 5.1 presents the defined IFT response for each solution tested in this research. The results suggest that an optimum concentration of sulfate is a critical criterion to design adequate mechanized/modified water based on the fluid-fluid interfacial mechanism. SSW+$2SO_4^{-2}$ had the highest IFT value, which means it also resulted in the

development of an elastic layer at the oil-brine interface. Therefore, the actual impact of both factors (rigid interfacial layer and coalescence-suppressing interfacial barriers) on oil recovery needs to be cleared from the core flooding experiments. Two main points can be derived from Table 5.1;

- Doubling the amount of sulfates in SSW resulted in a doubled value of IFT (compares to SSW).

  It is assumed that changes obey the ionic reaction happening at the interface. Interactions between divalent ions in the brine and oil polar compounds (asphaltene) at the interface formed a stable layer. The results of Mohamed and Alvarado [1] and Moustafa and Shedid [3] support this assumption. Morin et al. [35] proposed that this elastic layer at the interface correlates with producing more oil due to continuous oil flow because the layer is resistant to oil-phase rupture. The improved interfacial layer developed at the fluid interface helped produce higher IFT measurements for SSW+$2SO_4^{-2}$ brine.

- Quadrupling the sulfates in SSW resulted in a decrease in the IFT response.

  A possible explanation for this behaviour is the presence of an excessive amount of sodium in the brine. An excessive amount of sodium in the brine can implicate the development of naphthenic salts through the reaction between sodium in the brine and NAs in the oil. Naphthenic salts are accumulated at the oil-brine interface and soften the interfacial film [90]. According to Alvarado et al. [92] and Moradi and Alvarado [31], the controlling mechanism is associated with two coalescence-suppressing interfacial barriers between fluids.

Table 5.1: *Interfacial tension (IFT) between brines and crude oil at 22°C*

Brine	IFT 1	IFT 2	IFT (Average)
	mN/m	mN/m	mN/m
SSW	2.03	2.37	2.20
SSW+$2SO_4^{-2}$	4.66	4.28	4.47
SSW+$4SO_4^{-2}$	2.11	2.01	2.06
SSW-0NaCl	2.85	3.02	2.94
2*SSW	3.15	3.39	3.27

5.2.3 Oil-drop Snap-off Volume Measurements

Table 5.2 summarises the defined data. The observed behaviour appears to be in line with the results reported for the IFT response. SSW+$2SO_4^{-2}$ depicted the biggest drop size

before the drop snap-off point, and the drop was sustained on the needle for 43 minutes. It is assumed that this is due to the improved oil-brine interface layer developed by the slow and irreversible adsorption process of asphaltene-sulfate at the oil-brine interface, as discussed earlier [32] [30] [33]. This adsorption process of asphaltene-sulfates resulted in the development of a stable interface between the oil and brine [88]. Moreover, the induced interfacial layer made the oil-drop resistant to rupture, or the oil-drop snap-off from the needle occurred after a longer time interval. Both sulfate and NAs produced repulsion forces at the interface, as shown in Figure 5.6(B). The ability of NAs to improve the oil-brine interfacial elasticity was also reported by Havre and Sjoeblom [84]. These repulsive forces resulted in a higher IFT response at the fluid interface. This higher IFT indirectly resulted in the development of an interfacial elastic layer at the fluid interface. Hence, the stable and elastic interfacial layer continued to produce large oil drops with increasing oil influx until the buoyancy force overcame the interfacial force. The higher buoyancy force caused oil-drop snap-off from the needle. Moreover, the strong interfacial layer made the oil drop resistant to rupture or snap-off from the needle for 43 minutes, as be seen in Table 5.2.

Table 5.2: *Oil drop-size analysis before snap-off*

Brine	Time till Snap-off	Oil Drop Size
	Minutes	μL
SSW	21	7.5
SSW+$4SO_4^{-2}$	11	5.0
SSW+$2SO_4^{-2}$	43	12.5

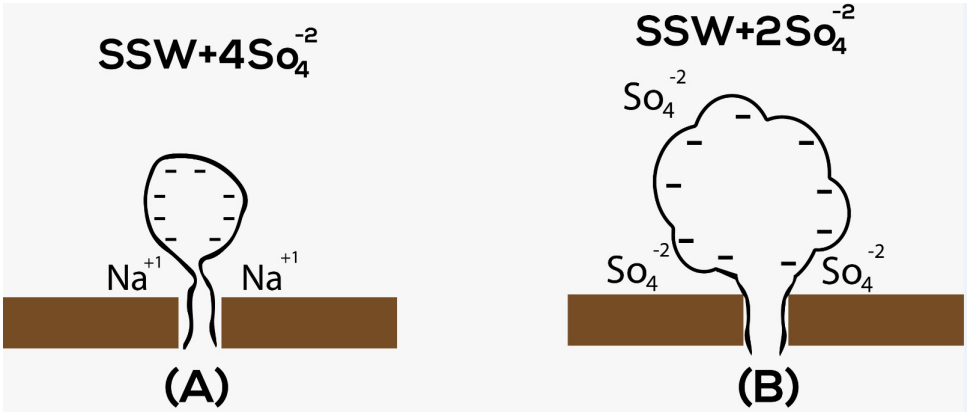

Figure 5.6: *Ionic activity of sodium and sulfate ions to develop small and large drops, respectively*

An additional point to note is that SSW+$4SO_4^{-2}$ had the smallest oil drop size at the snap-off point. A reason for this is an excessive amount of sodium can cause coalescence-suppressing interfacial barriers at the oil-brine interface. An excessive amount of sodium can promote the stability of microscale water-in-crude oil emulsions at the interface

and, hence, early snap-off of the oil drop from the needle, as shown in Figure 5.6 (A). According to Kiran at al. [90], an excessive amount of sodium results in the formation of naphthenic salts at the interface, which, in turn, softens the interfacial barrier. In simple words, attractive forces are developed at the oil-brine interface as the result of an excessive amount of sodium ions and negative oil polar compounds (NAs), as presented Figure 5.6 (A). These attractive forces result in microscale soap formation at the interface, which results in a decrease of IFT. Hence, buoyancy becomes dominant at the small oil-drop size, which results in earlier oil-drop snap-off from the needle.

A series of images shown in Figure 5.7 through Figure 5.9 depict the oil-drop size development during the snap-off evaluation. As shown, the oil drop in SSW brine developed drop volume up to 7.5μL, which was sustained for 21 minutes (Figure 5.7), while in SSW+4SO_4^{-2} brine, the drop volume reached only 5.0μL and was sustained for 11 minutes before snap-off (see Figure 5.8). Moreover, in SSW+2SO_4^{-2} brine, the largest oil drop size developed, at 12.5μL volume, with snap-off occurring at 43 minutes (Figure 5.9).

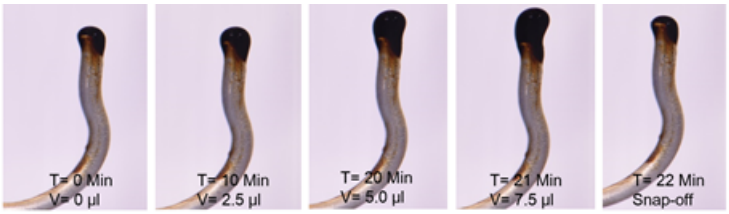

Figure 5.7: *Oil drop volume increased till the snap-off point in SSW brine (Fluid interfacial interactions)*

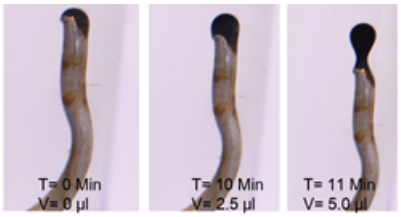

Figure 5.8: *Oil drop volume increased till the snap-off point in SSW+4SO_4^{-2} brine (Fluid interfacial interactions)*

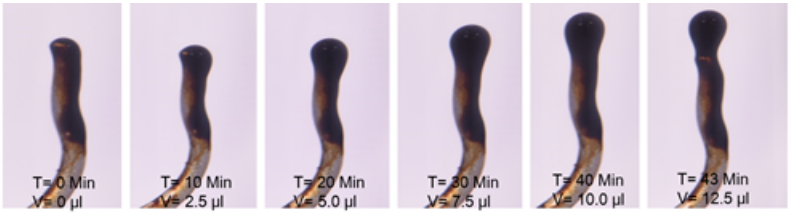

Figure 5.9: *Oil drop volume increase till snap-off point in SSW+2SO_4^{-2} brine (Fluids interfacial interactions)*

As an overall observation, doubling amount of sodium sulfate improved the asphaltene-sulfate adsorption process at the oil-brine interface and helped develop a stable interfacial barrier. This improved elastic response resulted in the higher IFT values and the production of larger oil drops. Further, increasing the amount of sodium sulfate, catalysed the ionic reaction between sodium ions in the brine and NAs in the oil. This reaction produced a negative impact on the oil-brine interfacial film, resulting in lower IFT values and hence small oil drop production.

5.2.4 Steady Shear Rheology (Shear Viscosity)

Figure 5.10 shows the shear viscosity of polymer solutions (injected in the tertiary mode). The selection criteria for polymer viscosity was described in Chapter 3 as Nr. 2 in Table 3.3. The main idea is to select a polymer concentration that provides half of the dead oil viscosity (≈4.0 mPas at a shear rate of 10 s^{-1}); hence, 750-ppm polymer concentrations were injected in the tertiary mode for the core flooding experiments.

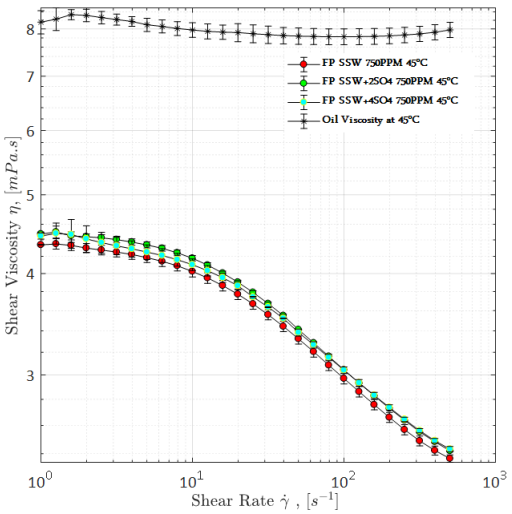

Figure 5.10: *Steady shear viscosity of polymer solutions at a temperature of 45°C. Polymer solutions are prepared in three injection brines*

5.3 Oil Recovery and Pressure Response

5.3.1 Core Flooding Sequence

Core flooding was performed according to the sequence described in Table 3.7. Cores were initially flooded in secondary-mode brine flooding through oil-saturated core plugs with

initial water saturation, as mentioned as CG2 in Table 3.5. The injected brines shown as BG3 in Table 3.1. Subsequently, as the second phase of injected fluids, polymer flooding was performed as the tertiary mode. Polymer diluted solution viscosities at 45°C and concentrations are reported as Nr. 2 in Table 3.3. Polymer viscosity was selected as half of the oil viscosity. Bump rate injection was also performed between secondary- and tertiary-mode flooding to eliminate fingering effects, if present.

5.3.2 Core Flooding and Oil Recovery Observations

Table 5.3 and Figure 5.11 summarise the results obtained for the core flooding experimental workflow defined in Table 3.7. The recovery factor (RF) indicates strong dependency on the chemical composition of the formation brine, injection brine, and, presumably, the fluid-fluid/rock-fluids interactions, as previously discussed. The most relevant observations from Table 5.3 and Figure 5.11 can be grouped into these categories:

- SSW as formation brine.
- Double SSW as formation brine.

Table 5.3: *Summary of core flooding experiment results and comparison of obtained recoveries (per Table 3.7)*

Nr.	Form. Brine	Inj. Brine	Core Name	ϕ	k, brine	Soi	RF Sec.	Inj. PV	RF BR	Inj. PV	RF Tert.	Inj. PV	Total RF (%)	ROS (%)
1	SSW	SSW	T2	26.53	2067	84.34	34.27	3	7.55	3	13.94	3	55.76	44.24
2		SSW+2SO_4^{-2}	T7	26.76	1952	82.11	45.69	3	7.07	3	8.84	3	61.60	38.40
3		SSW+4SO_4^{-2}	T8	26.06	1970	81.33	38.98	3	9.28	3	9.90	3	58.16	41.84
4		SSW-0NaCl	T1	27.18	2148	79.39	32.01	3	14.95	3	12.56	3	59.52	40.48
5	2*SSW	SSW	T6	26.41	1944	82.20	34.56	3	10.36	3	12.67	3	57.59	42.41
6		SSW+2SO_4^{-2}	T4	26.20	2113	79.48	41.37	3	13.59	3	10.05	3	65.01	34.99
7		SSW+4SO_4^{-2}	T5	28.56	1946	79.03	51.78	3	11.50	3	8.83	3	72.11	27.89
8		SSW-0NaCl	T3	26.22	2051	78.61	45.35	3	9.67	3	16.32	3	71.34	28.66

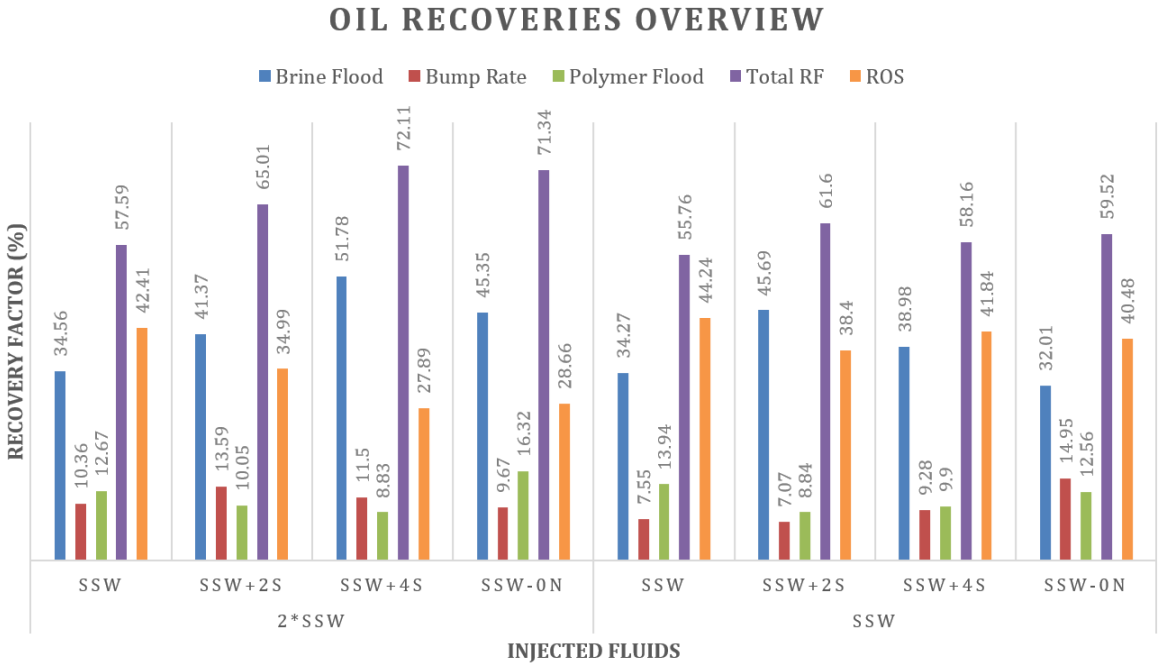

Figure 5.11: *Graphical overview of oil recovery and remaining oil saturation demonstrated in Table 5.3*

5.3.3 SSW as Formation Brine (Secondary-mode Brine Flooding)

- Secondary-mode SSW injection (T_2 core) resulted in the least RF at around 34%. A similar result was obtained under the same flooding conditions in the work outlined in Chapter 4.
- Injection of chemically modified brines disturbed the ionic equilibrium system inside the core plug. However, the aging of core plugs resulted in the attachment of polar compounds on the rock surface (previously confirmed in this work).
- Core plug T_7 had in the lowest remaining oil saturation (54.31%) after secondary-mode sulfate-modified water injection (SSW as formation brine). This response is assumed to correlate with improved fluid-fluid interfacial interaction (previously discussed). SSW+2SO_4^{-2} had the highest fluid-fluid interfacial interaction (IFT and oil-drop snap-off volume measurements). During core flooding, the wettability alteration process is initiated through modified brine, resulting in detachment of the oil from the rock formation. In parallel, in the oleic phase, contact with the injected brine forms an ionic interfacial layer. Presumably, this ionic interfacial layer helps with the continuous flow of oil. This further restricts the oil drop's reattachment on the rock surface, hence the plugging and entrapment of the oleic

phase.

- Flooding SSW+4SO_4^{-2} produced the second-highest oil recovery of 38.98%. This significantly lowered the remaining oil saturation compared to SSW brine and SSW-Na injection, which may be associated with improved fluid-fluid interaction. It is believed that the excessive spiked amount of sulfates (4SO_4^{-2}) helped to decrease IFT to 2.06 mN/m. Related to the IFT and oil-drop snap-off evaluations, the smallest drop-size detachment was observed, and the improved oil-brine interface reaction helped produce microscale water-in-oil emulsions (or microscale soap formation).
- The oil recovery results are in line with the results obtained by Mohamed and Alvarado [1]. Maximum oil recovery was obtained by increasing the sulfates in SSW by three and five times. According to the authors, three and five times more sulfate results in the highest interfacial viscoelasticity.
- It can be seen from experiments Nr.1 through 4 of Table 5.3 that the improved fluid-fluid properties have a dominant role compared to microscale water-in-oil emulsions for higher oil production. Moreover, the amount of sulfate added to designed modified water is a critical parameter that requires attention. Injecting SSW and SSW-0NaCl did not lead to additional oil production due to a lack of active sulfate ions. It is assumed that neither of the brines could disturb the established ROB ionic equilibrium and hence could not improve oil recovery (weaker fluid-fluid interaction).

5.3.4 Double SSW as Formation Brine (Secondary-mode Brine Flooding)

- Focusing on the second group of experiments (Nr. 5 through 8 from Table 5.3), SSW injection produced the lowest recovery of 34.56%, leaving a significant amount of remaining oil saturation (65.44%) in the core.
- Injecting SSW+4SO_4^{-2} resulted in the highest RF of 51.78% and the lowest remaining oil saturation of 48.22%. This behaviour is in contrast with injecting SSW+2SO_4^{-2} (Nr. 1 through 4 from Table 5.3), which produced the highest recovery with SSW as formation brine. The same result can be reasonably expected for remaining oil saturation (ROS) with 2*SSW formation brine. However, this did not happen and instead, SSW+4SO_4^{-2} produced the highest recovery. This is associated with the relationship between the chemical composition of injection and formation brines. As the formation brine composition is doubled to 2*SSW, the

sulfate amount must be quadrupled in the injection brine. This process is necessary to compensate for the ionic reaction based on fluid-fluid interaction. Therefore SSW+4SO_4^{-2} produced the highest recovery with 2*SSW formation brine.

- The second-lowest ROS (54.65%) was achieved by injecting SSW-0NaCl brine. This result is in line with the results reported by Zhang et al. [22]. The higher recovery is believed to be connected to the role of the PDI and non-PDI ions in the system. 2*SSW formation brine was saturated with PDI (Ca^{+2} and Mg^{+2} ions) while the injection brine had no non-PDI (Na^{+1}). An additional supporting argument for higher recovery is the reduced TDS. TDS of SSW-0NaCl were less than half that of SSW. Therefore, in this case, the low concentrations of salts could also play a role. It can be claimed that the combined scenario of PDI and non-PDI ions and low salinity played a crucial role in lowering the ROS. However, the ROS obtained in the T_1 core plug indicates otherwise, suggesting that the role of low concentrations of salts was negligible. Finally, the activity of PDI and non-PDI ions support the lowered ROS in the T_3 core flood.

Summarising the results of secondary-mode injection for both formation brines, it is clear that combined mechanisms of wettability alteration in porous media and improved fluid-fluid interfacial interactions are responsible for the higher oil recovery. Further, the spiked amount of sulfates in injection brine significantly lowered the ROS. In addition, both sets of experiments further explained that the relationship between the amount of sulfates added and oil recovery is not strictly linear. Hence, having an optimum amount of sulfates is an important parameter to achieve the lowest ROS. These experiments also suggest that the chemical relationship between injection brine and formation brine is essential.

5.3.5 Bump Rate: Remaining Oil Saturation

- The RF bump rate results in Table 5.3 indicate the oil produced through the bump rate. Bump-rate injection is performed at a higher rate (more than doubled) than brine flooding, as described earlier. This higher injection rate could cause a higher-pressure differential along the core and cause oil to be trapped due to capillary end effects.

- Looking at the figures for oil recovery, the T_4 and T_1 plugs produced the maximum oil, reducing the highest ROS. There is no specific trend regarding the relationship between the bump rate and RF based on the chemical composition of the previously injected brine. The RF obtained for the bump rate provides significant

insights into the production of trapped oil due to capillary end effects. A higher recovery (14.95%) from T_1 is expected because of the highest ROS (67.98%) after secondary-mode brine flooding. Interestingly, however T_4 also produced significant oil (13.59%). Comparing the RF of the T_4 and T_5 experiments (secondary mode), the difference becomes significant (10%). It is assumed that some oil is released due to improved fluid-fluid interaction in T_4 and could not be recovered due to the strong capillary end effects. However, the bump rate helped to release this trapped oil due to the excessive pressure drop.

5.3.6 Remaining Oil Saturation after Tertiary-mode Polymer Flooding

- Polymer flooding in the tertiary recovery mode also resulted in a significant reduction in ROS, as shown in Table 5.3. As previously mentioned, the objective is to lower ROS due to viscosity support from tertiary-mode flooding. Therefore, the viscosity of the polymer is defined as half that of the oil viscosity so the viscosity value lies between that of the brine and oil. It can be argued that this oil recovery is only due to mobility control of the polymer flood. However, Shaker Shiran and Skauge [7] found that hybrid EOR (combined EOR techniques) flooding results in higher recovery compare to a single EOR technique.

- Looking at the recovery numbers, polymer flooding after SSW-0NaCl significantly decreased ROS in the T_3 core (with 2*SSW as formation brine). The combined effect of PDI ions in the formation fluid and removal of non-PDI ions in the injected fluid released oil from the core surface, but this oil could not be produced even with the bump rate. The changes in viscosity due to the polymer flood made it possible for this detached oil to flow. Therefore, this contributed to lower the ROS to 16.32%. Interestingly enough, polymer flooding after SSW flooding contributed to significant recovery (12.67% and 13.4%), but the reason for this is the higher amount of ROS (in both T_2 and T_6 plugs). Moreover, comparing the final ROS from T_2 and T_6, the data depict the highest values among all scenarios. It is likely that polymer flooding produced higher recoveries due to the higher ROS of T_2 and T_6 plugs. Subsequently, polymer flooding after sulfate-modified water flooding reduced ROS by 9% to 11%, which is significant.

5.3.7 Final Recovery and Remaining Oil Saturation

- Table 5.3 shows that the improved fluid-fluid interfacial interaction significantly reduced the ROS (T_7 and T_5 cores) in both groups of formation brines.
- Depleted Na^{+1} in injection brine and a spiked amount of Ca^{+2} and Mg^{+2} ions in formation brine also produced significant oil recovery (71.34%). This result is in agreement with the data reported by Zhang et al. [27].
- According to the final ROS data of the T_3 and T_5 experiments, the flooding process of T_5 (SSW+4SO_4^{-2}) is commercially economical. The main reason for this is the brine processing cost of SSW-0NaCl for T_3. Na^{+1} removal from SSW can cost much more compared to the addition of a small amount of sulfate in the injection brine to design the modified water. Economically and technically, the spiked amount of sulfate is a feasible process on a commercial scale.
- The highest ROS was seen after the injection of SSW in both groups of experiments, as shown in Table 5.3. As previously described, this is because the injection and formation brines shown in Table 3.1 have the same hardness value. The modification of SSW to design modified water established a contrast in hardness between injected and formation brine. This process further manipulates the ionic equilibrium in the reservoir system. As seen in Table 3.1 and Table 5.3, the lowest ROS values were observed when the hardness contrast between injection and formation brine is significant. To summarise, the combined EOR process worked efficiently, contributing to significant oil recovery.
- Maximum total oil recovery was observed for the hybrid EOR process of SSW+4SO_4^{-2} and SSW+2SO_4^{-2} injection in the secondary mode and polymer flooding in the tertiary mode (SSW as formation brine). Similarly, in the case of 2*SSW formation brine, the highest total recovery was achieved through a hybrid EOR process comprising injecting SSW+4SO_4^{-2} and SSW-Na in the secondary mode followed by polymer flooding in the tertiary mode. However, SSW-Na preparation is not commercially economical, which further indicates that sulfate-modified brine should be injected in the secondary mode. To sum up, hybrid EOR processes worked efficiently, contributing to significant oil recovery, as found by Shaker Shiran and Skauge [7] and Tahir et al. [69].

5.3.8 Modified Water Injection in the Tertiary Mode

Table 5.4 describes the injection of modified water in the tertiary mode after SSW injection (core T_{10}). Note that the bump rate, before modified water injection, produced

significant oil; this is assumed to eliminate possible capillary end effects. On one hand, sulfate-modified water injection worked well in the tertiary mode contributing to a 9.64% reduction in ROS. In contrast, sulfate-modified water injection in the secondary mode (T_7 in Table 5.3) contributed to 2% increased recovery compared to the combination of SSW in the secondary mode and sulfate-modified water injection in the tertiary mode (Table 5.4). This comparison leads to the recommendation to adopt sulfate-modified water injection in the secondary mode as the best strategy.

Table 5.4: *Core flooding experiment with tertiary-mode sulfate-modified water injection (per Table 3.7)*

Nr.	Form. Brine	Inj. Brine	Core Name	ϕ (%)	k_b (mD)	Soi	RF Sec. (BF)	Inj.PV	RF BR	Inj. PV	RF Tert. (MWF)	RF Post-Tert. (PF)	Total RF (%)
1	SSW	SSW	T10	26.43	2108	73.64	34.04	3	10.21	3	9.64	3.97	57.857

5.3.9 Oil Recovery Profile versus PV Injected

It was challenging to develop the oil production profile over the pore volume injected after the brine breakthrough. Before the breakthrough, both oil and brine phases were stable in the fraction collector due to the continuous one-phase flow. Hence, it was possible to measure oil produced over time. After the breakthrough, oil and brine production overlapped in the calibrated collector. Oil drop movement towards the top and brine movement towards the bottom was observed in the fraction collector due to gravitational differences. This opposite fluid movement created phase entrapment and a kind of emulsion, as can be seen in Figure 5.12(left). One reason for this could be the oil viscosity, since before the aging process, oil viscosity was measured to be 8.0 mPa.s. However, during the six-week aging period, the evaporation of lighter oil components reduced the oil level. Oil refilling was performed twice during the aging process to keep core plugs inside the oil phase. Therefore, it is expected that lighter components evaporated, leaving behind the heavier components. Moreover, core flooding was performed at 45°C and the fraction collector was at room temperature (i.e., 22°C). It is expected that the combined action of the temperature difference and enriched heavier oil components in the core caused phase entrapment and emulsion development in the fraction collector, as shown in Figure 5.12(left). This problem was solved by providing phase settlement time at a higher temperature (45°C) for 3 hours. After each flooding experiment, the fraction collector was kept in an oven for 3 hours, and the volume of both phases (oil and brine) were measured afterward, as shown in Figure 5.12(right). Unfortunately, this technique could not provide the after-breakthrough produced oil values over time to draw a production profile. Therefore, the final recovery data and pressure response are the outputs of flooding experiments.

5.3.10 Pressure Response Observations

Figure 5.13 to Figure 5.17 represent the pressure response of selected core flooding experiments described in Table 5.3. Figure 5.18 describes the pressure behaviour of the experiments described in Table 5.4. As can be seen, the pressure response is nearly the same for both the secondary-mode brine flooding and bump-rate injection. Figure 5.16 presents an exception of the measured pressure data. A slightly higher but unstable pressure was observed. One explanation could be the presence of small air bubbles in the pipe that connects the pressure sensor (experimental artefact). Overall, pressure trends for all flooding experiments are about the same. A significant increase in pressure was observed for polymer flooding after brine flooding for all experiments, resulting in an increase in pressure until the breakthrough.

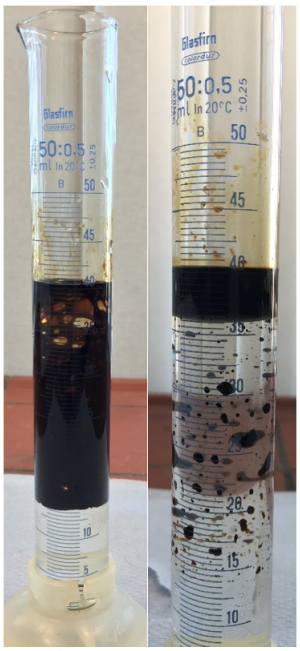

Figure 5.12: *Oil produced after the brine flooding in the secondary mode. Phase entrapment during core flooding (left) and the same fluids after phase settlement in an oven (right)*

5.4 Polymer Degradation and Stability Analysis

Figure 5.19 depicts the viscosity loss in the polymer solution and hence the degradation rate (according to Equation 3.2). Polymer solutions are sensitive to the amount of sulfate added to the brine while designing the modified water. The steady shear viscosity curve shows that the higher the amount of added sulfates, the higher the mechanical degradation observed. Moreover, the highest mechanical degradation, and hence the highest viscosity loss, happens when the polymer solution enters the core. Therefore, two main insights can be drawn here:

- Mixing polymer solutions in sulfate-modified water may not be an excellent solution or a promising approach.
- Mixing polymer solutions in SSW can result in mechanically stable polymer solutions, subsequently affecting economics (utility factor).

The impact of polymer degradation can be clearly seen from Table 5.3 and Figure 5.11. The polymer prepared in SSW produced higher recovery compared to the polymer prepared in modified water in the tertiary mode. A spiked amount of sulfate made the polymer solution sensitive to mechanical degradation and sweep efficiency in porous media was an issue. This indicates that polymer-SSW flooding after sulfate-modified water injection can produce higher recovery compared to polymer-SSW+$2SO_4^{-2}$. The

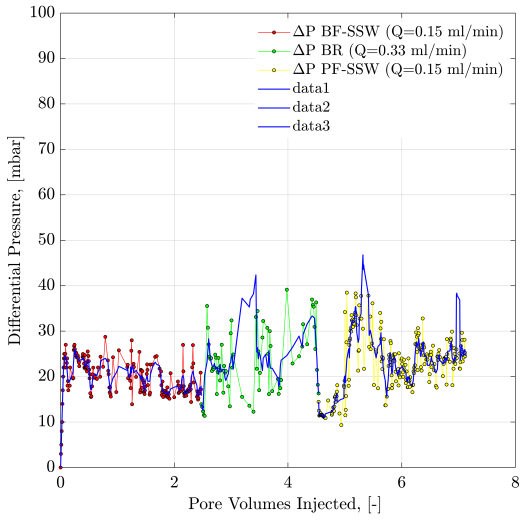

Figure 5.13: *Pressure drop versus PV injected for the T_6 core plug. Red represents the experimental data for secondary-mode injection of brine flood, green represents the experimental data for the bump rate, and yellow represents tertiary-mode injection of polymer flood. The blue line represents the smoothed data function. 2*SSW is the formation brine.*

same polymer sensitivity results with the spiked amount of sulfates were also obtained in Chapter 4.

5.5 Results and Remarks

Based on the experimental investigation and the evaluation of the obtained results in this chapter, it can be concluded that the proposed sulfate-modified water application helped to reduce ROS significantly.

Combined evaluations of fluid-fluid interfacial interaction measurements lead to the conclusion that a spiked amount of sulfates in the injected brine allowed a stable ionic interfacial layer to develop at the oil-brine interface. This stable layer formed due to the ionic reaction, which turned into fluid-fluid interaction. Later core flood experiments proved that the injection of sulfate-modified water disturbed the established ROB ionic equilibrium in the reservoir. This disturbance caused detachment of the oil phase from the rock surface, and sulfates developed an interfacial layer at the interface. This improved the fluid interface, helping to produce continuous oil flow and hence reducing the ROS.

Furthermore, it can also be concluded that the chemical relationship between injection and formation brines is essential to design the modified water. With SSW as formation brine, SSW+$2SO_4^{-2}$ injection resulted in the lowest ROS. With 2*SSW as

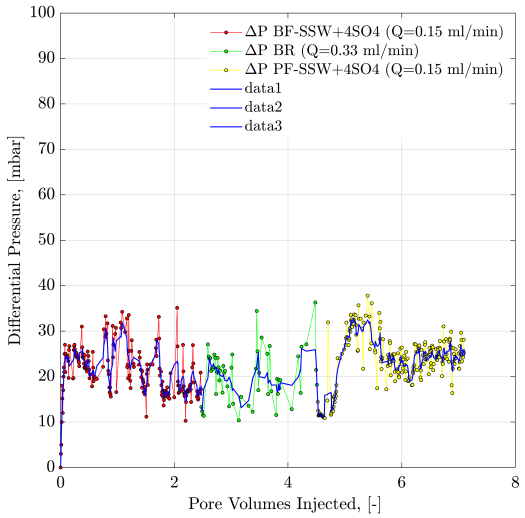

Figure 5.14: *Pressure drop versus PV injected for the T_5 core plug. Red represents the experimental data for secondary-mode injection of brine flood, green represents the experimental data for the bump rate, and yellow represents tertiary-mode injection of polymer flood. The blue line represents the smoothed data function. 2*SSW is the formation brine.*

formation brine, SSW+$4SO_4^{-2}$ injection resulted in the lowest ROS. This relationship is due to ionic interaction between divalent cations in the formation brine and sulfate ions of the injection brine. Moreover, the role of PDI (Ca^{+2} and Mg^{+2}) in the formation brine and removal of non-PDI (Na^{+1}) in the injection brine is also significant in ROS reduction.

Looking at the synergies and benefits of sulfate-modified water with polymer flooding, the lowest ROS was achieved after the secondary mode of modified water and tertiary-mode polymer flooding. Finally, the addition of sulfate when designing sulfate-modified water worked perfectly, resulting in less ROS. However, polymer solutions should not be prepared in modified water. A higher amount of sulfates can make the solutions sensitive to mechanical degradation and hence higher viscosity loss.

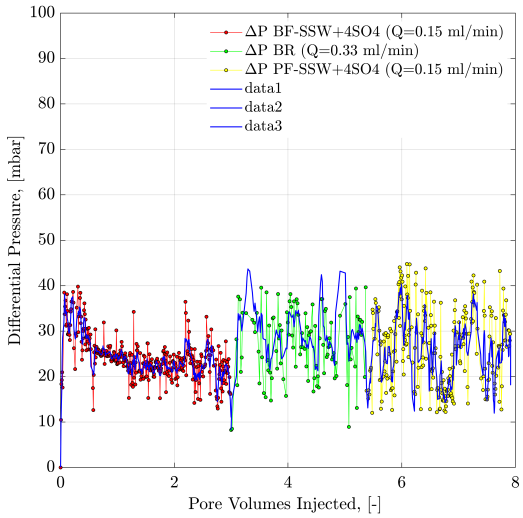

Figure 5.15: *Pressure drop versus PV injected for the T_8 core plug. Red represents the experimental data for secondary-mode injection of brine flood, green represents the experimental data for the bump rate, and yellow represents the tertiary-mode injection of polymer flood. The blue line represents the smoothed data function. SSW is the formation brine.*

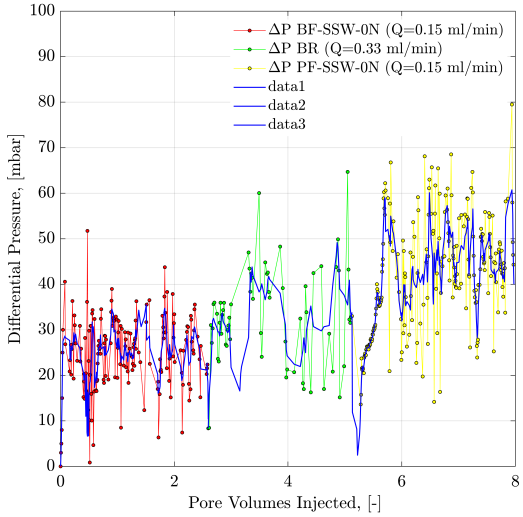

Figure 5.16: *Pressure drop versus PV injected for the T_1 core plug. Red represents the experimental data for secondary-mode injection of brine flood, green represents the experimental data for bump rate, and yellow represents the tertiary-mode injection of polymer flood. The blue line represents the smoothed data function. SSW is the formation brine.*

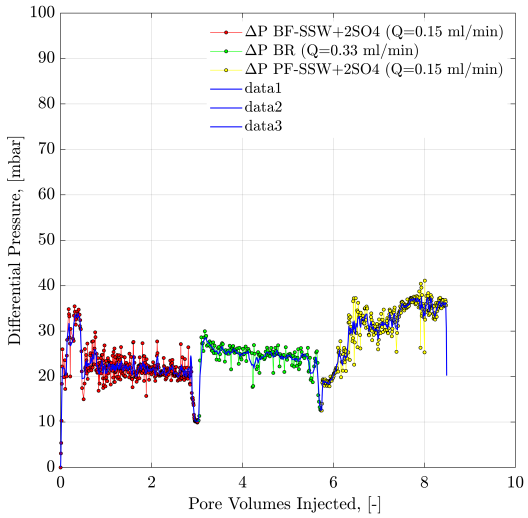

Figure 5.17: *Pressure drop versus PV injected for the T_7 core plug. Red represents the experimental data for secondary-mode injection of brine flood, green represents the experimental data for the bump rate, and yellow represents the tertiary-mode injection of polymer flood. The blue line represents the smoothed data function. SSW is the formation brine.*

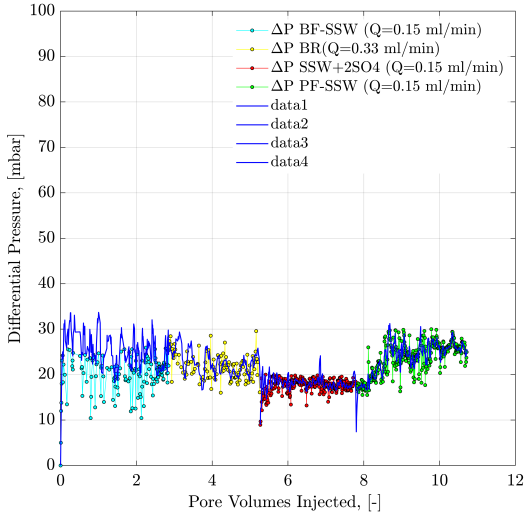

Figure 5.18: *Pressure drop versus PV injection for the T_{10} core plug. Cyan represents the experimental data for secondary-mode injection of brine flood, yellow represents the experimental data for the bump rate, red represents the tertiary-mode injection of modified water ($SSW+2SO_4^{-2}$), and green represents the post-tertiary-mode polymer flood. The blue line represents the smoothed data function. SSW is the formation brine.*

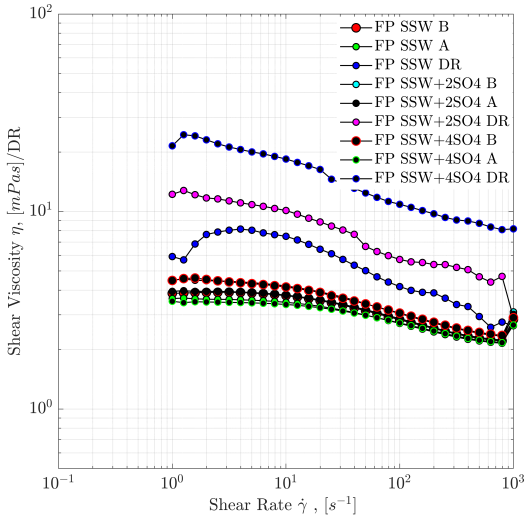

Figure 5.19: *Viscosity loss and mechanical degradation of polymer solutions through stainless steel pipe before entering the core plug. B represents the fresh solution, and A represents the degraded solution through stainless steel pipe connections.*

Chapter 6

Sulfate-modified Seawater in Micromodels

This chapter describes the flow behaviour of the oil recovery obtained by the injection of sulfate-modified/low-salinity water in micromodels with different wettabilities. It provides a detailed microscopic visualization of the displacement taking place during modified water flooding at a pore-scale level while evaluating the effect of wettability on oil recovery. A comprehensive workflow for the evaluation is proposed that includes fluid-fluid and rock-fluid interactions. The methods studied comprise flooding experiments with micromodels. Artificial and real structure water-wet micromodels are used to understand flow behaviour and oil recovery. Subsequently, water-wet, complex-wet, and oil-wet micromodels help understand wettability and rock-fluid interaction. The effect of the sulfate content present in the brine is a key variable in this work. The results of micromodel experiments conducted in this work indicate that sulfate-modified water flooding performs better in mixed-wet/oil-wet (artificial structure) than water-wet systems. This slightly differs from observations of core flood experiments (Chapter 5), where oil-wet conditions provided better process efficiency. As an overall result, sulfate-modified water flooding recovered more oil than SSW injection in oil-wet and complex-wet systems compared to water-wet systems. Figure 6.1 summarises the adopted workflow and experimental procedures. The findings of this chapter were organized for journal publication with title "Flow Dynamics of Sulfate-Modified Water/Polymer Flooding in Micromodels with Modified Wettability" in Applied Sciences 2020 (ISSN 2076-3417), 10(9), 3239; https://doi.org/10.3390/app10093239.

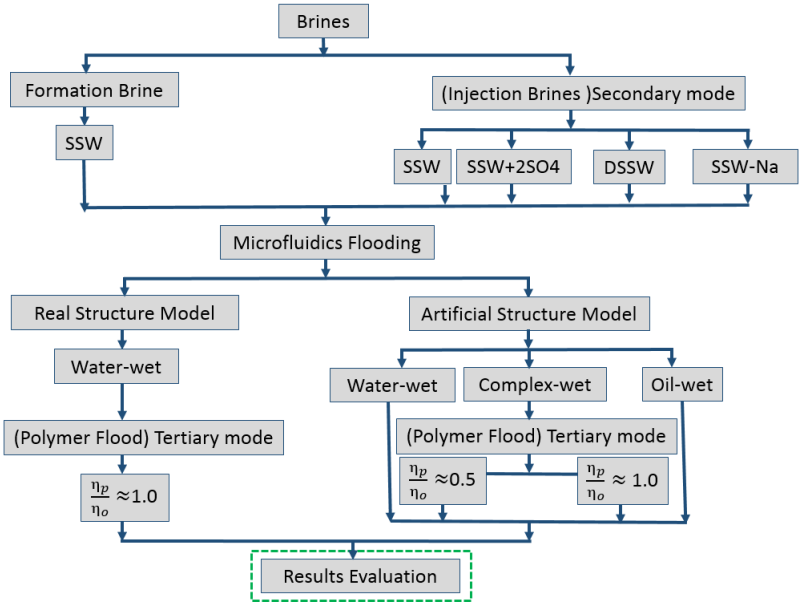

Figure 6.1: *Adopted workflow for hybrid EOR process in micromodels*

6.1 General Methodology and Approach

The proposed workflow helps create an understanding of the role of fluid-fluid interfacial interaction as a recovery mechanism other than wettability alteration. Furthermore, an attempt is made to analyse the success of the mechanism of a hybrid EOR comprising modified water application in combination with a polymer flood. The following steps were completed to achieve the objectives of this chapter:

- ***Brine Preparation and Optimization***: Four different injection brines were prepared to correlate and cross-validate the fluid-fluid interaction and oil recovery results (BG2 and BG3 in Table 3.1). The amount of sulfate in the brine and TDS were the key parameters for comparison.
- ***Polymer Diluted Solutions Preparation***: Polymer solutions with an oil-to-polymer viscosity ratio of 1 and 2 at a shear rate 10 s^{-1} were prepared to inject in the tertiary mode for viscosity control. Polymer viscosity and concentrations are reported as Nr. 3 and Nr. 4 in Table 3.3.
- ***Wettability and Geometry of the Porous Media***: Micromodels with three wettability conditions, summarised in Table 3.9, were used to investigate the role of wettability on fluid-fluid interfacial interaction. Moreover, two types of water-wet micromodels with different rock geometries/characteristics were further investigated to cross-analyse the results presented in Table 3.8.
- ***Two-phase Modified Brine Injection Combined with Polymer Flooding in Micromodels***: Flooding experiments were performed with oil-saturated mi-

cromodels with established initial water saturation. Brines were injected as the secondary mode and polymer flooding was performed in the tertiary mode with a mix-wet micromodel to evaluate and define the benefits and synergies of the combined EOR process.

6.2 Steady Shear Viscosity

Figure 6.2 shows the steady shear viscosity of polymer solutions injected in the tertiary mode (after brine flooding). As mentioned earlier, two (2) concentrations of 1,000 ppm and 1,500 ppm diluted solutions were selected based on the viscosity selection. The 1,000-ppm diluted solution had half the viscosity of the oil while the 1,500-ppm diluted solution had almost the same viscosity as the oil at a shear rate of $10s^{-1}$. Table 6.1 presents shear viscosity values at a shear rate of $10s^{-1}$. The same concentration of polymers was also prepared in sulfate-modified water. As described in previous chapters (4 and 5), the viscosity contrast was not substantial, both with and without sulfate.

The results of fluid-fluid interaction between the brine-oil interface, static interfacial tension, and oil-drop snap-off volume are briefly described in Chapter 5. Therefore, the critical outcomes of both measurements (IFT and oil-drop snap-off volume) from the work completed were used to interpret the impact on oil recovery.

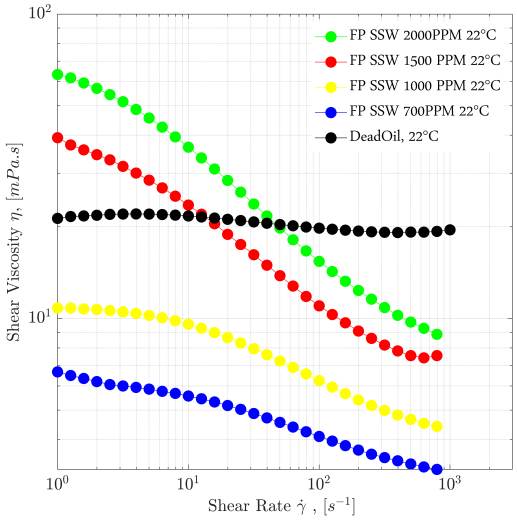

Figure 6.2: *Steady shear viscosity of polymer solutions at 22°C*

Table 6.1: *Polymer concentrations and viscosity at a shear rate of* $10s^{-1}$

HPAM Polymer at 22 °C	
Conc. (ppm)	**η at $10s^{-1}$ [mPa.s]**
700	5.56
1000	**9.58**
1500	**23.58**
2000	36.54
Dead Oil	**21.71**

6.3 Wettability Conditions of Micromodels

Wettability of the micromodel was confirmed by visual observation, through the concave/convex interface of the reservoir fluids (oil and brine) with a circular matrix structure. The concave shape of the wetting phase spreading over the rock matrix can be seen in Figure 7.5 with oil initialization. However, the non-wetting phase adopted the convex shape at the fluid interface. The water-wet micromodel had the concave shape of the water phase (in blue) and the convex shape of the oil phase (in green). Similarly, the oil-wet micromodel had the concave shape of the oil phase (in green) and the convex shape of the water phase (in blue). For the complex-wet micromodel, some parts were water-wet while other parts were oil-wet.

6.4 Oil Recovery and Pressure Response for Secondary-mode Brine Flooding

6.4.1 Flooding Sequence

Similar to the processes described in Chapter 4 and Chapter 5, brine flooding (BG2 and BG3 from Table 3.1) was performed in the secondary mode with the oil-saturated micromodels. Polymer flooding was performed in the tertiary mode as the second phase to investigate the hybrid EOR process for viscosity control. The viscosity of the oil sample and polymer solutions are presented as Nr. 3 and Nr. 4 in Table 3.3.

6.4.2 Oil-Wet Artificial Model

SSW injection was performed as the base case, and SSW flooding was repeated in the cleaned model to observe the reproducibility of the oil recovery data. Figure 6.4 and Figure 6.5 show oil recovery and pressure data for SSW flooding. Looking at the pressure response and final RFs, similar values are observed for both experiments. From Figure

6.3, the main flooding was a straight flow path between the injection and production points. For further investigation of the effect of brine composition on oil recovery, four injection brines of Table 3.1 were flooded in the secondary mode. Figure 6.6 and Figure 6.7 describe RF profiles and pressure responses for the four injection brines. Table 6.2 summarises further details with regards to additional oil recovery with modified brines flooding (compared to SSW injection).

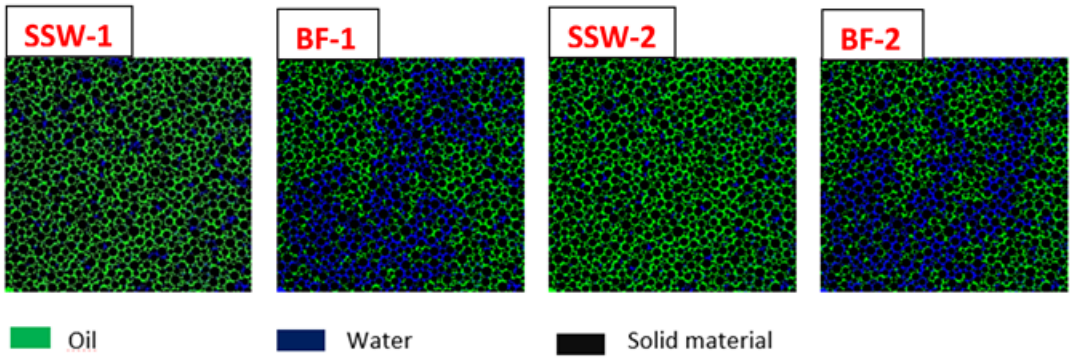

Figure 6.3: *Artificial structure oil-wet micromodels used for SSW flooding. SSW-1/SSW-2 represents the oil initialization, and BF-1/BF-2 represents after 10PV injected brine*

Table 6.2: *Summary of the artificial structure oil-wet micromodel with initial oil saturation, connate water saturation, and final oil RF.*

Nr.	Flooding Brine	Soi	Swc	RF	Add. RF
		(%)			
1	**SSW**	85.02	14.98	32.84	-
2	**SSW**	83.44	16.56	32.38	-
3	**SSW**+$2SO_4^{-2}$	85.13	14.87	35.01	2.63
4	**SSW-Na**	85.64	14.36	33.66	1.27
5	**DSSW**	83.48	16.52	34.84	2.46

The slightly higher additional oil recovery from brine (3-5 from Table 6.2) flooding compared to SSW injection was due only to the fluid-fluid interfacial interaction developed between the oil and brine. The main reason for this could be negligible local wettability alteration (rock-fluid interaction) of the micromodel established by injected brines. Sulfate-modified water and DSSW do not show a strong ability to disturb the hydrophobic layer coated on the matrix of the micromodel for wettability alteration. It is believed that this additional oil recovery was obtained due to the improved ionic interfacial response at the interface (fluid-fluid interaction). This ionic interfacial interaction developed due to a slight increase in the static IFT at the interface between the modified brines and the oleic phase. Further, the concept of PDI/non-PDI ions for SSW-Na brine flood did not work as expected and produced only 1.27% additional oil. Hence, this indicates that adding/removing the PDI/non-PDI ions works, focusing on the concept of

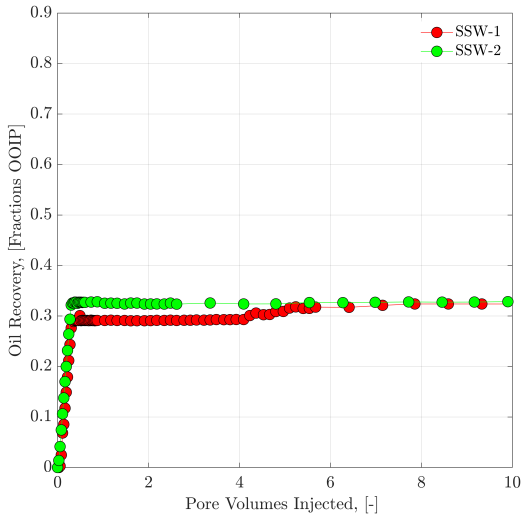

Figure 6.4: *Oil recovery versus PV injected for the artificial structure oil-wet micromodel. SSW injection was performed as the secondary mode for both flooding experiments.*

wettability alteration as a main recovery mechanism. Considering the economical aspect of the project, sulfate-modified (SSW+$2SO_4^{-2}$) injection proved to be a suitable brine when comparing the extra oil recovery and brine preparation (the removal of NaCl from SSW or dilution of the SSW).

Figure 6.8 is the final image after ≈ 10PV brine flood (Table 3.1 injection brines). Table 6.2 describes the initial oil saturation and connate water saturation, which fall in the same range. RF represents the final RF after 10 PV injected. Further, additional oil RF represents the additional oil produced after brine flood compared to SSW. Looking at the flooded flow paths of Figure 6.8, it is clear that two brines (SSW+$2SO_4^{-2}$ and DSSW) swept slightly better than the other two brines. The reason is the previously discussed improved fluid-fluid interfacial interaction.

6.4.3 Mixed/Complex-Wet Artificial Model

As previously mentioned, a model with the same characteristics as the oil-wet model and pore geometry was used. Some parts of this model were oil-wet while others were water-wet, leading to its name—a complex-wet model. Three injection brines of Table 3.1 were flooded at injection flux of 1.0 ft/day to compare the RFs. For reproducibility of the results, modified water (SSW+$2SO_4^{-2}$) injection was repeated to observe the RFs, as displayed in Figure 6.9 and Figure 6.10.

Almost the same final oil RF and pressure responses were measured for both experiments, confirming reproducibility of the data. For further investigation, SSW and

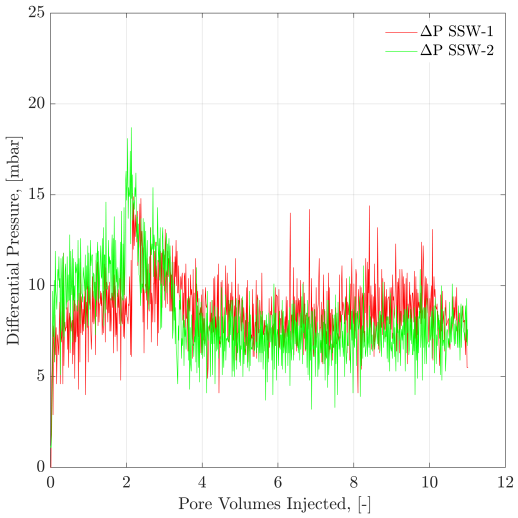

Figure 6.5: *Pressure drop versus PV injection for artificial structure oil-wet micromodel. SSW injection was performed as the secondary mode for both flooding experiments*

SSW-Na brines were injected through this model to compare the RFs presented in Figure 6.11.

Both brines (SSW+$2SO_4^{-2}$, SSW-Na) produced higher recovery compare to SSW injection (see Table 6.3). Again, the mechanism behind the increased production is the higher ionic interaction at the brine-oil interface compared to SSW. Furthermore, the wettability alteration mechanism (rock-fluid interaction) is not strong enough to produce additional oil, compared to core flooding, as discussed in Chapters 4 and 5. Moreover, the pressure profile for the complex-wet model was the same as for the oil-wet model for all brines except SSW-Na (Figure 6.12). Figure 6.13 shows the flooding patterns for fluids after 10 PV brine injection.

Table 6.3: *Summary of the artificial structure complex-wet micromodel with initial oil saturation, connate water saturation, and final oil RFs*

Nr.	Flooding Brine	Soi	Swc	RF	Add. RF
		(%)			
1	**SSW**	81.28	18.73	39.58	-
2	**SSW+$2SO_4^{-2}$**	80.66	19.34	42.71	3.13
3	**SSW-Na**	76.40	23.6	41.55	1.97

6.4.4 Water-Wet Artificial Model

SSW injection showed the reproducibility of the results in the water-wet micromodel, as shown in Figure 6.14. Furthermore, water-wet micromodel experiments showed slightly higher oil recovery from SSW flooding compared to SSW+$2SO_4^{-2}$ injection, as shown

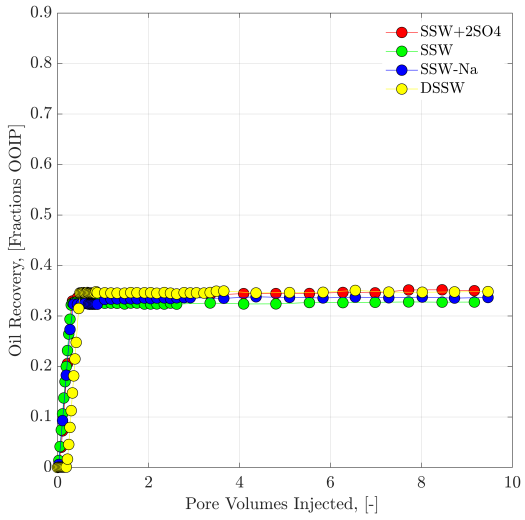

Figure 6.6: *Oil recovery versus PV injected for the artificial structure oil-wet micromodel. Four injection brines of Table 3.1 were flooded as the secondary mode.*

in Table 6.4. As described earlier, SSW+2SO_4^{-2} works effectively if the reservoir is oil-wet or mixed-wet. This approach was confirmed during the micromodel experimental investigation. Furthermore, it can be seen that pressure response is almost half that of the pressure profiles of both previously discussed systems, as can be seen in Figure 6.15. Negative additional RF in Table 6.4 represents lower oil recovery through SSW+2SO_4^{-2} flooding compared to SSW. Figure 6.16 and Figure 6.17 show the recovery profiles and pressure responses of both injected brines for water-wet micromodels. Further, Figure 6.18 represents the flooding pattern after 10 PV of both brine flooding.

Table 6.4: *Summary of the artificial structure water-wet micromodel with initial oil saturation, connate water saturation, and final oil RFs.*

Nr.	Flooding Brine	Soi	Swc	RF	Add. RF
		(%)			
1	**SSW**	93.19	6.82	53.77	-
2	**SSW**+2SO_4^{-2}	92.74	7.26	52.85	-0.92

6.4.5 Water-Wet Real Structure Model

Three brine floods were performed as mentioned in Table 6.5 and described in Figure 6.19 and Figure 6.20. The final RFs were similar for SSW and SSW+2SO_4^{-2}. The results are in line with the oil recovery results of the artificial structure water-wet micromodel discussed. Furthermore, DSSW produced slightly less oil (0.58%) compared to the other two brines. This small difference in oil recovery may be due to experimental artefacts and can considered to be the same oil recovery.

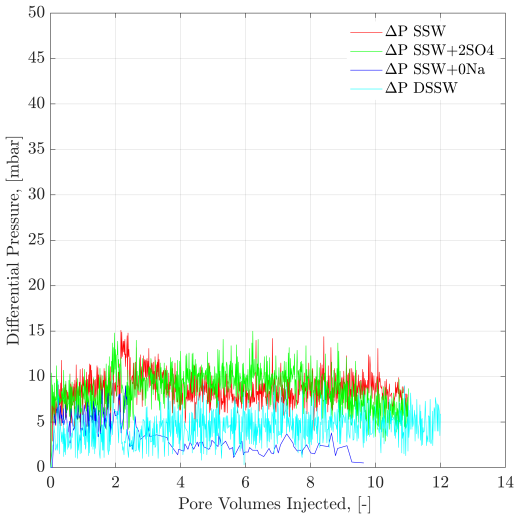

Figure 6.7: *Pressure drop versus PV injected for the artificial structure oil-wet micromodel. Four injection brines of Table 3.1 were flooded as the secondary mode.*

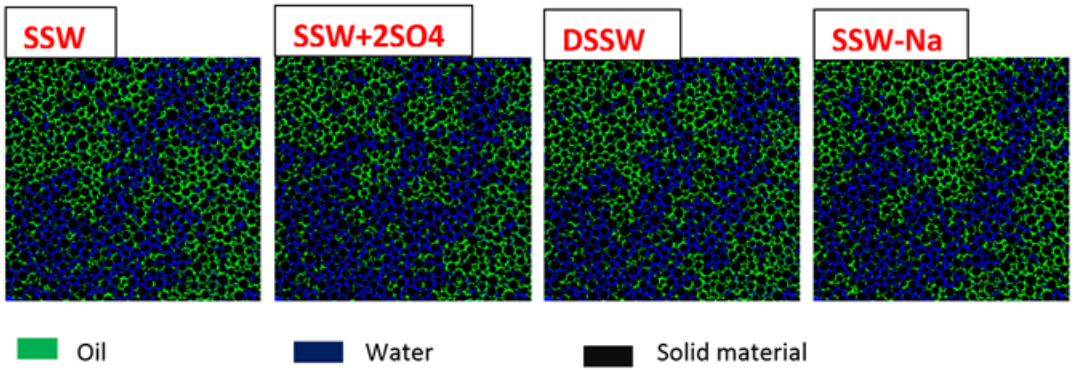

Figure 6.8: *Artificial structure oil-wet micromodels used for injection brines in Table 3.1. The figures represent the recovery after 10PV injected brine.*

This analysis justifies that oil-wet or complex-wet porous media systems are important for producing extra oil with sulfate-modified seawater or low saltwater. Figure 6.19 explains that SSW+2SO_4^{-2} produces the maximum oil at breakthrough. Furthermore, DSSW requires higher injected PV to achieve oil recovery close to the other two brines. Compared with the micromodel discussed in the previous section (water-wet artificial model), the difference between oil recovery was less than 1% for both models for SSW and SSW+2SO_4^{-2} flooding. This comparison emphasizes the hypothesis that sulfate-modified water flooding in the water-wet system will not work efficiently and produced brine/SSW is favourable to perform secondary-mode brine flooding. Figure 6.21 shows the oil initialization condition and after 10PV brine flood for three brines. Comparing the final RFs with the RFs of all previous experiments, the artificial structure water-wet model is closer. This comparison further justifies that under the same wetting conditions, brine could recover oil within a margin of 3%. This difference increased to 22%

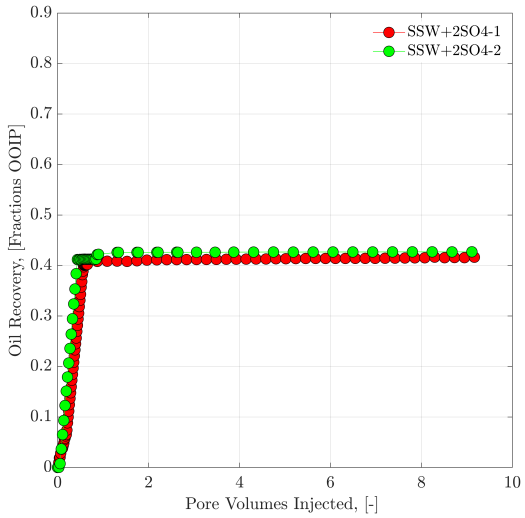

Figure 6.9: *Oil recovery versus PV injected for the artificial structure complex-wet micromodel. Sulfate-modified water injection was performed as the secondary mode for both flooding experiments.*

by changing the wettability of the system (oil-wet model).

Table 6.5: *Summary of the real structure water-wet micromodel with initial oil saturation, connate water saturation, and final oil RFs.*

Nr.	Flooding Brine	Soi	Swc	RF	Add. RF
				(%)	
1	**SSW**	91.15	8.85	55.01	-
2	**SSW+2SO_4^{-2}**	96.49	3.51	55.4	0.39
3	**DSSW**	95.32	4.68	54.43	-0.58

6.5 Oil Recovery and Pressure Response for Tertiary-mode Polymer Flooding

6.5.1 Polymer Viscosity with Half the Oil Viscosity in the Complex-wet Model

As described earlier, polymer (1,000 ppm) with half the viscosity of the oil (9.58 mPa.s) was injected in the tertiary mode to observe additional oil recovery. The micromodel with complex wettability was used for polymer flooding. First, bump-rate injection at a rate five times higher than that of the brine flood was performed to eliminate any possible capillary end effects. A minor amount of recovered oil and increased pressure response for the bump rate can be seen in Figure 6.22 and Figure 6.23. The polymer

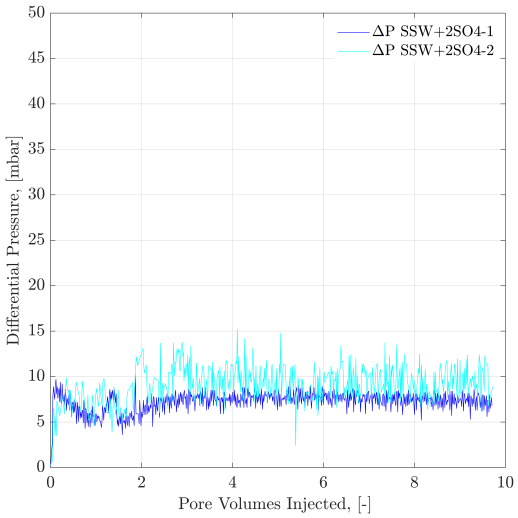

Figure 6.10: *Pressure drop versus PV injected for the artificial structure complex-wet micromodel. Sulfate-modified water injection was performed as the secondary mode for both flooding experiments.*

flood results for the tertiary mode are also shown. Figure 6.22 shows that no additional oil was produced by polymer injection in either experiments. One reason for this could be that the polymer followed the pre-flushed path of the brine and could not contribute additional recovery due to lower aqueous viscosity compared to the oil. Furthermore, the pressure of the polymer flood was lower compared to the bump rate in both experiments, as shown in Figure 6.23. This analysis supports the assertion that the lower pressure difference for polymer flooding was the reason for no additional recovered oil.

6.5.2 Polymer Viscosity Equal to the Oil Viscosity in the Complex-wet Model

As a further step, the impact of increased polymer viscosity (equal to the oil viscosity) on oil recovery was investigated. To do so, 1,500-ppm polymer was injected through the micromodels described in the previous sections. Figure 6.24 to Figure 6.27 describe the additional oil recovered and the impact on pressure response. Polymer diluted in SSW resulted in additional oil recovery of 4.33% (Figure 6.24), and the polymer prepared in SSW+2SO_4^{-2} resulted in additional oil recovery of 6.91% (Figure 6.26). Overall recovery from both micromodels was approximately 50%. Brine flooding was also performed after post-tertiary-mode polymer flooding to observe further recovery due to any bypass flow through the micromodel, but, in both cases, no oil was recovered. This reason for this could be a loss of polymer viscosity due to mechanical degradation while flowing through flow lines and the pump. This degradation caused a reduction in polymer

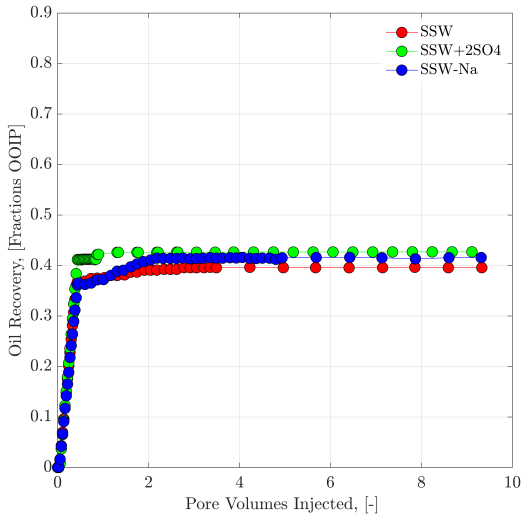

Figure 6.11: *Oil recovery versus PV injected for the artificial structure complex-wet micromodel. Three injection brines of Table 3.1 were flooded as the secondary mode.*

viscosity, resulting in lower viscosity than that of the oil. Later, brine flooding was performed for the pre-flushed flow paths of polymer solutions due to lower viscosity of the aqueous phase compared to the viscosity of the trapped oil. This investigation and the comparison of its results with those outlined in the previous section suggest injecting polymer solution with a viscosity at least equal to the oleic phase in porous media. Lower polymer viscosity (half that oil) do not contribute to the economics of a polymer injection project.

6.5.3 Polymer Viscosity Equal to Oil Viscosity in the Water-wet Real Structure Model

The same polymers described in Section 6.5.2 were injected through the real structure model. The results are presented in Figure 6.28 and Figure 6.29. Polymer flooding was performed after bump rate injection at a rate five times that of brine injection. Looking at the oil production profiles, the bump rate after SSW+2SO_4^{-2} produced more oil compared to SSW flooding. This could be due to detached and trapped oil drops in porous media, which are produced through high-pressure support of the bump rate. However, the polymer solution diluted in SSW+2SO_4^{-2} produced 2.61% additional oil recovery after the bump rate, and the polymer prepared in SSW produced 1.69% additional recovery. This marginal 1% difference in oil recovery was due to the increase in pressure across the model, as can be seen in Figure 6.29. This rapid increase in pressure was caused by microgel plugging the flow channels. Furthermore, comparing the results of the same polymer flood in the artificial structure model shows that this model produced more

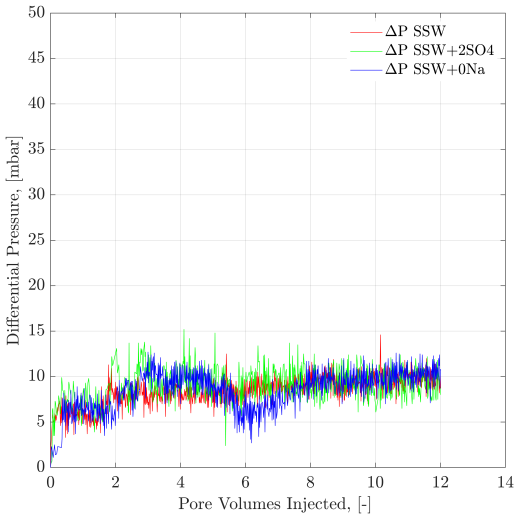

Figure 6.12: *Pressure drop versus PV injected for the artificial structure complex-wet micromodel. Three injection brines in Table 3.1 were flooded as the secondary mode.*

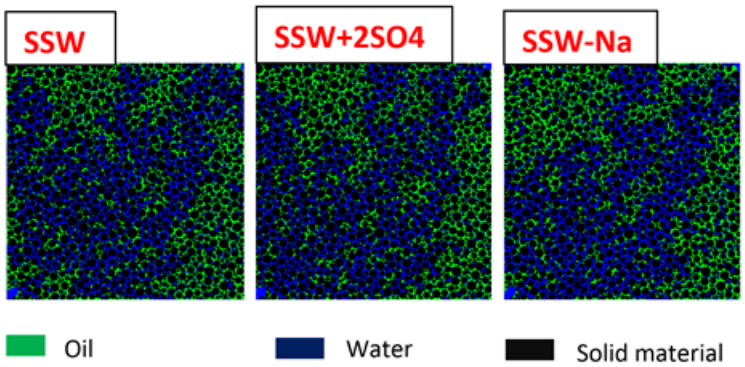

Figure 6.13: *Artificial structure complex-wet micromodels used for three injection brines mentioned in Table3.1. The figure represents the oil recovery after 10PV injected brine.*

recovery with polymer flooding. This higher oil recovery could be due to the wettability difference between the systems. Polymer flooding in the complex-wet micromodel was more efficient than in the water-wet micromodel. Brine injection helped to develop fluid-fluid interfacial interaction and the follow-up higher viscosity aqueous phase efficiently swept the detached oil, resulting in higher recovery.

6.6 Results and Remarks

Based on the experimental investigation and collected data outlined in this chapter, it can be concluded that mechanisms of both wettability alteration and fluid-fluid interfacial interaction are of great importance for reducing the ROS. However, in the oil-wet micromodel, only fluid-fluid interaction helped to produce the additional oil from

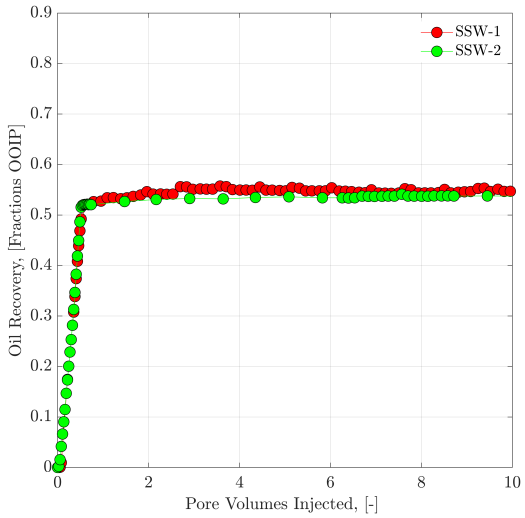

Figure 6.14: *Oil recovery versus PV injected for the water-wet artificial structure micromodel. SSW injection was performed as the secondary mode for both flooding experiments*

SSW+$2SO_4^{-2}$. Additionally that there was no rock-fluid interaction in the oil-wet micromodel. One reason for this is that the oil-wet condition is achieved by applying a chemical layer adsorbed at the matrix structure, which is difficult to change to water-wet by modified water. The results also confirm that SSW+$2SO_4^{-2}$ or low-salt water flooding work efficiently only in oil-wet and complex-wet reservoir systems (for the conditions presented in this work). In a water-wet system, the fluid-fluid/rock-fluid interaction concept could not work in a promising manner.

Moreover, it was observed that polymer injection with a viscosity equal to that of oil can contribute to additional oil recovery through the micromodels. Polymer flooding after SSW+$2SO_4^{-2}$ contributed 2% higher recovery compared to polymer injection after SSW, which proposes as the appropriate combination of modified water flooding following polymer flooding. Subsequently, it was observed that the pore distribution and rock properties do not have a significant impact on oil recovery under the same wettability conditions (for the conditions presented in this work). Comparing the two types of water-wet models artificial and real structure), nearly the same RF of 55% through SSW flooding was achieved.

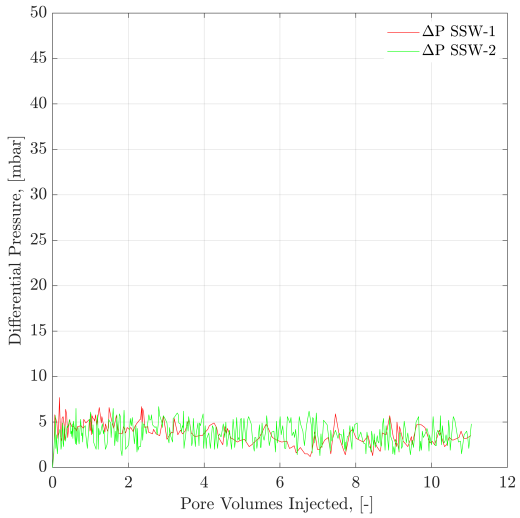

Figure 6.15: *Pressure drop versus PV injected for the water-wet artificial structure micromodel. SSW injection was performed as the secondary mode for both flooding experiments.*

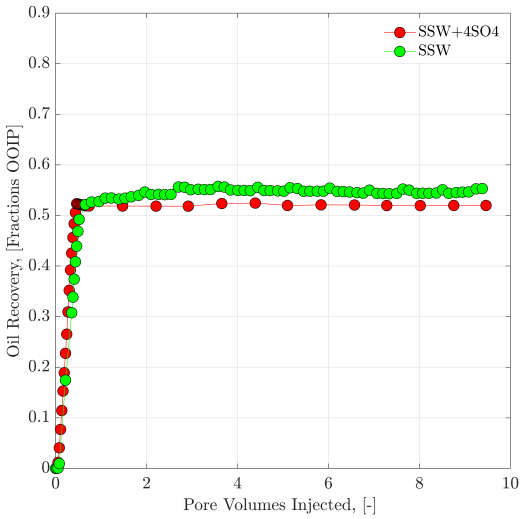

Figure 6.16: *Oil recovery versus PV injected for the water-wet artificial structure micromodel. Two injection brines of Table 3.1 were flooded as the secondary mode.*

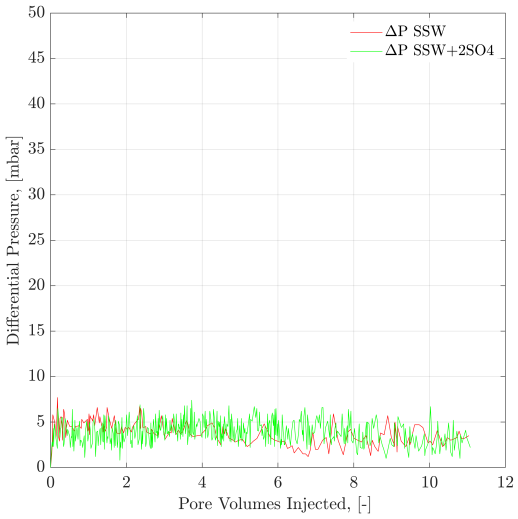

Figure 6.17: *Pressure drop versus PV injected for the water-wet artificial structure micromodel. Two injection brines of Table 3.1 awere flooded as the secondary mode.*

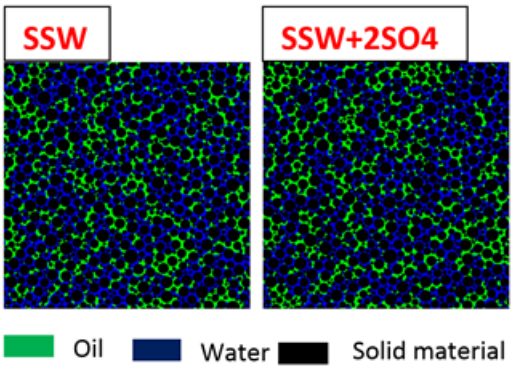

Figure 6.18: *Artificial structure water-wet micromodels used for two injection brines in Table 3.1. The figure represents oil recovery after 10PV injected brine.*

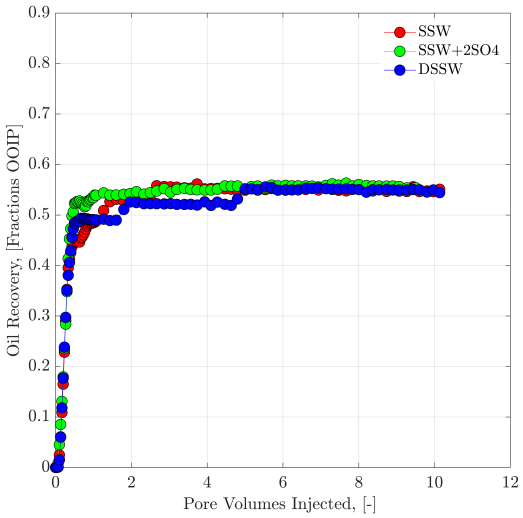

Figure 6.19: *Oil recovery versus PV injected for the water-wet real structure micromodel. Three injection brines of Table 3.1 were flooded as the secondary mode.*

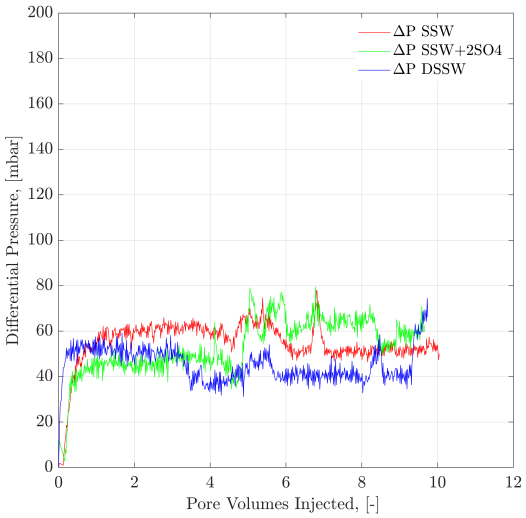

Figure 6.20: *Pressure drop versus PV injected for the water-wet real structure micromodel. Three injection brines of Table 3.1 were flooded as the secondary mode.*

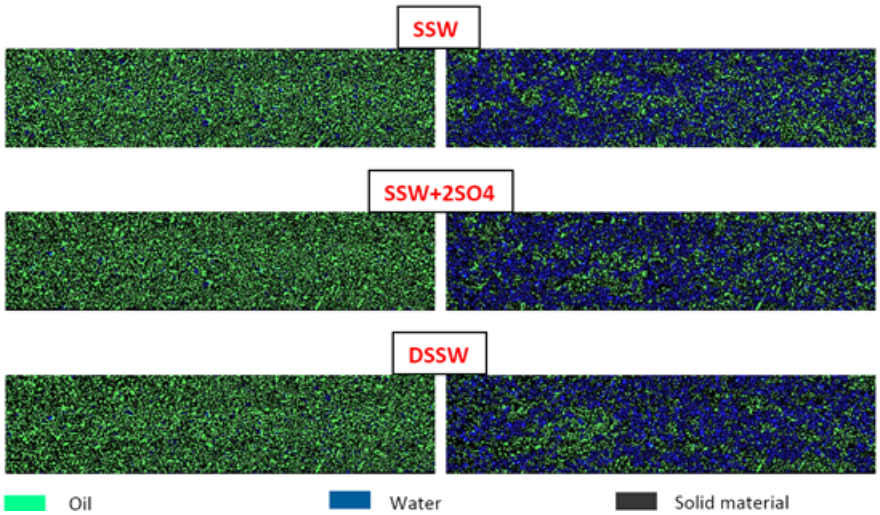

Figure 6.21: *Real structure water-wet micromodels used for three injection brines in Table3.1. The figures on the left represent oil initialization, and those on the right represent oil recovery after 10PV brine flooding.*

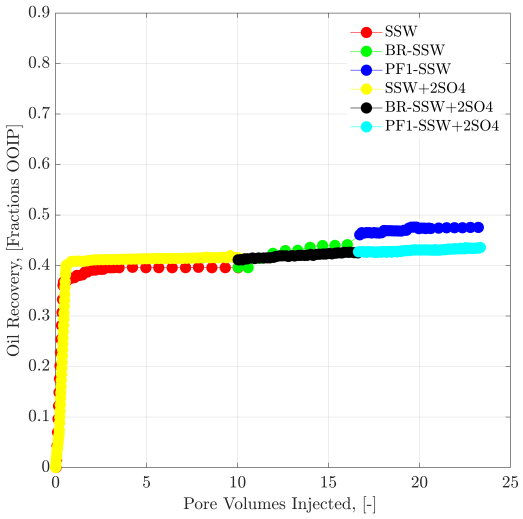

Figure 6.22: *Oil recovery versus PV injected for the complex-wet artificial structure micromodel. Polymer (with half the viscosity of oil) flooding in the tertiary mode was performed after brine flooding in the secondary mode.*

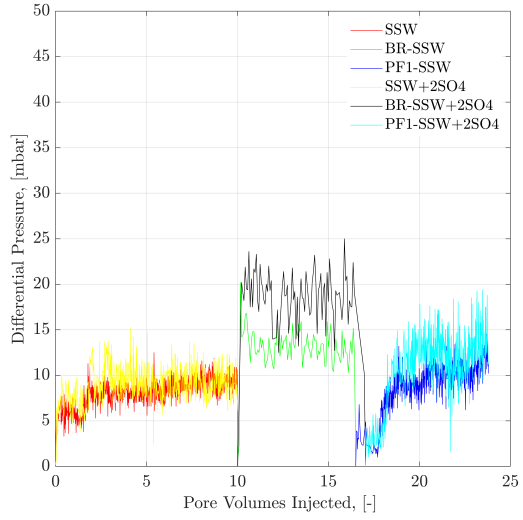

Figure 6.23: *Pressure drop versus PV injected for the complex-wet artificial structure micromodel. Polymer (half the viscosity of oil) flooding in the tertiary mode was performed after brine flooding in the secondary mode.*

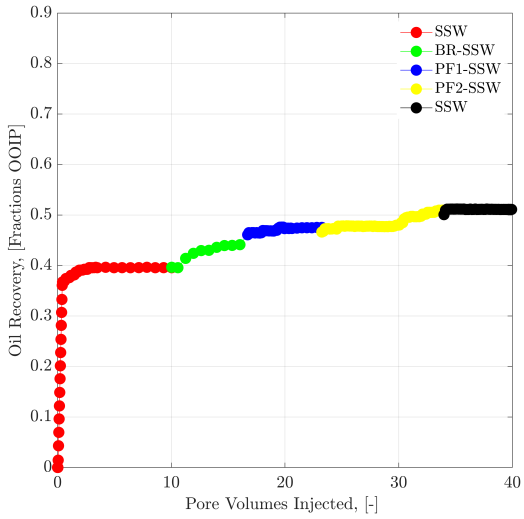

Figure 6.24: *Oil recovery versus PV injected for the complex-wet artificial structure micromodel. Polymer (equal to the viscosity of oil) flooding was performed in the post-tertiary mode after SSW brine flooding in the secondary mode.*

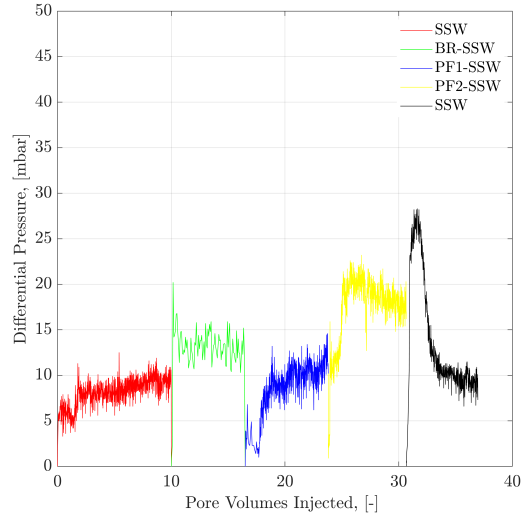

Figure 6.25: *Pressure drop versus PV injected for the complex-wet artificial structure micromodel. Polymer (equal to the viscosity of oil) flooding was performed in the post-tertiary mode after SSW brine flooding in the secondary mode.*

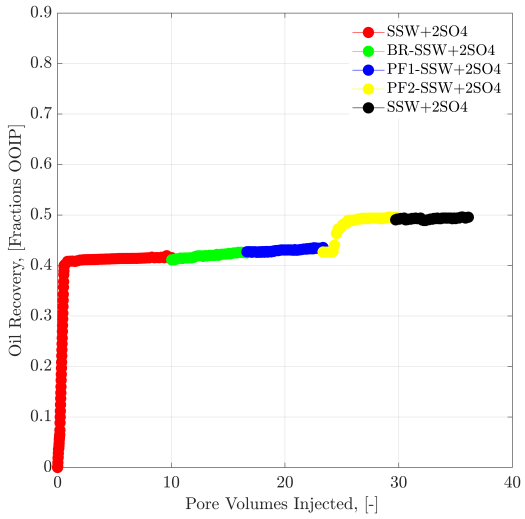

Figure 6.26: *Oil recovery versus PV injected for the complex-wet artificial structure micromodel. Polymer (equal to the viscosity of oil) flooding in the post-tertiary mode was performed after SSW+2SO_4^{-2} brine flooding in secondary mode*

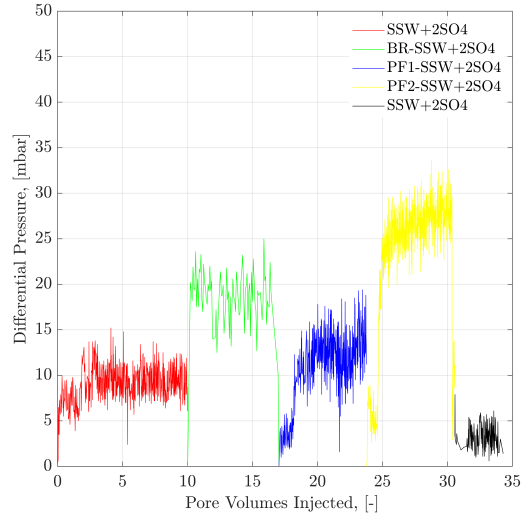

Figure 6.27: *Pressure drop versus PV injected for the complex-wet artificial structure micromodel. Polymer (equal to the viscosity of oil) flooding in the post-tertiary mode was performed after SSW+2SO_4^{-2} brine flooding in the secondary mode.*

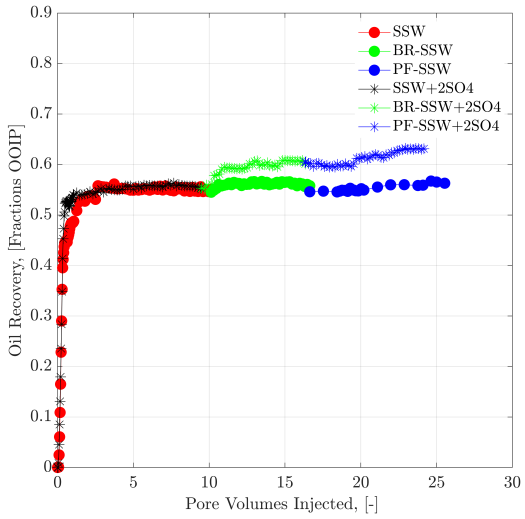

Figure 6.28: *Oil recovery versus PV injected for the water-wet real structure micromodel. Polymer (equal to the viscosity of oil) flooding in the tertiary mode was performed after SSW+2SO_4^{-2}/SSW brine flooding in the secondary mode.*

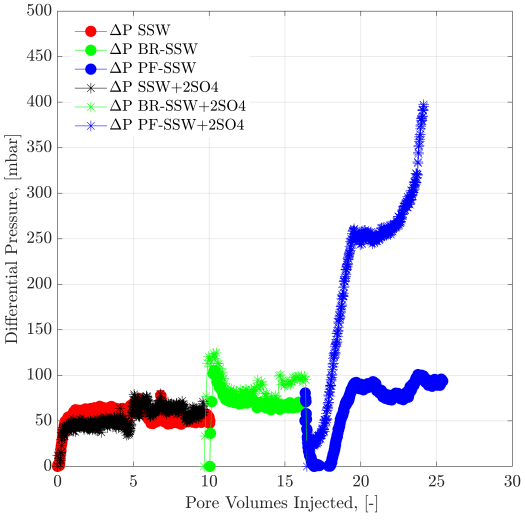

Figure 6.29: *Pressure drop versus PV injected for the water-wet real structure micromodel. Polymer (equal to the viscosity of oil) flooding in the tertiary mode was performed after SSW+2SO_4^{-2}/SSW brine flooding in the secondary mode.*

Chapter 7

Coupling Microfluidics Data With Core Flooding Experiments

The injection of sulfonated-modified water could be an attractive application as it results in the formation of a mechanically rigid oil-water interface and, hence, possible higher oil recovery in combination with polymer. Therefore, detailed experimental investigation and fluid-flow analysis into porous media are required to understand the possible recovery mechanisms. This chapter evaluates the potential influence of sulfate-modified water injection in oil recovery by coupling microfluidics data and core flooding experiments. Fluid characterisation is achieved by detailed rheological investigation focused on steady shear viscosity. Moreover, two-phase core floods and micromodel experiments helped to define the behaviour of different fluids. The data obtained was cross-analysed to draw conclusions about the process effect and performance.

This chapter compares the information presented in previous chapters (4-6), with a focus on the design of sulfate-modified water flooding for core plugs and micromodels. The comparison is presented to support the hypothesis that the primary recovery mechanism is either the rock-fluid interaction (wettability alteration) or the fluid-fluid interaction for modified water flooding based on sulfate content. The workflow for the study of the leading recovery mechanism is described in Figure 7.1. The findings of this chapter were organized for journal publication "Coupling Microfluidics Data with Core Flooding Experiments to Understand Sulfonated/Polymer Water Injection" in Polymers 2020 (ISSN 2073-4360), 12(6), 1227; https://doi.org/10.3390/polym12061227.

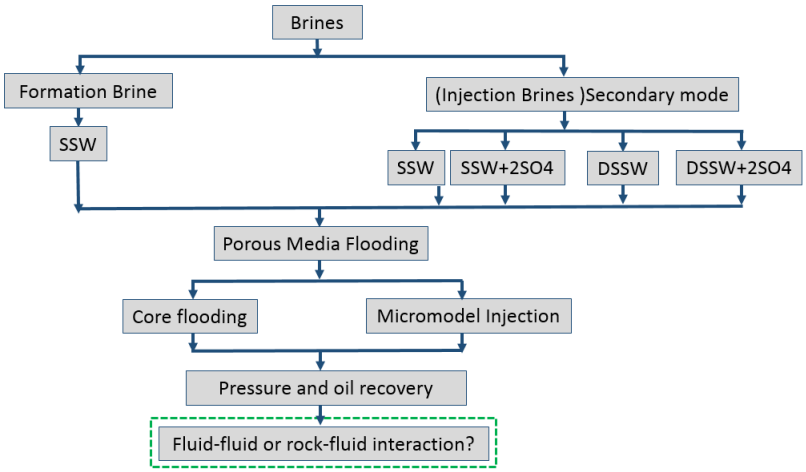

Figure 7.1: *Adopted workflow to establish the recovery mechanism*

7.1 General Methodology and Approach

- ***Fluid-fluid and rock-fluid investigations***: Fluid-fluid interaction was investigated in oil and brine samples using interfacial tension and oil-drop snap-off volume measurements. However, rock-fluid interaction was defined by the wettability alteration.
- ***Two-phase flooding experiments in core plugs and micromodels***: These experiments were conducted to understand the oil recovery contribution through fluid-fluid and rock-fluid interactions. The comparison helped determine the main recovery mechanism.
- ***Two-phase flooding experiments combining polymer with modified water***: These experiments were conducted to evaluate and define the synergies and benefits between modified water and polymer flooding as a combined EOR technique. Polymer was injected in the tertiary mode in the complex-wet micromodel and aged core plugs.

7.2 Fluid Optimization

7.2.1 Steady Shear Viscosity

The steady shear viscosity measurements can be seen as Nr. 1 through 4 in Table 3.3. Data are presented for the different fluids used in this work and are shown at a reference shear rate of $10s^{-1}$. Important observations can be grouped as the following:

- A diluted solution of 1,000 ppm resulted in viscosity half that of oil while a diluted solution of 1,500 ppm has a viscosity equal to that of oil at room temperature.

- Diluted solutions of 300 ppm and 750 ppm resulted in the same viscosity due to TDS in the mixing brine. Brine 2 and Brine 3 (BG2 in Table 3.1) had TDS of around 4.5g/L while Brine 4 and Brine 5 (BG3 in Table 3.1) had TDS of around 45g/L. This predicts the significance of salt activity in designing polymer solution with the desired viscosity. One brine always has a higher sulfate content than the other.

- At a lower polymer concentration of 300 ppm, it was impossible to differentiate the viscoelastic properties of the polymer solutions based on the sulfate present (Chapter 4).

7.2.2 IFT Results

Figure 7.2 presents the static interfacial measurements between the brines mentioned in Table 3.1 and dead oil. The results show that the amount of TDS has a significant impact on IFT. The lowest values were measured for the SSW and SSW+$4SO_4^{-2}$. Figure 7.2 also shows that doubling the amount of sulfate in SSW also doubled the IFT values and that a further increase in sulfate reduced the static IFT at the fluids interface. Moreover, diluted brines resulted in the highest values of IFT for both brines. These results are in agreement with Sohrabi et al. [36], who concluded that the interfacial layer is more stable and elastic in the case of low-salt brine. This IFT response also predicts the ionic reaction between brine and oil at the interface. Active ionic interaction at the fluid-fluid interface is expected to develop a bond of divalent ions in brine and polar oil compounds (asphaltene and NAs) [34] [35]. This interaction results in the development of a stable interfacial layer at the interface and hence increased IFT values.

This mechanism enhances the development of the elastic layer at the interface, which corresponds to higher recovery [1] [35] [3]. However, increasing the amount of sulfates in SSW by four times results in a water-in-crude oil microemulsion at the fluid-fluid interface. According to previous studies [92] [31], the controlling mechanism is associated with two coalescence-suppressing interfacial barriers between fluids. Summarising the IFT response, higher values of IFT at the interface enhance the ionic interfacial properties (indirectly, elasticity), which, in turn, is expected to produce larger oil drops.

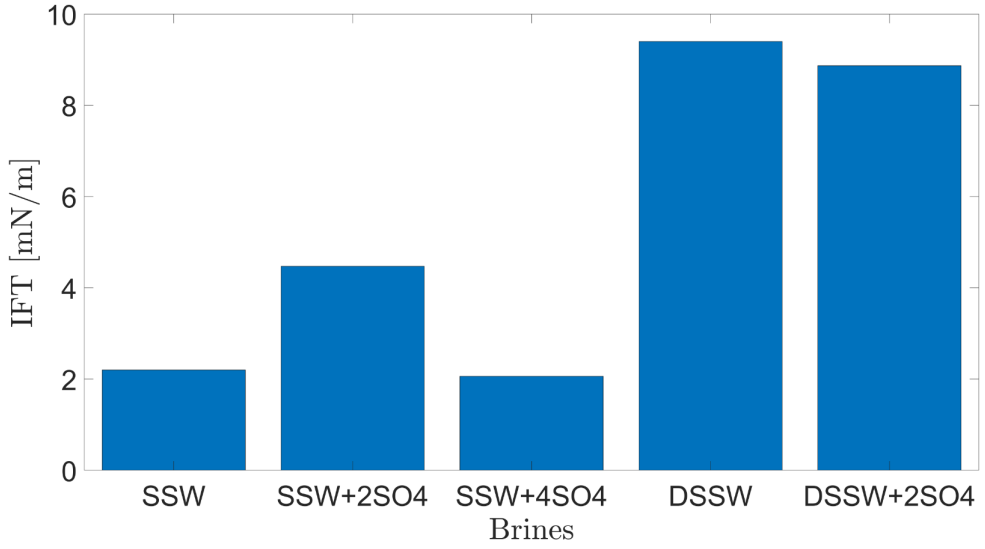

Figure 7.2: *Interfacial tension (IFT) between brines and crude oil at 22°C*

7.2.3 Oil Drop Volume Measurements at Snap-off Point

Figure 5.7 shows the measured oil-drop volume in SSW brine. The oil drop was sustained on the needle for 21 minutes before snap-off, resulting in 7.5 μL oil volume. Similarly, the oil drop volume and snap-off time was measured for two more brines, as presented in Figure 7.3. The interfacial response of fluids (oil-brine) appears to be in line with the results of IFT measurements. As IFT data depicted the lowest value for SSW+4SO_4^{-2} brine, the smallest drop size was expected for this brine. Small drop volume was produced due to a water-in-crude oil microemulsion at the fluid-fluid interface (coalescence-suppressing interfacial barriers), which resulted in quick oil-drop snap-off from the needle.

Moreover, SSW+2SO_4^{-2} resulted in two times the IFT compare to SSW; presumably, this is due to the generated stable layer (at the interface) due to sulfates in brine and polar oil compounds (asphaltene). The higher IFT value generated a larger oil drop of 12.5 μL. Note that it was expected that larger oil drops would be produced in both diluted brines (Brine 2 and Brine 3 of BG2 group) of Table 3.1.

Overall, it was observed that a slightly higher IFT indicates an improved and stable interfacial layer developed at the oil-brine interface. This improved interfacial layer assists with continuous oil flow, resulting in larger oil drops (ganglia) during brine flooding and hence is expected to recover more oil.

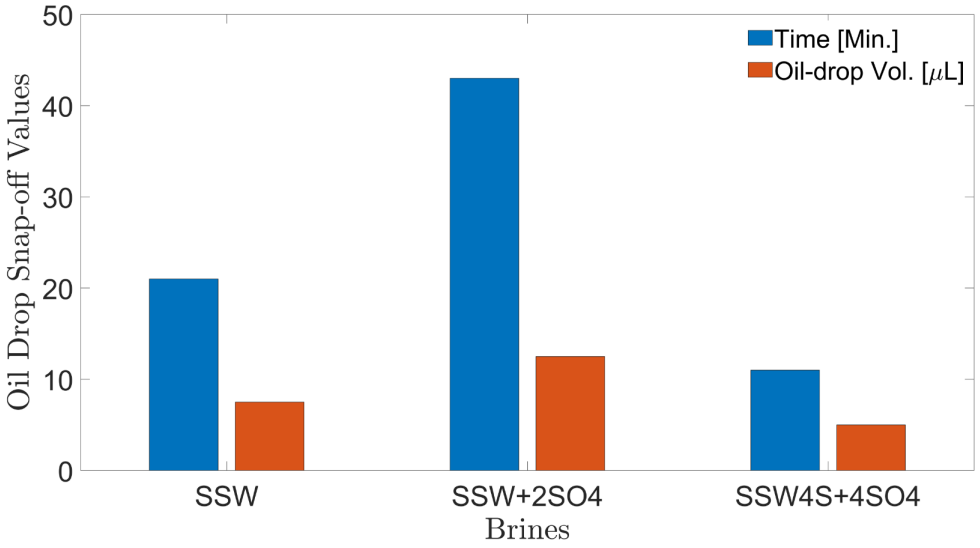

Figure 7.3: *Oil drop size analysis before snap-off for different brines at 22°C*

7.2.4 Wettability Conditions of Porous Media

Contact angle data after the six-week aging process, presented in Figure 7.4, helped to preliminarily confirm the wettability alteration of core plugs. Chapter 5 provides a detailed description of contact angles for aged and unaged cores for wettability alteration. It is believed that this wettability alteration process happened after three weeks of aging. It is assumed that for plugs with a three-week aging period, the wettability condition of mix-wet to oil-wet can be achieved. Skauge et al. [102] also proposed polar compound attachment for the Bentheimer sample.

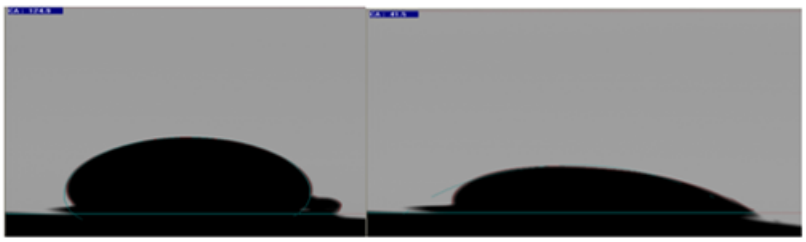

Figure 7.4: *Pendant drop method for contact angle measurement between oil-saturated, six-week aged core plug and oil drop at 0 minutes (left) and after 60 minutes (right) at 22°C*

Moreover, the wettability of the micromodel was confirmed by visual observation, through the concave/convex interface of the reservoir fluids (oil and brine) with a circular matrix structure. The concave shape of the wetting phase spreading over the rock matrix can be seen in Figure 7.5. However, the non-wetting phase adopted a convex shape at the fluid interface. The water-wet micromodel has the concave shape of the water phase (in blue) and the convex shape of the oil phase (in green), as presented in Figure 7.5. Similarly, the oil-wet micromodel has the concave shape of the oil phase (in green) and

the convex shape of the water phase (in blue), as shown in Figure 7.5. For the complex-wet micromodel, some parts are water-wet while other parts are oil-wet. It is believed that the oil-wet model resembles the six-week aged core plugs while the complex-wet micromodel resembles the three-weeks aged core plugs for flooding result comparisons.

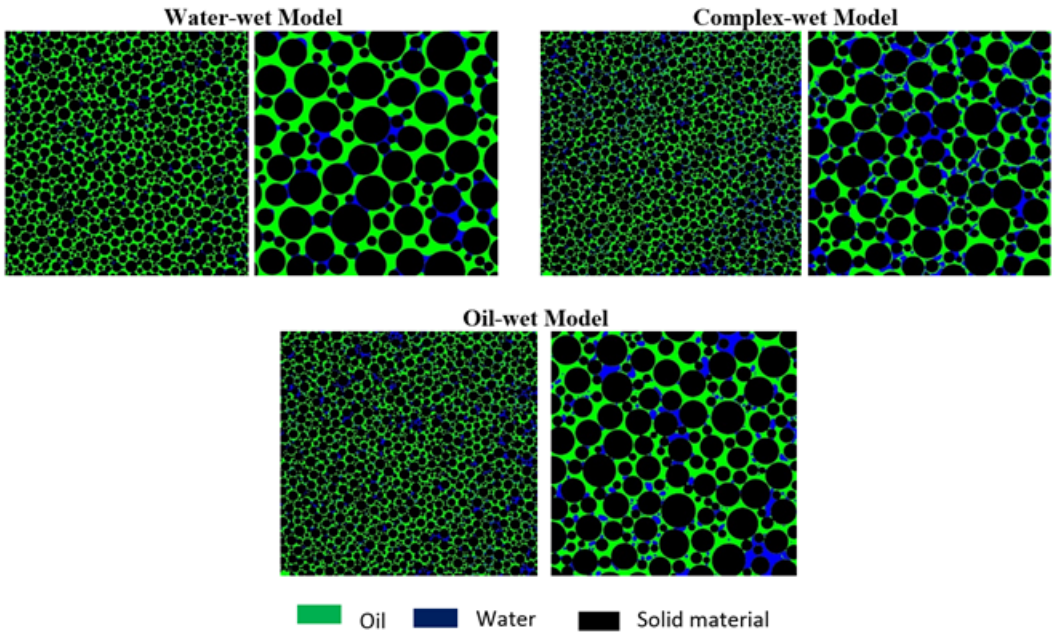

Figure 7.5: *Micromodel with different wettability conditions. The left side of each wettability condition represents the micromodel with initial oil saturation while the right side is the zoomed-in image of the bottom-right corner for each micromodel at 22°C*

7.3 Oil Recovery and Pressure Response of Secondary-mode Brine Flooding

7.3.1 Flooding Sequence

Brine flooding was performed as the secondary mode in the micromodels and aged core plugs for comparison purposes to investigate the recovery mechanisms. Further polymer flooding was performed as the tertiary mode in the mix-wet micromodels and three-week and six-week aged core plugs to cross-validate the synergies and benefits of the hybrid EOR process. Oil and polymer viscosities are listed as Nr. 1 through 4 in Table 3.3. For this investigation, the flooding sequences and results previously obtained in Chapters 4 through 6 were used to determine the primary recovery mechanism.

7.3.2 Oil-Wet Porous Media

Table 7.1 and Figure 7.6 describe the secondary-mode RFs of different brine floods for six-week aged core plugs and the oil-wet micromodels. Additional RF (Add. RF) in Table 7.1 describes the additional RF compared to the RF of SSW while Diff.CF/ Diff.MM in Figure 7.6 describes the difference in the RF of the brine flood minus the RF through SSW injection. As can be seen from Table 7.1 and Figure 7.6, the highest RF was achieved for both porous media when flooded with SSW+$2SO_4^{-2}$.

Oil-wet Micromodel

Brine flooding through the micromodel produced lower RFs (32-35%) for all of the brines presented in Table 7.1 and Figure 7.6. There was additional oil recovery of 2%, as seen from Table 7.1, for the sulfate-modified water and DSSW compared to the base brine. This 2% additional recovery can be attributed to the fluid-fluid interaction developed in the reservoir. Mahzari and Sohrabi [34] and Sohrabi et al. [36] and Morin et al. [35] also reported higher oil recovery through the improved fluid-fluid interaction.

Further, similar additional recovery from sulfate-modified water and DSSW supported the assumption that fluid-fluid interfacial interaction can only contribute an additional 2% oil (from the oil-wet micromodel). Significantly higher recovery from DSSW due to stronger static IFT values can be reasonably expected (Figure 7.2), but this was not observed during the flooding process. The recovery also confirms that no additional oil was produced due to wettability alteration. It was not possible to alter the micromodel wettability to water-wet through sulfate-modified water injection or low-salt brine flooding, presumably due to the adsorption of the hydrophobic layer at the matrix. Figure 6.8 confirms that the wettability of oil-wet micromodels remains unchanged after 10 PV brine flooding was performed (concave-convex contact of fluids with the matrix).

Six-Week Aged Core Plugs

There was significantly higher oil recovery using SSW+$2SO_4^{-2}$ for Bentheimer core plugs compared to the micromodel (Table 7.1 and Figure 7.6). It is assumed that this high recovery of 45.69% was obtained through the combined recovery mechanisms of wettability alteration and fluid-fluid interfacial interaction. Sulfate-modified water injection through the micromodel confirmed the 2.17% additional oil recovery through fluid-fluid interfacial interaction. Moreover, a 9.31% difference between the micromodel and core plug RFs was contributed through the wettability alteration mechanism (core plug wet-

tability alteration to water-wet). Oil polar compounds' attachment on the rock matrix during the aging process was not permanent, and wettability alteration was achieved through ionic interaction between the rock-oil-brine systems. The data are in good agreement with those presented for wettability alteration of core plugs through low-salt water injection or sulfate-modified water flooding ([79] [80] [81] [82]). Therefore, wettability alteration (rock-fluid interaction) in core plugs is a more straightforward approach than comparing wettability alteration in the micromodels. Hence, significantly higher oil recovery was obtained with the core plugs. The IFT and oil-drop snap-off volume measurements indicate that SSW+$4SO_4^{-2}$ cannot develop a stronger fluid-fluid interaction. Further, oil recovery through SSW+$4SO_4^{-2}$ flooding should be lower than that through SSW+$2SO_4^{-2}$ flooding due to a weaker fluid-fluid interfacial interaction. The lower RF from SSW+$4SO_4^{-2}$ is confirmed in Table 7.1, which is in line with the results obtained for IFT and oil-drop snap-off volume measurements.

These results suggest that interfacial interaction as well as wettability alteration produce higher oil recovery compared to the base SSW injection. Moreover, the primary recovery mechanism in micromodels is only fluid-fluid interfacial interaction with negligible wettability alteration. Note that for the core plugs evaluated here, wettability alteration is the main recovery mechanism. Hence, the oil contributed from wettability alteration was much greater than the oil produced by fluids' interfacial interaction.

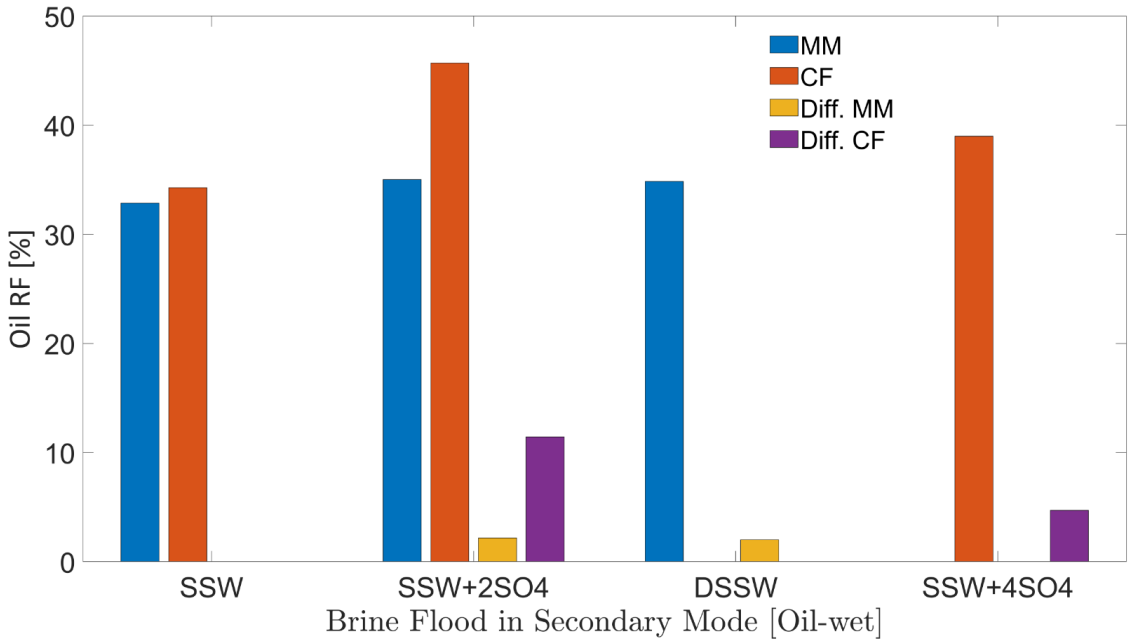

Figure 7.6: *Oil RFs of secondary-mode brine flooding through oil-wet core plugs and micromodels.*

Table 7.1: *Oil-wet cores and micromodel flooding with initial fluid saturations and oil recovery in secondary-mode brine flooding*

Porous Media	Brine Flood	Soi	Swc	RF	Add. RF
		%			
6-week Aged CF	SSW	84.34	15.66	34.27	-
	SSW+$2SO_4^{-2}$	82.11	17.89	45.69	11.42
	SSW+$4SO_4^{-2}$	81.33	18.67	38.98	4.71
Oil-wet MM	SSW	85.02	14.98	32.84	-
	SSW+$2SO_4^{-2}$	85.13	14.87	35.01	2.17
	DSSW	83.48	16.52	34.84	2.00

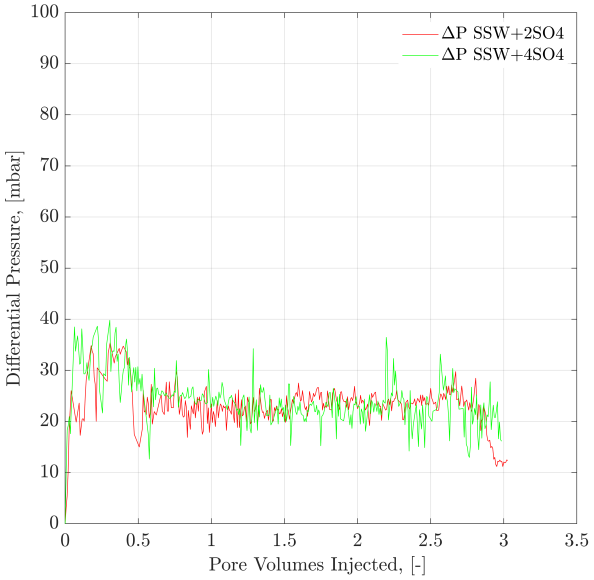

Figure 7.7: *Pressure response of secondary-mode brine flooding through six-week aged Bentheimer core plugs at a flux rate of 1ft/day.*

Pressure Profiles

Figure 7.7 and Figure 7.8 present the pressure profiles for the injected brines in the core plugs and micromodels, respectively. The pressure response through core plugs is slightly unstable with large bumps compared to the micromodel. Such bumps are expected due to the low injection rate compared to the oil drop movement. Further, nearly the same pressure response was observed for the injected fluids through a specific porous media (core plugs or micromodels). Brine flooding was performed at the flux rate of 1ft/day, but core flooding resulted in almost doubled pressure values compared to micromodel flooding.

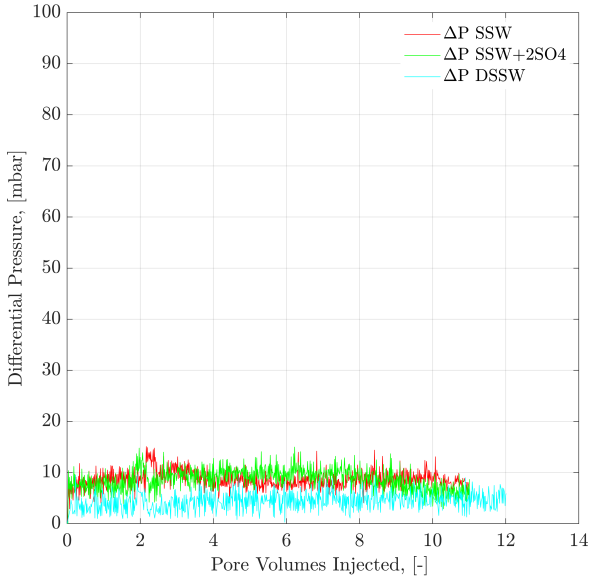

Figure 7.8: *Pressure response of secondary-mode brine flooding through the oil-wet micromodel at a flux rate of 1ft/day*

7.3.3 Mixed-Wet Porous Media

RFs of injected brines from three-week aged core plugs and the complex-wet micromodel are presented in Table 7.2 and Figure 7.11. The comparison in the previous section (oil-wet system) with the mix-wet system further deepened the investigation based on the fluid-fluid and rock-fluid interactions (wettability alteration).

Table 7.2: *Complex-wet cores and micromodels with initial fluid saturations and oil recovery in secondary-mode brine flooding*

Porous Media	Brine Flood	Soi	Swc	RF	Add. RF
				%	
3-week Aged CF	SSW	79.4	20.6	32.22	
	DSSW	75.4	24.6	36.9	4.68
	DSSW+$2SO_4^{-2}$	75.5	24.5	37.87	5.65
Complex-wet MM	SSW	81.28	18.73	39.58	
	DSSW	80.27	19.74	43.56	3.98
	SSW+$2SO_4^{-2}$	80.66	19.34	42.71	3.13

Mix-wet Micromodel

Oil RFs for the mixed-wet micromodel are presented in Table 7.2 and Figure 7.11. It can be seen that both modified brines (DSSW and SSW+$2SO_4^{-2}$) produced higher oil recovery (3-4%) compared to the base brine (SSW). Similar to the previous section (oil-wet), additional oil recovery was produced only through the fluid-fluid interfacial interaction

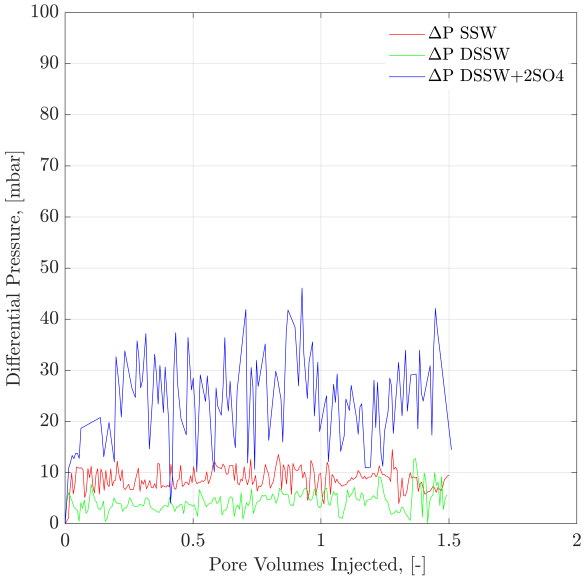

Figure 7.9: *Pressure response of secondary mode brine flooding through three-week aged Bentheimer core plugs at a flux rate of 1ft/day*

at the oil-brine interface. No wettability alteration was achieved using modified water or through low-salt brine ionic activity.

Three-Week Aged Core Plugs

Oil RFs of the three-week aged core plugs presented in Table 7.2 were significantly lower than the RF from six-week aged plugs in Table 7.1. The first reason for lower oil recovery is the difference in the wettability conditions of core plugs. During the three-week aging process, fewer polar compounds were attached to the rock matrix compared to the six-week aging period. This led to less wettability alteration during DSSW+$2SO_4^{-2}$ flooding in the three-week aged core plugs. The second reason is that there was 10 times less sulfate in DSSW+$2SO_4^{-2}$ compared to the SSW+$2SO_4^{-2}$ brine. Hence, oil recovery from the three-week aged core plugs was achieved mainly due to fluid-fluid interaction, with a weaker effect of the wettability alteration as a recovery mechanism.

Pressure Profiles

Pressure profiles of the brine floods are presented in Figure 7.9 and Figure 7.10 for core and micromodel flooding. Pressure profiles for brine flooding in micromodel are smoother than for core flooding. Core flood pressure responses with bumps over a wide range were also observed for oil-wet core plugs, as discussed in the previous section.

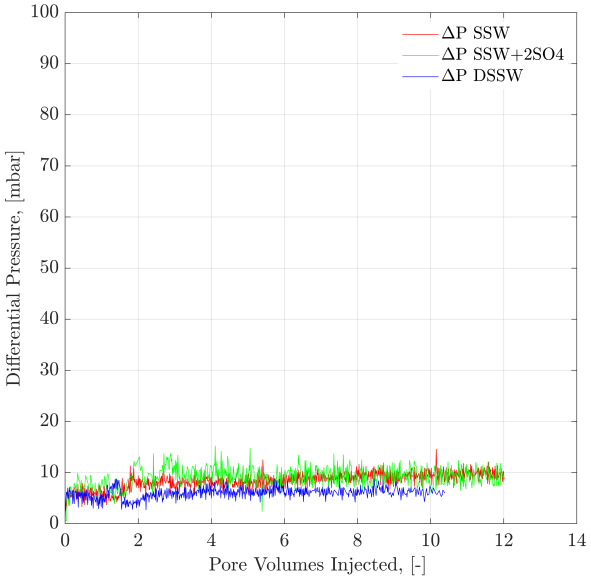

Figure 7.10: *Pressure response of secondary-mode brines flood through complex-wet micromodel at a flux rate of 1ft/day*

Theoretically, the difference in the additional recovery between three-week aged core flooding and mixed-wet micromodel flooding should be smaller than the difference discussed for the oil-wet system. This difference is confirmed through RFs of SSW+2SO_4^{-2}/DSSW+2SO_4^{-2} between CF and MM in oil-wet and complex-wet systems. The recovery difference of 2.52% in the mixed-wet system is much smaller than the difference of 9.25% for the oil-wet system. This difference in RFs emphasizes the critical role of wettability alteration as the leading oil recovery mechanism compared to fluid-fluid interfacial interaction.

7.4 Brine Bump-rate Flooding

After secondary-mode brine flooding, brine bump-rate injection was performed for all of the experiments mentioned above to eliminate any capillary end effects before performing tertiary-mode polymer flooding. Through MM, bump rate injection was performed at an injection rate five times greater than the brine rate. The core flooding was performed at a rate 2.3 times greater than the brine flooding. Oil RFs and pressure profiles for bump rate injection are excluded in this chapter to focus on the recovery comparison between secondary- and tertiary-mode flooding.

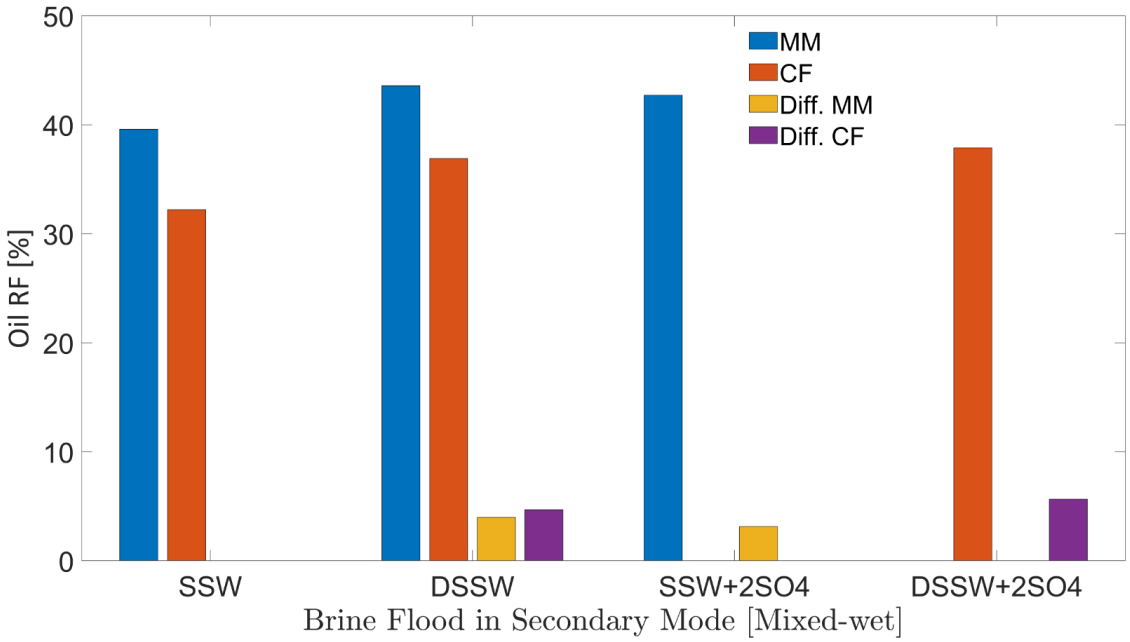

Figure 7.11: *Oil RFs of secondary-mode brine flooding in mixed-wet core plugs and micromodels*

7.5 Oil Recovery and Pressure Response for Tertiary-mode Polymer Flooding

7.5.1 Complex-wet Micromodel

Polymer Viscosity Half of the Oil Viscosity (Tertiary Mode)

No additional oil recovery was obtained with tertiary-mode polymer flooding, as shown in Figure 6.22 and Figure 6.23. There are two possible reasons for this:

- There is a lower polymer viscosity compared to oil viscosity. Moreover, mechanical degradation of the polymer solution while flowing through flow lines can result in an even lower viscosity of the polymer solution than the actual polymer viscosity. Hence, polymer viscosity is expected to be less than half that of oil. Injected polymer follows the flow path of the pre-injected brine flood and cannot displace the oil due to lower aqueous viscosity.
- The pressure drop for polymer flooding is less than the pressure drop of the bump rate (pressure profiles in Figure 6.23). Hence, the bump rate produced additional oil due to the greater pressure drop. However, polymer flooding resulted in less of a pressure drop compared to the bump rate and hence no further oil was produced.

Polymer Viscosity Equal to the Oil Viscosity (Post-tertiary Mode)

Looking at the final oil RFs of the micromodel in Table 7.3, the combination of brine flooding with polymer resulted in 5.71% higher recovery for SSW+$2SO_4^{-2}$ compared to the combination of SSW with the polymer. As previously discussed, no wettability alteration occurred in the micromodel. This difference in oil recovery was due to the fluid's ionic interfacial mechanism plus viscosity support of the polymer flood. This difference in oil recovery was due to the combined EOR techniques of sulfate-modified water flooding with polymer flooding. SSW+$2SO_4^{-2}$ helped develop a stable ionic layer around the oil phase and produce oil ganglia inside the reservoir while follow-up polymer flooding helped produce these ganglia due to improved aqueous phase viscosity. Pressure profiles of both micromodels are presented in Figure 6.25 and Figure 6.27. This post-tertiary polymer injection resulted in a higher-pressure response for polymer prepared in SSW+$2SO_4^{-2}$ brine (28 mBar) compared to polymer prepared in SSW (20 mBar). This higher pressure drop, in turn, played a vital role in higher oil recovery, as seen in Table 7.3.

Table 7.3: *Oil recovery of core plugs and mix-wet micromodels in secondary-mode brine flooding and tertiary-mode polymer flooding*

Aging/ Wettability	Porous Media	Brine Flood	Soi	Swc	Brine RF	Polymer RF	Total RF
			%				
3-week aging	CF	**SSW**	79.40	20.6	32.22	-	-
		DSSW	75.40	24.6	36.90	6.90	43.80
		DSSW+$2SO_4^{-2}$	75.50	24.5	37.87	9.60	47.47
Mix-wet	MM	**SSW**	81.28	18.73	39.58	4.33	43.91
		SSW+$2SO_4^{-2}$	80.66	19.34	42.71	6.91	49.62
6-week aging	CF	**SSW**	84.34	15.66	34.27	13.94	48.21
		SSW+$2SO_4^{-2}$	82.11	17.89	45.69	8.84	54.53
		SSW+$4SO_4^{-2}$	81.33	18.67	38.98	9.90	48.88

7.5.2 Three-Week Aged Core Plugs

Figure 7.12 presents pressure profiles for tertiary-mode polymer flooding in three-week aged cores. Polymer solutions with half the viscosity of oil were selected for tertiary-mode injection. Looking at the RF of polymer floods for three-week aged core plugs in Table 7.3, 2.7% more oil was obtained from polymer flooding after DSSW+$2SO_4^{-2}$. This higher recovery can be attributed to the combined effect of greater pressure drop with polymer injection combined with fluid-fluid interaction. Moreover, comparing the final RFs after combined EOR techniques, 3.67% higher recovery was produced from sulfate-modified water combined with polymer flood compared to low-salt brine combined with polymer

flooding. With the three-week aging process, wettability alteration was not the main recovery mechanism for brine flood. The main contribution of oil recovery is expected from the interfacial interaction of fluids. Pressure response for polymer prepared in the spiked amount of sulfate brines (DSSW+2SO_4^{-2}) was higher than for the DSSW brine (almost doubled at 2.5 PV). This higher pressure response also supports higher oil recovery with polymer flooding (polymer- DSSW+2SO_4^{-2}).

7.5.3 Six-Week Aged Core Plugs

Figure 7.13 presents the pressure profiles of six-week aged core plugs for secondary-mode brine flooding and tertiary-mode polymer flooding. Polymers injected in the tertiary mode have viscosity half that of oil. Polymer-SSW produced the maximum amount of oil with an additional RF of 13.94%. This higher recovery was contributed due to higher ROS in the core plugs after secondary-mode SSW brine flooding. This higher amount of unflushed oil (ROS) was produced through tertiary-mode polymer flooding resulting in higher recovery. However, comparing the combined EOR effects of brine in combination with polymer flooding, sulfate-modified water (SSW+2SO_4^{-2}) produced the highest oil recovery. The combined EOR of sulfate-modified water resulted in additional oil recovery of 6.32% compared to SSW due to strong fluid-fluid/rock-fluid interaction and follow-up higher aqueous viscosity of polymer flooding.

7.5.4 Final RFs

A summary of the final/total RFs for both porous media—core plugs and the complex-wet micromodel—can be seen in Table 7.3. For the data obtained, the combination of sulfate-modified water (SSW+2SO_4^{-2} and DSSW+2SO_4^{-2}) always led to higher recovery compared to the base brine flood (SSW). This investigation concludes that the spiked amount of sulfate plays a significant role in disturbing the ionic equilibrium in a reservoir, which, in turn, initiates fluid-fluid and rock-fluid interactions. Comparing the final RFs obtained for SSW+2SO_4^{-2} flooding combined with polymer flood in Table 7.3, rock-fluid interaction is the dominant mechanism compared to fluid-fluid interaction. Although higher viscosity polymer was injected through the micromodels (compare to core flooding), less oil recovery was obtained. This low recovery was due to the lack of rock-fluid interaction in the micromodel. This study concludes that both mechanisms (fluid-fluid interfacial interactions and wettability alteration) are essential for higher oil recovery during low-salt or sulfate-modified water flooding, but wettability alteration is the dominating and primary recovery mechanism.

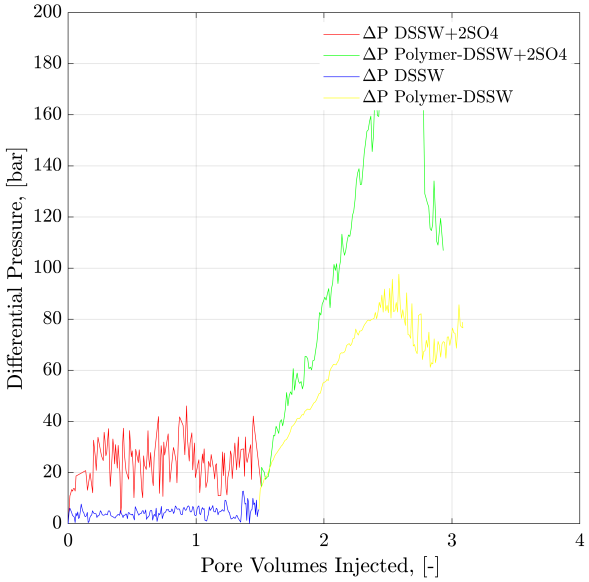

Figure 7.12: *Pressure drop versus PV injected for three-week aged core plugs. Brine injection (5g/L TDS) was performed in the secondary mode while polymer flooding (half the viscosity of oil) was performed in the tertiary mode.*

7.6 Results and Remarks

This chapter helps with the understanding of the main recovery mechanism for modified water flooding based on sulfate content and outlines the benefit of using coupled data obtained from core plugs and micromodel flooding. Furthermore, it helps confirm whether the main recovery mechanism of sulfate-modified water injection is fluid-fluid interfacial interaction or wettability alteration or a combination of these.

Base on the static interfacial tension and oil-drop snap-off volume measurements, it is clear that the doubled amount of sulfates in SSW improved the fluid-fluid interaction. This improvement in fluid-fluid interaction led to large oil drop formation in SSW+2SO_4^{-2} brine, which assisted with continuous oil flow while limiting the oil trapped in porous media, and is hence associated with higher oil recovery. Additionally, two-phase sulfate-modified water flooding in oil-wet and mixed-wet micromodels confirmed that the additional oil recovery can be mainly attributed to fluid-fluid interfacial interaction.

Comparison of sulfate-modified water flooding in the oil-wet core plugs with the oil-wet micromodel leads to the assumption that rock-fluid interaction is the dominating recovery mechanism in core plugs. The strong rock-fluid interaction in core plugs helped produce significantly higher oil recovery compared to the oil recovery obtained from the micromodel. Moreover, comparing the six-week aged core plug and the three-week aged core plug indicates that the oil-wetting condition of the reservoir is the primary

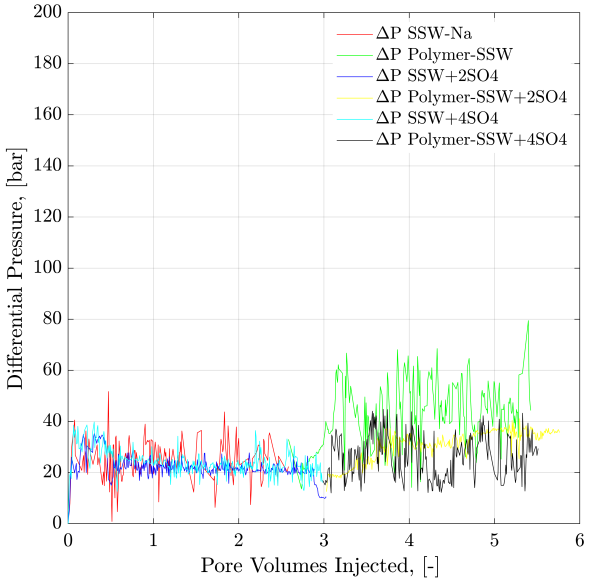

Figure 7.13: *Pressure drop versus PV injected for six-week aged core plugs. Brine injection (17-41g/L TDS) was performed in the secondary mode while polymer flooding (half the viscosity of oil) was performed in the tertiary mode.*

requirement for the rock-fluid interaction.

On one hand, RFs between fluid-fluid interaction and rock-fluid interaction indicate that rock-fluid interaction is the dominating recovery mechanism in oil-wet reservoirs. On the other hand, oil recovery results show that secondary-mode sulfate-modified water injection and tertiary-mode polymer flooding resulted in the lowest ROS, hence proposing the synergies and benefits of combined EOR techniques.

Chapter 8

Polymer Viscoelastic Properties

This chapter evaluates the viscoelastic phenomenon in high-molecular-weight polymers (24-28 M Daltons) used for EOR applications based on single-phase polymer core flooding experiments. The evaluation refers to the polymer discussed in the previous chapters and others that were used only for screening and comparison purposes. First, the investigation of the impact of sulfates on polymer viscoelastic properties during polymer flooding is studied. Chapters 4 and 5 determined the sensitivity of spiked sulfate brine for polymer mechanical degradation. However, Chapter 7 indicated a higher pressure drop of the polymer with spiked sulfate in the mixed-wet micromodel/core plugs. These contradictory results motivate the further investigation of polymer viscoelastic properties using single-phase polymer flooding.

Second, an evaluation of the impact of semi-harsh conditions (salinity, hardness, and temperature) is performed. The addition of sulfate to modified water changes the salinity and hardness of the brine. Hence, the roles of salinity and hardness are also investigated for polymer viscoelastic properties using two different brines. The findings of this chapter were organized, prepared, and split for journal publications 1) "Coupling Microfluidics Data with Core Flooding Experiments to Understand Sulfonated/Polymer Water Injection" in Polymers 2020 (ISSN 2073-4360), 12(6), 1227; and 2) "Elongational and Shear Evaluation of Polymer Viscoelasticity during Flow in Porous Media" in Applied Sciences 2020 (ISSN 2076-3417), 10(12), 4152; https://doi.org/10.3390/app10124152.

8.1 General Methodology and Approach

This work investigates the polymer viscoelastic properties, focusing on single-phase polymer flooding through Bentheimer core plugs. The objectives of this chapter were achieved

using the following methodologies:

- ***Brine preparation***: Four brines were prepared, focusing on salinity, hardness, and increasing the sulfates for mixing polymer solutions, presented as BG4 Table 3.1.
- ***Polymer diluted solutions***: High concentrations (2,000 ppm and 3,000 ppm) of polymer solutions were prepared using Flopaam 6035 S and Hengfloc 63026 polymer to investigate the pore-scale mechanism of viscoelasticity. Polymer solution viscosities are Nr. 5 and Nr. 6 in Table 3.3.
- ***Single-phase polymer flooding***: Bentheimer core plugs saturated with brine, described as CG3 in Table 3.5, were used for the single-phase polymer flooding. Polymer flooding was performed over increasing injection rates to observe the corresponding pressure response. Core flooding experiments were performed at room temperature (22°C) and a higher reservoir temperature (45°C).

8.2 Single-phase Core Flooding

8.2.1 Impact of Sulfates on Polymer Viscoelasticity

Chapters 4 and 5 discussed that a spiked amount of sulfate in polymer solutions makes them sensitive to mechanical degradation while flowing through flow lines. Polymer solutions' viscosity is significantly decreased before entering the core plugs because an increase in the amount of sulfate in polymer solutions increases the sensitivity to mechanical degradation while flowing through flow lines (Chapters 4 and 5). However, looking at the pressure profiles through mixed-wet micromodels and three-week aged core plugs, pressure response for polymer solution with a spiked amount of sulfate is significantly higher compared to the polymer solution in SSW. This higher pressure during polymer flooding is in contradiction to the mechanical degradation that happens before entering the core plugs. There are two main reasons for the high pressure of the spiked sulfate polymer in porous media.

- The first reason is the improvement in polymer viscoelastic properties while flowing through the multiple converging-diverging geometries of the porous media. Improved viscoelastic properties cause resistance in flow due to stretching of long-chain polymer molecules and hence an increase in pressure is observed.
- The second reason is the improved interfacial bondage developed at the brine-oil interfaces, which either develops oil ganglia or holds the water-phase attachment

with the remaining oil due to a fluid's ionic interaction. This fluid-fluid interaction indirectly narrows the flow path for polymer molecules and hence results in the higher-pressure response.

To understand the leading cause of the higher pressure drop, single-phase polymer flooding was performed through the Bentheimer core plugs, with SSW and brine with four times the spiked amount of sulfate (Brine 9 and Brine 10 of BG4 from Table 3.1). Polymer injection (2,000 ppm) was performed over a wide range of increasing flux rates of 1 ft/day to 33 ft/day, as described in Figure 8.1 and Figure 8.2. The shear pressure drop corresponds with the pressure value calculated after matching the polymer viscosity values measured by a viscometer (using Darcy's equation) against the apparent viscosity in the core while the CF/total pressure drop corresponds with the pressure measured for core flooding. The difference in values corresponds with the values of SSW minus the values of SSW+$4SO_4^{-2}$ at the same flux rate. The pressure profile for SSW polymer flooding is always slightly higher than for SSW+$4SO_4^{-2}$ polymer.

Moreover, the difference in pressure drop remained constant for all flux values with the same trend line. The pressure ratio presented in Figure 8.2 indicates that polymer-SSW presented higher values than polymer-SSW+$4SO_4^{-2}$ (flux rate higher than 1*10^{-4} m/s). At flux values higher than 1*10^{-4} m/s, the slope of both polymer solutions increased due to the dominance of viscoelastic response. However, this dominance was observed for both polymer solutions. This justifies that a spiked amount of sulfates cannot improve the viscoelastic response of polymer solutions while flowing through porous media. Further, increased sulfates make polymer solution sensitive to mechanical degradation, which resulted in a slightly lower pressure drop compared to polymer prepared in SSW in single-phase flooding. Hence, it can be concluded that the high-pressure profiles for polymer with the spiked amount of sulfates though micromodels and three-week aged core plugs were due to the presence of strong interfacial layer at the oil-brine interface.

8.2.2 Impact of Semi-harsh Conditions on Polymer Viscoelasticity

Two synthetic high-molecular-weight viscoelastic polymers, Hengfloc 63026 and Flopaam 6035 S (MW=24-28MD), were used to prepare the diluted solutions at concentrations of 3,000 ppm using two brines (Brine 7 and Brine 8 of BG4 from Table 3.1). The viscoelastic phenomenon was observed in polymers via a similar approach to that proposed by Heemskerk et al. [130], where the pressure drop measured during polymer flooding experiments is plotted against interstitial velocity. Heemskerk's work described

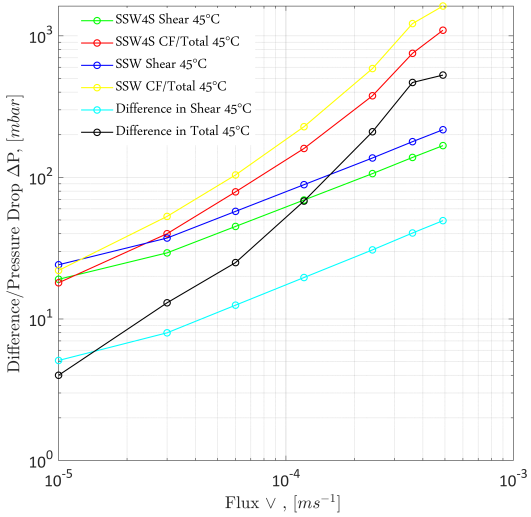

Figure 8.1: *Pressure drop/difference in pressure drop for two polymer solutions as a function of the injection rate.*

shear-thinning behaviour for a slope below 45º, shear thickening for a slope higher than 45º, and a Newtonian response for a slope of precisely 45º. The results presented here are in excellent agreement with those reported by Heemskerk et al. [130]. Figure 8.3 illustrates the following observed behaviours of HPAM polymer solutions at different temperatures prepared in both brines: a characteristic slope for a Newtonian response at 45º, shear thinning below 45º, and shear-thickening behaviour above 45º. A seen in Figure 8.3, Flopaam polymer has higher viscoelastic properties (pressure drop) compared to Hengfloc polymer at a specific temperature and in the same brine. Furthermore, for Flopaam polymer, the pressure drop of the polymer solution prepared in GB (German brine from Table 3.1) at 22°C is higher than the pressure drop of the same polymer prepared in SSW2 (from Table 3.1) at 45°C. This behaviour indicates that temperature has a stronger effect on decreasing polymer viscoelastic properties compared to the brine hardness.

Figure 8.4 shows a typical plot that represents the pressure response related to injection interstitial velocity for different conditions. The plots consider the total pressure (ΔP_T) obtained during core flooding measurement. The pressures associated with shear (ΔP_S) are determined by Darcy's law using rheometer viscosity data, and pressure drops due to elongation (ΔP_E) are measured using e-VROC. These results allow any additional pressure drop to be classified as an excessive pressure drop caused by turbulence. This excessive pressure drop could be caused by the mingling of flow lines, which changes the flow sequence and causes resistance. From Figure 8.4, it appears that the calculated pressure drop matched the experimental data only at low interstitial velocity. The calculation is performed with;

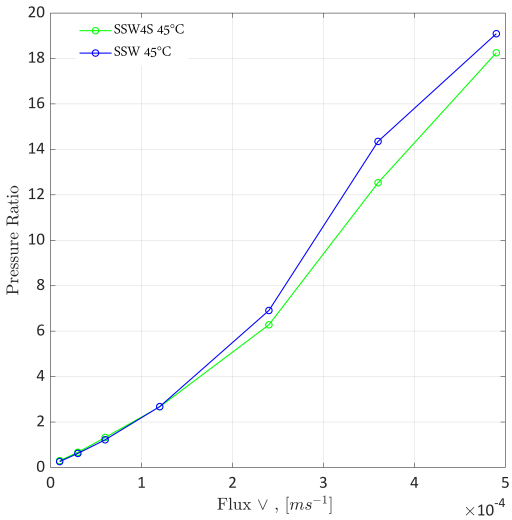

Figure 8.2: *Pressure ratio for two polymer solutions as a function of the flux rate. The pressure ratio is defined as the polymer pressure drop at each flux rate divided by the pressure drop for brine flooding at a flux rate of 10 ft/day.*

$$\Delta P_T = \Delta P_S + \Delta P_E + \Delta P_t,$$

where, ΔP_T is total pressure obtained during core flooding, ΔP_S is determined using Darcy's equation and the Carreau-Yasuda flow curve fitted to rheometer data, ΔP_E is the e-VROC measurement, and ΔP_t is the excessive pressure drop happening in porous media (ΔP_T - ΔP_E-ΔP_S)

Shear forces dominate at low interstitial velocities, which can be seen by comparing the experimental pressure data with the rheometer data. Figure 8.4 clearly shows that, at low flux values, the elongational pressure drop is lower and can be neglected. As for flux increases, the viscoelastic nature of polymer becomes dominant, resulting in a higher total pressure drop. This behaviour causes the total pressure drop to deviate from the rheometer data. The viscoelastic response of the polymer is also confirmed via the increase in the elongational pressure drop from intermediate to high flux values. Figure 8.4 also shows that, at high injection rates, the elongational pressure drop almost matches the total pressure drop during core flooding. The triangular area at medium flux (crossover of pressure drop lines) represents excessive pressure drop in porous media, which is not measured using e-VROC or a rheometer.

8.3 Results and Remarks

The results of single-phase polymer flooding indicate that the spiked amount of sulfates in mixing brine does not enhance polymer's viscoelastic properties. It also proves that

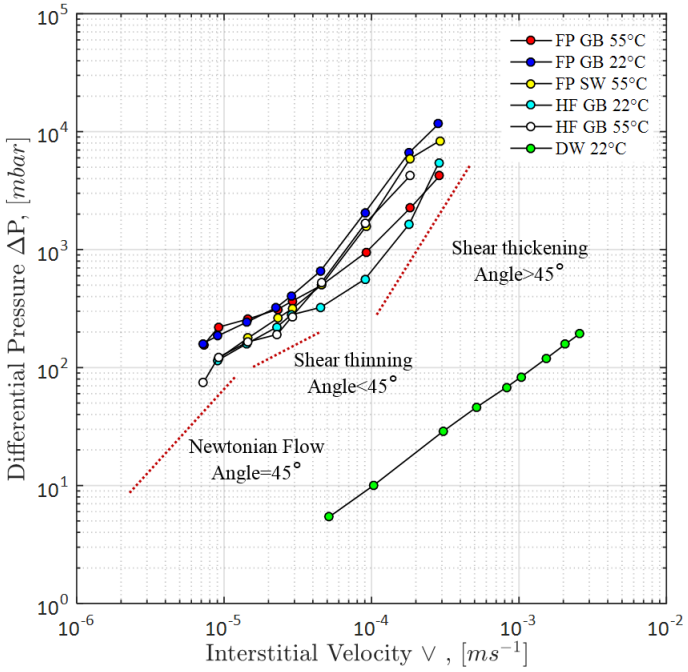

Figure 8.3: *Measured pressure drop as a function of the interstitial velocity for solutions through Bentheimer core plugs. The data plotted is for HPAM Flopaam 6035 S/Hengfloc 63026 at different temperatures prepared in Brine 7 and Brine 8 from Table 3.1*

the pressure drop of a spiked sulfate solution is slightly less than a solution with no or fewer sulfates. Spiked sulfate polymers demonstrate a higher pressure drop in two-phase flooding due to improved interfacial layer at the oil-brine interface developed during pre-flushed modified water. Moreover, semi-harsh reservoir conditions significantly damage the viscoelastic properties of polymers. The presence of divalent ions at high temperatures makes it difficult for polymers to retain good viscoelastic properties. This issue can be minimized using water-softening techniques for makeup water (solvent for polymer) and prior low-salt water injection. Comparing the results obtained for pressure drop in the core in with e-VROC and rheometer data provides insightful information about turbulence-dominated excessive pressure drops occurring inside porous media. The existence of this excessive pressure drop in porous media helps with the understanding of pore-scale mechanisms in reservoirs.

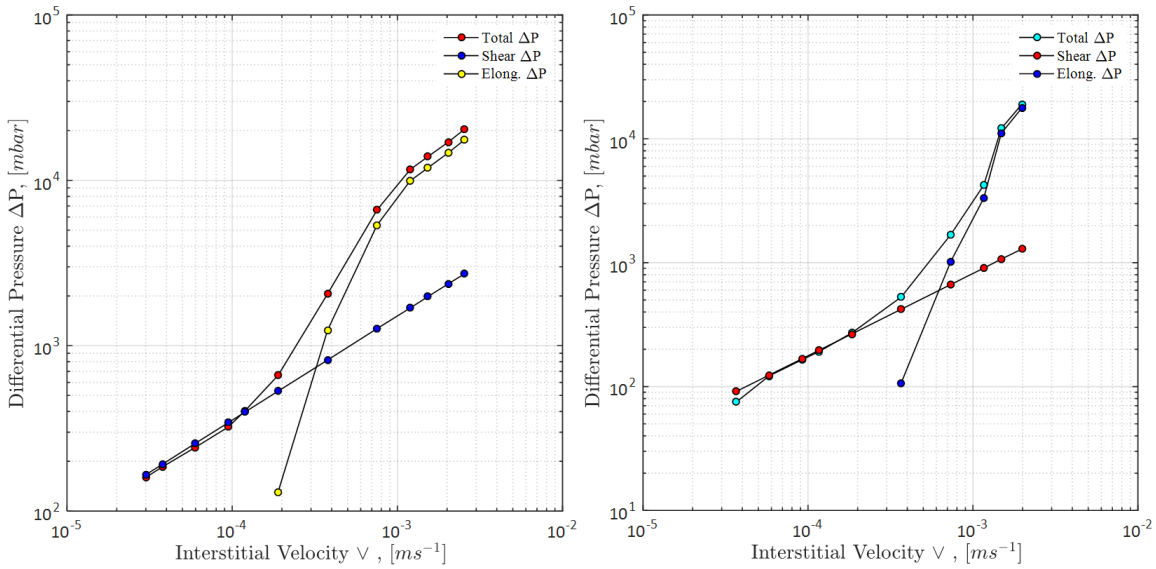

Figure 8.4: *Pressure drops as a function of interstitial velocity for an HPAM solution through a Bentheimer core. The data plotted is for Flopaam 6035 S with 3,000ppm at 22°C in SSW (left) and Hengfloc63026 with 3,000 ppm at 55°C in GB (right). The calculated pressures were obtained using Darcy's equation and the Carreau-Yasuda flow curve fitted to rheometer data. Elongation was measured via e-VROC.*

Chapter 9

Economic Perspective – An Estimate

Low-salt/modified water is expected to be a cheaper EOR technique compared to other chemical methods. This chapter outlines a basic, straightforward approach for economic evaluation, focusing on the cost of modified water preparation. Modification of injected water involves either the removal or addition of specific salts, which directly affects the investment/cost incurred for a low-salt or modified water injection project. Previous chapters (4-7) summarised the various types of modified water injected in combination with polymer flooding. Here, economic evaluation is performed to select the most economical injection water recipe. Note that this economic evaluation approximates the possible scenarios to assist with understanding the potential impacts of each technique.

9.1 Low-salt Brines–BG2 Group in Table 3.1

Chapter 4 discusses brines prepared through the dilution process to reduce the TDS $\leq$ 5g/L. A low-salt process occurs when the salinity of injection brine ranges 1,000 to 5,000 ppm. However, on a commercial scale, a significant amount of modified or diluted brine is required to execute a project. Low-salt brines can be obtained through two scenarios:

- First, they can be obtained through available resources (shallow reservoir). Low-salinity injection can be performed either by direct injection of freshwater or diluting freshwater with produced brine. Nevertheless, in both scenarios, a significant amount of resources is essential. Most of the time, oil fields are located in barren places or far away from freshwater resources. Moreover, in some countries,

there are restrictions on using freshwater for EOR, limiting the application of low-salt/sulfate-modified water injection at the field scale.

- Second, low-salt brines can be produced through the desalination process of the produced water. However, the desalination process is not cost-effective. A cost estimation study from Sarai Aftab et al. [62] concluded that the desalination of seawater (15,000 ppm) required an investment of 11.3 GBP to obtain water with low salt (1,600 ppm). Further, it required 0.8 GBP/m^3 in operational costs. Total expenses (investment and operational cost) can significantly increase the cost of a commercial project. Qtaishat et al. [61] performed a similar economic analysis for brackish water desalination used for irrigation in the Jordan Valley. The authors concluded an average desalination investment of JD 63.5 (m^3/h), with an average desalination cost of JD 0.38 per cubic meter.

Oil RFs of secondary-mode brine floods from Table 4.1 indicate that without polymer flooding, it may not be economical to perform low-salt/sulfate-modified water flooding in intermediate oil-wet reservoirs (2.60% to 5.65% extra oil recovery). Nevertheless, with follow-up tertiary-mode polymer flooding, modified water with a spiked amount of sulfates can make the project economical (12.20% to 15.25% extra oil recovery).

9.2 Spiked Sulfate Brine BG3 Group in Table 3.1

This group of brines was modified through the addition of sulfates in SSW. The commercial price of Na_2SO_4 is USD 80-120/Ton. The average price of this salt is around 0.1 USD/kg, which is much lower than the average price of polymer, alkaline, and co-solvent (3 USD/kg, 0.25 USD/kg, and 3 USD/kg, respectively [10]). The spiked amount of sulfate to design sulfate-modified water for this study is 8-16g/L (two times and four times the sulfates in SSW). Comparing the price of Na_2SO_4 and the required amount of this salt, it seems attractive and commercially economical to apply sulfate-based modified water at field scale. Sulfate-modified water produced 11.42% to 17.22% extra oil recovery compared to SSW flooding, which holds significant promise. Figure 9.1 presents the cost of sodium sulfate to make the desired modified injection brine for the RF obtained. The expense for a doubled amount of sulfates is less than the expense for a quadrupled amount of sulfates in terms of the oil produced. SSW-CF represents the core plug with SSW as the formation brine while 2*SSW-CF represents the core plug with doubled seawater as the formation brine.

A high RF of SSW without sodium chloride salts can be seen in Table 5.3. However, this technique can be expensive due to expenditures to remove non-PDI monovalent ions

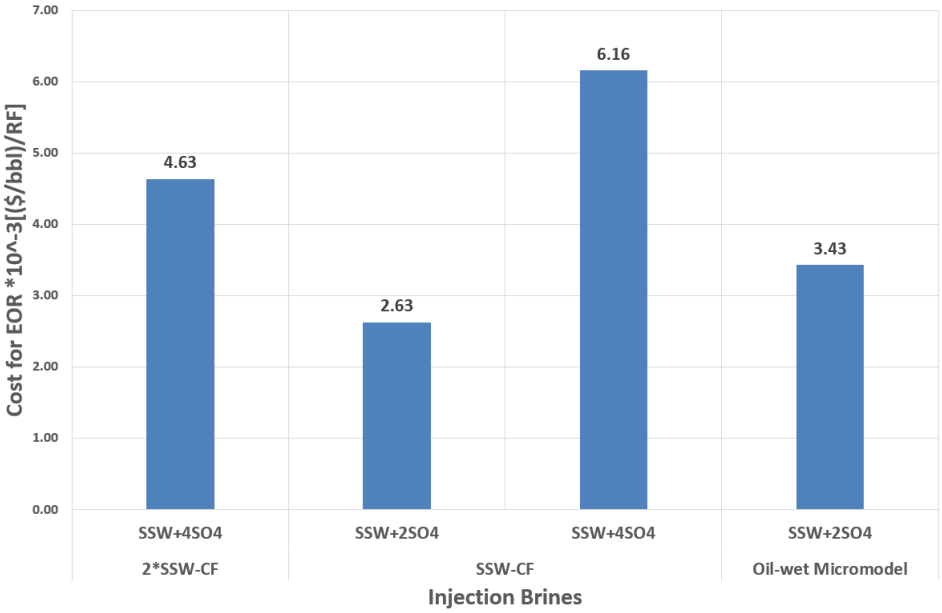

Figure 9.1: *Price of the spiked amount of sulfates in [USD/bbl]/RF of injected modified SSW to obtain the RF from core plugs.*

from the brine (sodium ions). This technique is similar to the desalination method in terms of capital investment as well as operational costs.

9.3 Results and Remarks

According to the observations, the proposed combination of techniques could lead to cost optimization. A doubled amount of spiked sulfate in SSW resulted in a cost-effective modified water process for injection in an oil-wet reservoir. No capital investment is required and no special equipment needs to be installed for mixing the small amount of sulfate in the injection brine. This recipe costs significantly less and will produce higher oil recovery. Moreover, low-concentration polymer flooding in the tertiary mode after modified water flooding can recover extra oil.

Chapter 10

Conclusions

This study aimed at investigating the physical aspects and recovery mechanisms of sulfate-modified water injection in combination with polymer flooding in sandstone reservoirs. Multiple brine preparation recipes and injection schemes were investigated to screen out the most effective modified water composition from technical and economic perspectives. This work compares core floods and micromodels to cross-validate the principal results and to deepen the investigation of the primary recovery mechanism (wettability alteration or fluid-fluid interfacial interaction or both). Synergies of polymer flooding in combination with brine injection were also investigated to evaluate the potential oil recovery. Further, the comparison of different wettability micromodels confirmed that the concept of modified water works only in oil-wet/mixed-wet reservoirs.

For a detailed description of the findings, please refer to the results and remarks of each chapter (4-9). Some of the key conclusions are summarised here to support the objectives of the thesis.

- ***Modified low-salinity flooding combined with polymer flooding***: Oil RFs obtained during low-salt/low-salt sulfate-modified brine injection demonstrated the potential results of wettability alteration through aged core plugs. It was concluded that low-salt and low-salt sulfate-modified water injection should be performed before polymer flooding to initiate the wettability alteration process. Follow-up polymer flooding displaced the detached and trapped oil droplets due to improved polymer viscoelastic properties. It was observed that polymer solutions prepared in sulfate-modified brine resulted in a higher-pressure drop during flooding, which supports the significantly higher oil recovery after sulfate-modified low-salinity flooding. The concept of modified water and polymer flooding synergies works efficiently, resulting in promising oil recovery. However, linear viscoelastic mea-

surements could not completely predict the polymer viscoelastic response at low polymer concentrations.

- ***Modified seawater flooding combined with polymer flooding***: The role of the interfacial layer (oil-brine interaction) was investigated in parallel with the wettability alteration (rock-fluid interaction) process to accomplish higher oil recovery. High salinity (close to SSW) modified water recipes were investigated. Static interfacial tension and oil-drop snap-off volume measurements confirmed the development of the stable and elastic layer at the oil-brine interface by sulfate-active ionic interactions. Later, core flood experiments proved that sulfate-modified brine injection disturbed the established ionic equilibrium in the reservoir, which resulted in wettability alteration and the development of a stable interfacial layer. However, the amount of sulfate added in the injection brine must be compatible with the amount of divalent cations in the formation brine. Oil recovery results indicated that secondary-mode sulfate-modified brine injection and tertiary-mode polymer flooding resulted in the lowest ROS, hence proposing the synergies and benefits of combined EOR techniques.

- ***Sulfate-modified seawater flooding in micromodels***: The concept of fluid-fluid interaction was further investigated through flooding performed in the micromodels with the various brines. It was not possible to alter the wettability (rock-fluid interaction) of oil-wet micromodels with modified brine flooding. Oil-wettability was established by applying a chemical layer at the matrix structure, which was impossible to remove with the injected modified brine. Hence, additional oil recovery obtained from low-salt/sulfate-modified seawater was only through the recovery mechanism of fluid-fluid interaction. Moreover, it was confirmed that low-salt/sulfate-modified seawater injection produced additional oil recovery only in the oil-wet/complex-wet micromodels.

- ***Comparative investigation of modified water injection***: Comparative investigation of micromodels and core plug flooding concluded that rock-fluid interaction (wettability alteration) was the dominating recovery mechanism compared to fluid-fluid interaction. Significant additional oil recovery was contributed from wettability alteration compared to the oil-brine interaction. Additional oil recovery was obtained from the core plugs by low-salt/sulfate-modified seawater flooding from both recovery mechanisms of wettability alteration and fluid-fluid interaction. However, the additional oil recovery from oil-wet and mixed-wet micromodels was achieved only by fluid-fluid interaction.

- ***Polymer viscoelastic properties***: The results of single-phase polymer flooding showed that a spiked amount of sulfate did not enhance the polymer viscoelastic

properties. Moreover, the higher-pressure drop with polymer flooding with a spiked amount of sulfates in the two-phase mixed-wet micromodel and core plugs was due to improved interfacial interaction at the oil-brine interface developed during pre-flushed modified/low-salt water flooding. It was also determined that single-phase polymer flooding under semi-harsh conditions (salinity, hardness, reservoir temperature) sharply decreased the polymer viscoelastic properties. High temperature and the presence of divalent cations in the formation brine developed worse conditions for polymer viscoelastic response. This issue can be minimized through the use of low-salinity/sulfate-modified water pre-flush. Additionally, comparing the core flood pressure drop with e-VROC and rheometer data provided insightful information about turbulence-dominated excessive pressure drop occurring inside the porous media.

- ***Economic perspective analysis***: Doubling the amount of sulfates of seawater resulted in optimum modified water for sandstone reservoirs in terms of lower expenses and maximum oil recovery. This sulfate-modified water required neither the installation of special equipment at field scale nor significant capital investment.

Bibliography

[1] Mohamed Ibrahim Mohamed and Vladimir Alvarado. Smart water flooding in berea sandstone at low temperature: Is wettability alteration the sole mechanism at play? Society of Petroleum Engineers.

[2] V. Alvarado, G. Garcia-Olvera, and E. J. Manrique. Considerations of adjusted brine chemistry for waterflooding in offshore environments. In *OTC Brasil*. Offshore Technology Conference.

[3] El-Abbas A. A. Moustafa and Shedid A. Shedid. Effects of magnesium and potassium sulfates on oil recovery by water flooding. 27(4):649–656.

[4] Taha Sochi. Non-newtonian flow in porous media. 51(22):5007–5023.

[5] Rafael E. Hincapie. *Pore-Scale Investigation of the Viscoelastic Phenomenon during Enhanced Oil Recovery (EOR) Polymer Flooding through Porous Media*. Papierflieger.

[6] Muhammad Tahir, Rafael E. Hincapie, Michael Be, and Leonhard Ganzer. A comprehensive combination of apparent and shear viscoelastic data during polymer flooding for EOR evaluations. 5(4):585–600.

[7] Behruz Shaker Shiran and Arne Skauge. Enhanced oil recovery (EOR) by combined low salinity water/polymer flooding. 27(3):1223–1235.

[8] OCA optical contact angle measuring and contour analysis systems - DataPhysics instruments.

[9] Calvin Gaol, Jonas Wegner, Leonhard Ganzer, Nicole Dopffel, Felix Koegler, Ante Borovina, and Hakan Alkan. Investigation of pore-scale mechanisms of microbial enhanced oil recovery MEOR using microfluidics application. Society of Petroleum Engineers.

[10] Bettina Schumi, Torsten Clemens, Jonas Wegner, Leonhard Ganzer, Anton Kaiser, Rafael E. Hincapie, and Verena Leitenmueller. Alkali/cosolvent/polymer flood-

ing of high-TAN oil: Using phase experiments, micromodels, and corefloods for injection-agent selection.

[11] R. R. Elhajjaji, R. E. Hincapie, M. Tahir, A. Rock, J. Wegner, and L. Ganzer. Systematic study of viscoelastic properties during polymer-surfactant flooding in porous media (russian). Society of Petroleum Engineers.

[12] Rafael Hincapie, Francisco Deomar Tovar, and Carlos Eduardo Alvarez. Feasibility for the application of in situ combustion in faja petrolifera del orinoco (FPO) based in a novel screening criteria for the technology. Society of Petroleum Engineers.

[13] Larry W Lake. *Enhanced oil recovery*. Prentice Hall.

[14] K. S. Sorbie. *Polymer-improved oil recovery*. Blackie.

[15] S. Thomas. Enhanced oil recovery - an overview. 63(1):9–19.

[16] Vladimir Alvarado and Eduardo Manrique. Enhanced oil recovery: An update review. 3(9):1529–1575.

[17] A. Lager, K. J. Webb, C. J. J. Black, Michael Singleton, and Kenneth Stuart Sorbie. Low salinity oil recovery - an experimental investigation. 49(1):28–35.

[18] John C. Martin. The effects of clay on the displacement of heavy oil by water. Society of Petroleum Engineers.

[19] A. Lager, K. J. Webb, and C. J. J. Black. Impact of brine chemistry on oil recovery.

[20] K. J. Webb, C. J. J. Black, and H. Al-Ajeel. Low salinity oil recovery - log-inject-log. Society of Petroleum Engineers.

[21] G. Q. Tang and N. R. Morrow. Influence of brine composition and fines migration on crude oil/brine/rock interactions and oil recovery. 24(2):99–111.

[22] Peimao Zhang, Medad T. Tweheyo, and Tor Austad. Wettability alteration and improved oil recovery by spontaneous imbibition of seawater into chalk: Impact of the potential determining ions ca2+, mg2+, and SO42−. 301(1):199–208.

[23] P. P. Jadhunandan and N. R. Morrow. Effect of wettability on waterflood recovery for crude-oil/brine/rock systems. 10(1):40–46.

[24] G.Q. Tang and N.R. Morrow. Salinity, temperature, oil composition, and oil recovery by waterflooding. 12(4):269–276.

[25] Mohammed B. Alotaibi, Ramez Masoud Azmy, and Hisham A. Nasr-El-Din. Wettability studies using low-salinity water in sandstone reservoirs. Offshore Technology Conference.

[26] N.R. Morrow, M. Valat, and H. Yidliz. Effect of brine composition on recovery of an alaskan crude oil by waterflooding. In *Annual Technical Meeting*. Petroleum Society of Canada. event-place: Calgary, Alberta.

[27] Yongsheng Zhang and Norman R. Morrow. Comparison of secondary and tertiary recovery with change in injection brine composition for crude-oil/sandstone combinations. Society of Petroleum Engineers.

[28] Griselda Garcia-Olvera and Vladimir Alvarado. Interfacial rheological insights of sulfate-enriched smart-water at low and high-salinity in carbonates. 207:402–412.

[29] Hasan N. Al-Saedi, Ralph E. Flori, and Soura K. Al-Jaberi. Eliminate the role of clay in sandstone: EOR low salinity water flooding. 9(2):1475–1483.

[30] Andrew P. Sullivan, Nael N. Zaki, Johan Sjoeblom, and Peter K. Kilpatrick. The stability of water-in-crude and model oil emulsions. 85(6):793–807.

[31] Mehrnoosh Moradi and Vladimir Alvarado. Influence of aqueous-phase ionic strength and composition on the dynamics of water–crude oil interfacial film formation. 30(11):9170–9180.

[32] Jan Czarnecki and Kevin Moran. On the stabilization mechanism of water-in-oil emulsions in petroleum systems. 19(5):2074–2079.

[33] Vincent J. Verruto and Peter K. Kilpatrick. Water-in-model oil emulsions studied by small-angle neutron scattering: Interfacial film thickness and composition. 24(22):12807–12822.

[34] Pedram Mahzari and Mehran Sohrabi. Crude oil/brine interactions and spontaneous formation of micro-dispersions in low salinity water injection. Society of Petroleum Engineers.

[35] Brendon Morin, Yafei Liu, Vladimir Alvarado, and John Oakey. A microfluidic flow focusing platform to screen the evolution of crude oil–brine interfacial elasticity. 16(16):3074–3081.

[36] Mehran Sohrabi, Pedram Mahzari, Seyed A. Farzaneh, John R. Mills, Pantelis Tsolis, and Shaun Ireland. Novel insights into mechanisms of oil recovery by use of low-salinity-water injection. 22(2):407–416.

[37] Gary A. Pope. Recent developments and remaining challenges of enhanced oil recovery. 63(7):65–68.

[38] Rafael Hincapie, Carlos Eduardo Alvarez, and Armando Jose Vargas. Technical feasibility of polymer injection in heavy oil reservoir BAINF60 and BAMED78: Intercampo norte - through predictive models. Society of Petroleum Engineers.

[39] R. E. Hincapie and L. Ganzer. Assessment of polymer injectivity with regards to viscoelasticity: Lab evaluations towards better field operations. Society of Petroleum Engineers.

[40] R. E. Hincapie, J. Duffy, C. O'Grady, and L. Ganzer. An approach to determine polymer viscoelasticity under flow through porous media by combining complementary rheological techniques. Society of Petroleum Engineers.

[41] M. Be, R. E. Hincapie, A. Rock, C. L. Gaol, M. Tahir, and L. Ganzer. Comprehensive evaluation of the EOR polymer viscoelastic phenomenon at low reynolds number. Society of Petroleum Engineers.

[42] Augustine Agi, Radzuan Junin, Jeffrey Gbonhinbor, and Mike Onyekonwu. Natural polymer flow behaviour in porous media for enhanced oil recovery applications: a review. 8(4):1349–1362.

[43] D. M. Jones and K. Walters. The behaviour of polymer solutions in extension-dominated flows, with applications to enhanced oil recovery. 28(6):482–498.

[44] W. M. Jones. Polymer additives in reservoir flooding for oil recovery: shear thinning or shear thickening? 13(5):L87–L88.

[45] Michael A. Nilsson, Ruta Kulkarni, Lauren Gerberich, Ryan Hammond, Rohitashwa Singh, Elizabeth Baumhoff, and Jonathan P. Rothstein. Effect of fluid rheology on enhanced oil recovery in a microfluidic sandstone device. 202:112–119.

[46] Joris van Santvoort and Michael Golombok. Sweep enhancers for oil recovery. 6(3):473–480.

[47] M. Tahir, R. E. Hincapie, M. Be, and L. Ganzer. Experimental evaluation of polymer viscoelasticity during flow in porous media: Elongational and shear analysis. Society of Petroleum Engineers.

[48] Umar Alfazazi, Waleed AlAmeri, and Muhammad R. Hashmet. Experimental investigation of polymer flooding with low-salinity preconditioning of high temperature–high-salinity carbonate reservoir. 9(2):1517–1530.

[49] M. A. Leveratto, J. Lauri, C. Sanz, J. Sigal, and S. M. Farouq Ali. EOR polymer screening for an oil field with high salinity brines. 4(1):73–81.

[50] E. Unsal, A. B. G. M. ten Berge, and D. A. Z. Wever. Low salinity polymer flooding: Lower polymer retention and improved injectivity. 163:671–682.

[51] E. J. L. Koning, E. Mentzer, and J. Heemskerk. Evaluation of a pilot polymer flood in the marmul field, oman. Society of Petroleum Engineers.

[52] J. Wang and M. Dong. Optimum effective viscosity of polymer solution for improving heavy oil recovery. 67(3):155–158.

[53] Abrar Al-Qattan, Abbas Sanaseeri, Zainab Al-Saleh, B. B. Singh, Hassan Al-Kaaoud, Mojdeh Delshad, Richard Hernandez, Winoto Winoto, Scott Badham, Chris Bouma, John Brown, and Kory Kumer. Low salinity waterflood and low salinity polymer injection in the wara reservoir of the greater burgan field. Society of Petroleum Engineers.

[54] W. Kleinitz and W. Littmann. Polymer flooding: Appraisal of four different field projects in germany. pages cp–107–00054. European Association of Geoscientists & Engineers.

[55] Demin Wang, Yuexing Hao, Eric Delamaide, Zhonggui Ye, Si Ha, and Xiangcheng Jiang. Results of two polymer flooding pilots in the central area of daqing oil field. Society of Petroleum Engineers.

[56] Haishan Luo, Emad W. Al-Shalabi, Mojdeh Delshad, Krishna Panthi, and Kamy Sepehrnoori. A robust geochemical simulator to model improved-oil-recovery methods. 21(1):55–73.

[57] J. J. Sheng. Critical review of low-salinity waterflooding. 120:216–224.

[58] James J. Sheng, Bernd Leonhardt, and Nasser Azri. Status of polymer-flooding technology. 54(2):116–126.

[59] Behruz Shaker Shiran and Arne Skauge. Similarities and differences of low salinity polymer and low salinity LPS (linked polymer solutions) for enhanced oil recovery. 35(12):1656–1664.

[60] Arne Skauge and Behruz Shaker Shiran. Low salinity polymer flooding. In *Saint Petersburg Russia - From Fundamental Science to Deployment: 17th European Symposium on Improved Oil Recovery, IOR*.

[61] Tala Qtaishat, Nayef Seder, Emad Al-Karablieh, Amer Salman, Mohammad Tabieh, and Hussain Al-Qudah. Economic analysis of brackish-water desalination used for irrigation in the jordan valley. 72.

[62] M. Sarai Atab, A. J. Smallbone, and A. P. Roskilly. An operational and economic study of a reverse osmosis desalination system for potable water and land irrigation. 397:174–184.

[63] James Sheng. *Modern Chemical Enhanced Oil Recovery: Theory and Practice*. Gulf Professional Publishing.

[64] Charles C. Patton. Water quality control and its importance in waterflooding operations. 40(9):1.123–1.126.

[65] Ali A. Yousef, Salah Al-Saleh, and Mohammed Saleh Al-Jawfi. Smart Water-Flooding for carbonate reservoirs: Salinity and role of ions. Society of Petroleum Engineers.

[66] Ramez A. Nasralla and Hisham A. Nasr-El-Din. Coreflood study of low salinity water injection in sandstone reservoirs. Society of Petroleum Engineers.

[67] Behruz Shaker Shiran and Arne Skauge. Wettability and oil recovery by low salinity injection. Society of Petroleum Engineers.

[68] Yogesh Kumar Suman, Ezeddin Shirif, Hussameldin Ibrahim, and Abdulsalam Ala-Ktiwi. Evaluation of low saline "smart water" enhanced oil recovery in light oil reservoirs. 02(1):13.

[69] Muhammad Tahir, Rafael E. Hincapie, Hendrik Foedisch, Hiwa Abdullah, and Leonhard Ganzer. Impact of sulphates presence during application of smart water flooding combined with polymer flooding. Society of Petroleum Engineers.

[70] Norman R. Morrow, Guo-qing Tang, Marc Valat, and Xina Xie. Prospects of improved oil recovery related to wettability and brine composition. 20(3):267–276.

[71] Scott Rivet, Larry W. Lake, and Gary A. Pope. A coreflood investigation of low-salinity enhanced oil recovery. Society of Petroleum Engineers.

[72] Quan Xie, Desheng Ma, Jiazhong Wu, Qingjie Liu, Ninghong Jia, and Manli Luo. Low salinity waterflooding in low permeability sandstone: Coreflood experiments and interpretation by thermodynamics and simulation. Society of Petroleum Engineers.

[73] Winoto Winoto, Nina Loahardjo, Sheena Xina Xie, Peigui Yin, and Norman R. Morrow. Secondary and tertiary recovery of crude oil from outcrop and reservoir rocks by low salinity waterflooding. Society of Petroleum Engineers.

[74] Zahra Aghaeifar, Skule Strand, Tina Puntervold, Tor Austad, and Farasdaq Muchibbus Sajjad. Smart water injection strategies for optimized EOR in a high temperature offshore oil reservoir. 165:743–751.

[75] M. A. AlGeer, A. Gmira, S. M. Al-Enezi, and A. A. Yousef. A new insight on the impact of individual ions on fluid/fluid interactions and SmarWater recovery. Society of Petroleum Engineers.

[76] Yongsheng Zhang, Xina Xie, and Norman R. Morrow. Waterflood performance by injection of brine with different salinity for reservoir cores. Society of Petroleum Engineers.

[77] Kholood Al-Nofli, Peyman Pourafshary, Nader Mosavat, and Ali Shafiei. Effect of initial wettability on performance of smart water flooding in carbonate reservoirs—an experimental investigation with IOR implications. 11(6):1–19.

[78] Aleksandr Mamonov, Tina Puntervold, and Skule Strand. EOR by smart water flooding in sandstone reservoirs - effect of sandstone mineralogy on initial wetting and oil recovery. Society of Petroleum Engineers.

[79] S. Bagci, Mustafa V. Kok, and Ulas Turksoy. Effect of brine composition on oil recovery by waterflooding. 19(3):359–372.

[80] Dick Jacob Ligthelm, Jan Gronsveld, Jan Hofman, Niels Brussee, Fons Marcelis, and Hilbert van der Linde. Novel waterflooding strategy by manipulation of injection brine composition. Society of Petroleum Engineers.

[81] Norman Morrow and Jill Buckley. Improved oil recovery by low-salinity waterflooding. 63(5):106–112.

[82] Kevin John Webb, Clifford James J. Black, and Gunnar Tjetland. A laboratory study investigating methods for improving oil recovery in carbonates. International Petroleum Technology Conference.

[83] Géza Horváth-Szabó, Jan Czarnecki, and Jacob Masliyah. Liquid crystals in aqueous solutions of sodium naphthenates. 236(2):233–241.

[84] Trond Erik Havre and Johan Sjoeblom. Emulsion stabilization by means of combined surfactant multilayer (d-phase) and asphaltene particles. 228(1):131–142.

[85] Jan Czarnecki and Kevin Moran. On the stabilization mechanism of water-in-oil emulsions in petroleum systems. 19(5):2074–2079.

[86] Vincent J. Verruto and Peter K. Kilpatrick. Water-in-model oil emulsions studied by small-angle neutron scattering: Interfacial film thickness and composition. 24(22):12807–12822.

[87] Andrew P. Sullivan, Nael N. Zaki, Johan Sjoeblom, and Peter K. Kilpatrick. The stability of water-in-crude and model oil emulsions. 85(6):793–807.

[88] Sócrates Acevedo, Belsay Borges, Felipe Quintero, Vincent Piscitelly, and Luis B. Gutierrez. Asphaltenes and other natural surfactants from cerro negro crude oil. stepwise adsorption at the water/toluene interface: film formation and hydrophobic effects. 19(5):1948–1953.

[89] Inge Harald Auflem, Arild Westvik, and Johan Sjoeblom. Destabilization of water-in-crude oil emulsions based on recombined oil samples at various pressures. 24(1):103–112.

[90] Sumit K. Kiran, Edgar J. Acosta, and Kevin Moran. Evaluating the hydrophilic-lipophilic nature of asphaltenic oils and naphthenic amphiphiles using microemulsion models. 336(1):304–313.

[91] William G. Anderson. Wettability literature survey- part 1: Rock/oil/brine interactions and the effects of core handling on wettability. 38(10):1.125–1.144.

[92] V. Alvarado, X. Wang, and M. Moradi. Role of acid components and asphaltenes in wyoming water-in-crude oil emulsions. 25(10):4606–4613.

[93] Muhammad Tahir, Rafael E. Hincapie, Hendrik Foedisch, Gion-Joèl Strobel, and Leonhard Ganzer. Potential benefits of fluid optimization for combined smartwater and polymer flooding: Impact on remaining oil saturation. Society of Petroleum Engineers.

[94] Seyed Jafar Fathi, Tor Austad, and Skule Strand. Water-based enhanced oil recovery (EOR) by "smart water" in carbonate reservoirs. Society of Petroleum Engineers.

[95] Merdhah, Amer Badr Bin, and Abu Azam Mohd Yassin. Laboratory study and prediction of calcium sulphate at high-salinity formation water. 1(1).

[96] Mingdong Yuan. Effect of temperature on barium sulfate scale inhibition of diethylene triamine penta (methylene phosphonic acid). In *Advances in Crystal Growth Inhibition Technologies*, pages 151–163. Springer, Boston, MA.

[97] K. I. Andersen, E. Halvorsen, T. Sælensminde, and N. O. Østbye. Water management in a closed loop - problems and solutions at brage field. Society of Petroleum Engineers.

[98] Bisweswar Ghosh, Lying Sun, and Samuel Osisanya. Smart-water EOR made smarter a laboratory development. International Petroleum Technology Conference.

[99] G. M. Graham, L. S. Boak, and C. M. Hobden. Examination of the effect of generically different scale inhibitor species (PPCA and DETPMP) on the adherence and growth of barium sulphate scale on metal surfaces. Society of Petroleum Engineers.

[100] Mehrnoosh M. Bidhendi, Griselda Garcia-Olvera, Brendon Morin, John S. Oakey, and Vladimir Alvarado. Interfacial viscoelasticity of crude oil/brine: An alternative enhanced-oil-recovery mechanism in smart waterflooding. 23(3):803–818.

[101] Hasan Al-Saedi, Ralph E. Flori, and Alsaba Mortadha. Investigation of smart water flooding in sandstone reservoirs: Experimental and simulation study part2. Society of Petroleum Engineers.

[102] Tormod Skauge, Ketil Djurhuus, and Roland Reichenbach-Klinke. Visualization of heavy oil mobilization by associative polymer. Society of Petroleum Engineers.

[103] Chun Huh and Gary Arnold Pope. Residual oil saturation from polymer floods: Laboratory measurements and theoretical interpretation. Society of Petroleum Engineers.

[104] Alexander Rock, Rafael E. Hincapie, Eugen Hoffmann, and Leonhard Ganzer. Tertiary low salinity waterflooding LSWF in sandstone reservoirs: Mechanisms, synergies and potentials in EOR applications. Society of Petroleum Engineers.

[105] Andrew Clarke, Andrew M. Howe, Jonathan Mitchell, John Staniland, Laurence Hawkes, and Katherine Leeper. Mechanism of anomalously increased oil displacement with aqueous viscoelastic polymer solutions. 11(18):3536–3541.

[106] Hongjun Yin, Demin Wang, and Huiying Zhong. Study on flow behavoirs of viscoelastic polymer solution in micropore with dead end. Society of Petroleum Engineers.

[107] Wang Demin, Cheng Jiecheng, Xia Huifen, Li Qun, and Shi Jingping. Viscous-elastic fluids can mobilize oil remaining after water-flood by force parallel to the oil-water interface. page 8.

[108] R. E. Hincapie, A. Rock, J. Wegner, and L. Ganzer. Oil mobilization by viscoelastic flow instabilities effects during polymer EOR: A pore-scale visualization approach. Society of Petroleum Engineers.

[109] Pengpeng Qi, Daniel H. Ehrenfried, Heesong Koh, and Matthew T. Balhoff. Reduction of residual oil saturation in sandstone cores using viscoelastic polymers. Society of Petroleum Engineers.

[110] Fulin Yang, Demin Wang, Gang Wang, Xinguang Sui, Weijie Liu, and Chunling Kan. Study on high-concentration polymer flooding to further enhance oil recovery. Society of Petroleum Engineers.

[111] M. Algharaib, A. Alajmi, and R. Gharbi. Improving polymer flood performance in high salinity reservoirs. 115:17–23.

[112] Subhash C. Ayirala, Ernesto Uehara-Nagamine, Andreas Nicholas Matzakos, Robert W. Chin, Peter Harold Doe, and Paul Jacob van den Hoek. A designer water process for offshore low salinity and polymer flooding applications. Society of Petroleum Engineers.

[113] Saeid Khorsandi, Changhe Qiao, and Russell T. Johns. Displacement efficiency for low salinity polymer flooding including wettability alteration. Society of Petroleum Engineers.

[114] Do Hoon Kim, Seungjun Lee, Chong Hyun Ahn, Chun Huh, and Gary Arnold Pope. Development of a viscoelastic property database for EOR polymers. Society of Petroleum Engineers.

[115] Andrew Clarke, Andrew M. Howe, Jonathan Mitchell, John Staniland, and Laurence A. Hawkes. How viscoelastic-polymer flooding enhances displacement efficiency. 21(3):675–687.

[116] Demin Wang, Gang Wang, and Huifen Xia. Large scale high visco-elastic fluid flooding in the field achieves high recoveries. Society of Petroleum Engineers.

[117] Mechanical degradation - an overview | ScienceDirect topics.

[118] Alejandro Mueller, L. Patruyo, Wilfrido Montano, D. Roversi-M, R. Moreno, N. Ramírez, and A. Sáez. Mechanical degradation of polymers in flows through porous media: Effect of flow path length and particle size. 50.

[119] Chemical degradation - an overview | ScienceDirect topics.

[120] Thermal degradation of polymer - an overview | ScienceDirect topics.

[121] Sudip Ray and Ralph Cooney. Thermal degradation of polymer and polymer composites. pages 213–242.

[122] Thomas Divers, Nicolas Gaillard, Stéphane Bataille, Antoine Thomas, and Cédrick Favéro. Successful polymer selection for CEOR: Brine hardness and mechanical degradation considerations. Society of Petroleum Engineers.

[123] Ahmad Moradi-Araghi and Peter H. Doe. Hydrolysis and precipitation of polyacrylamides in hard brines at elevated temperatures. 2(2):189–198.

[124] R. S. Seright. The effects of mechanical degradation and viscoelastic behavior on injectivity of polyacrylamide solutions. 23(3):475–485.

[125] Rene Tabary, Frederic Douarche, Brigitte Bazin, Pierre Maxime Lemouzy, Patrick Moreau, and Mikel Morvan. Design of a surfactant/polymer process in a hard brine context: A case study applied to bramberge reservoir. Society of Petroleum Engineers.

[126] A. Tay, F. Oukhemanou, N. Wartenberg, P. Moreau, V. Guillon, A. Delbos, and R. Tabary. Adsorption inhibitors: A new route to mitigate adsorption in chemical enhanced oil recovery. Society of Petroleum Engineers.

[127] Hendrik Foedisch, Hiwa Abdullah, Rafael E. Hincapie, and Leonhard Ganzer. Optimizing laboratory cEOR flooding evaluations to assess initial oil saturation and mobility ratio. Society of Petroleum Engineers.

[128] Florian Hauhs, Hendrik Foedisch, Rafael E. Hincapie, and Leonhard Ganzer. Novel evaluation of foam and immiscible gas flooding in glass-silicon-glass micromodels. Society of Petroleum Engineers.

[129] SEVERS, E. T. and AUSTIN, J. M. Ind. eng. chem. In *Ind. Eng. Chem.*, volume 46, pages 2369–2375.

[130] J. Heemskerk, R. Rosmalen, R. Janssen-van, R. J. Holtslag, and D. Teeuw. Quantification of viscoelastic effects of polyacrylamide solutions. Society of Petroleum Engineers.